2015

Light Controlled Drug Activation and Release

Jonathon Sheldon
sheldonje

Light Controlled Drug Activation and Release

A dissertation submitted in partial fulfillment of the requirements for the degree of

Doctor of Philosophy (Chemistry)

At

Virginia Commonwealth University (2015)

By

JONATHON ERVIN SHELDON

B.S. Chemistry (2010)

Longwood University, Farmville, Va

Advisor: **Matthew C. T. Hartman, Ph.D.**

Associate Professor, Department of Chemistry

Virginia Commonwealth University

And

The Massey Cancer Center

Richmond, Va

August, 2015

Acknowledgement

First and foremost, I would like to acknowledge my wife. Melissa has been a rock in my life and she has held strong to support me through this entire endeavor. Melissa has such an optimistic perception of life and people. It seems that she can always find a positive in places where I only see negative and I feel truly blessed to have found her and have her as a life partner. My entire family has always been supportive of my ideas and has encouraged me to educate myself as much as possible. My interest in "the way things work" stems from my family and none of this would have been possible without this cornerstone. It is through my parents and sister that I gained the confidence to push forward through any obstacle I might encounter. They have taught me, importantly, that family comes first and it is through their actions that I have come to adopt and live by this principle.

Entering graduate school, one of the first responsibilities of the graduate student is to choose an advisor. This is the person who will serve as a mentor and as the artist who molds graduate students in to scientists. I could not have made a better decision five years ago then to work for Matthew Hartman. Matthew is not only a remarkable scientific mind, but a moral, positive man who truly leads by example. My lab mates have further shaped me in to a scientist. It behooves me to mention David Hacker as a mentor and friend during my time at VCU. David brought a level of intelligence and comradery to Matthew's lab that I do not think I could have found anywhere else. Michael Dcona and I worked on similar projects under Matthew, and I learned the fine details of what it means to be a scientist from him. I would like to thank E. Railey White,

Daniela Selaya, Deboleena Mitra and Stacie Richardson for scientific discussion and for being leaders in the laboratory.

My committee members have been monumental in shaping my graduate work through the handling of my proposal and committee meetings. Richard Moran, James Terner, Ashton Cropp, and my chair, Vladimir Sidorov, deserve recognition for their help and advice. I would like to thank the Department of Chemistry, the Massey Cancer Center, and Virginia Commonwealth University for help and support.

Table of Contents

List of Figures

List of Schemes

Abstract

Cancer constitutes a terrible burden on modern society. In the United States there are an estimated 1,658,370 new cancer diagnoses resulting in 589,430 deaths in 2015 alone.[1] An estimated 41,170 of these cases will be diagnosed right here in Virginia. With new cancer patients comes the expanding demand for new treatments. As we all know, many modern chemotherapeutics cause adverse reactions to patients. This is because the toxic nature of these therapies often affects normal tissue alongside the tumors that are infesting the body. Therefore, researching novel ways to make chemotherapeutics selective for cancer, while leaving healthy tissue unscathed, is of paramount importance. There are a few ways in which we have approached cancer-specific chemotherapeutics. Through the use of light controlled toxicity and drug release and the targeting of tumor phenotypes such as overexpressed proteins and the Warburg effect, we begin to tackle the problem of non-specificity of current chemotherapeutics.

Combretastatin A-4 (CA4) is highly potent anticancer drug that acts as an inhibitor of tubulin polymerization.[2, 3] The core of the CA4 structure contains a cis-stilbene, and it is known that the *trans* isomer is significantly less potent. We prepared an azobenzene analog of CA4 (Azo-CA4) that shows 13-35 fold enhancement in potency upon external irradiation. G_{I50} values in the light were in the mid nM range. Due to its ability to thermally revert to the less toxic *trans* form, Azo-CA4 also has the ability to automatically turn its activity off with time. Therefore, this work establishes a novel strategy for switchable potency for cancer treatment.

Doxorubicin (Adriamycin) is an anthracycline type of chemotherapeutic that intercalates double-stranded DNA.[4] Although this drug has played a huge role in the treatment of cancer, its usefulness declines in cases of cancer recurrence because of the impact this drug has on the cardiovascular system. Therefore, we prepared this drug as a cell impermeable conjugate that gains penetrability through the use of external radiation.[5]

Folate receptor alpha (FRα) is overexpressed in a variety of cancer cells and accepts folic acid as a natural ligand.[6] Therefore, conjugation of drugs to folic acid introduces a promising way to bring these drugs to cancer cells with greater specificity. We took this concept one step further with the introduction of a photo-labile linker, connecting doxorubicin to folic acid, which offers dual-specificity through ligand targeting and light activation.

Finally, many cancer cells produce adenosine triphosphate, the energy currency of a cell, through an abnormal upregulation of glycolysis.[7] This pathway results in a larger-than-normal production of lactic acid and lowers the pH of cancer cells through a phenomenon known as the Warburg Effect. We hypothesized that through the use of L-canavanine, an L-arginine analog, we could construct short peptides that would gain cell permeability in a low pH environment. Attaching a cargo to these peptides, such as doxorubicin will ultimately allow for targeting the low pH extracellular environment of cancer cells. Through the use of these strategies we have furthered the fight against cancer. Targeting cancer by taking advantage of its phenotypes or through the use of light is vital in reducing negative side-effects of current chemotherapeutics. The

novel technologies offered above bring us a step closer to side-effect free treatment of cancer patients.

CHAPTER 1. INTRODUCTION

1.1 Cancer and Chemotherapy

Cancer remains one of the most dreaded diagnoses that a patient may receive. According to the American Cancer Society, cancer will affect one half of men and one third of women during their lifetimes. In 2015 there will be an estimated 1.7 million cancer diagnoses resulting in almost 600,000 deaths in the United States alone.[1] Thus, new treatments for cancer are in demand. Treatments for cancer have evolved over the years. Common treatments include surgery, radiation therapy, and chemotherapy.

Cancer chemotherapy began in the 1940's with the use of nitrogen mustards, which are DNA alkylating agents. Not long after this was the discovery of the anticancer properties of aminopterin,[8] a folic acid analog, which was later replaced by a similar, but more effective drug, methotrexate.[9] These discoveries ushered in an era of targeting cancer using chemotherapeutics.

1.1.1 Classes of Chemotherapeutics

Many types of cancer chemotherapeutics exist today. Among these include alkylating agents[10] such as the aforementioned nitrogen mustards. These agents work by alkylating guanine, damaging DNA, and ultimately preventing DNA replication, which is necessary for cell division and proliferation. Others inhibit the interaction of topoisomerase I & II with DNA[11] including irinotecan and topotecan. Topoisomerase inhibitors gain their lethality by blocking the ligation step of DNA coiling, which leads to diminished integrity of the genome and apoptosis. Similar to the topisomerase inhibitors are anthracyclines such as doxorubicin[12] which intercalates into double stranded DNA and prevents the progression of topoisomerase II. In the presence of doxorubicin, topoisomerase II is unable to re-seal double stranded DNA after the initial breakage of the base pairs. There is also a class of cancer drugs known as mitotic inhibitors that target a variety of proteins associated with mitosis[13]. Mitotic inhibitors generally gain effectiveness from inhibiting microtubule formation, which is involved in cell splitting. During my thesis work, I focused primarily on two of these drugs, doxorubicin, which is in an anthracycline class and combretastatin A-4, which falls into the mitotic inhibitor class.

1.1.2 Doxorubicin and Combretastatin A-4

Doxorubicin

Doxorubicin (Dox), also known as Adriamycin, bears close structural resemblance to the more abundant natural product daunomycin (Figure 1.1). Daunomycin, also known as daunorubicin, is produced by *Streptomyces peucetius,* a

species of bacterium. Dox is used in treating a variety of cancers including leukemia, breast, bone, lung and brain cancers and has several known mechanisms of action that result in cell death.[4] Dox is widely known as a DNA intercalator, but can be toxic in other ways. Dox is also known to bind to topoisomerases I and II preventing their dissociation from DNA and leading to DNA damage through double strand breaks.[14] Dox also stabilizes topoisomerase II and inhibits the enzyme from dissociating from DNA which leads to breaks which trigger an apoptotic pathway. Furthermore, stress on the genome of a cell can cause over activation of poly(ADP-ribose) polymerase-1 (PARP-1), depleting energy reserves and resulting in cell death.[15]

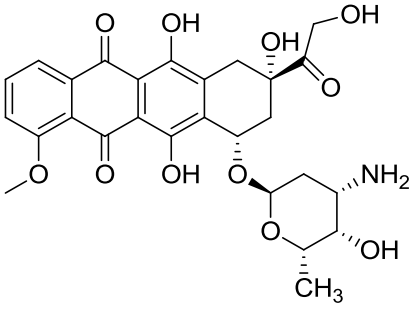

Doxorubicin (Adriamycin)

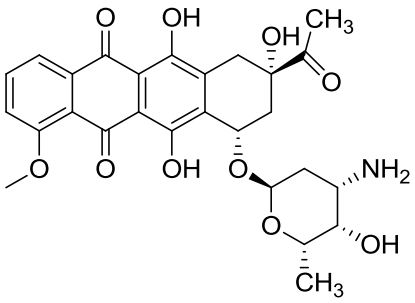

Daunomycin

Figure 1.1. Structures of doxorubicin (left) and daunomycin (right).

Combretastatin A-4

Combretastatin A-4 (CA4) and its water soluble phosphate prodrug CA4P (fosbretabulin) are a class of chemotherapeutics known as mitotic inhibitors. CA4 is known to bind at the colchicine binding site of β-tubulin, and is inhibitory at micromolar levels (IC_{50} = 1.9 ± 0.2 μM).[16] CA4 prevents heterodimer polymerization with α-tubulin *in vitro*. Destabilization of tubulin polymerization inside cells leads to cell cycle arrest and prevents mitosis, ultimately leading to activation of apoptosis via caspase-9 and PARP cleavage or through mitotic catastrophe.[17] CA4P is currently in clinical trials against a variety of cancer types with different combinations of chemotherapeutics.[18, 19][20] For example, CA4P has been used in conjunction with carboplatin and paclitaxel to treat platinum resistant ovarian cancer.[21]

1.2 Targeting Cancer

Off-target toxicity persists as a challenge with chemotherapeutics. A promising avenue towards treating cancer involves finding what makes cancer cells unique from healthy cells and how we might target these anomalies. There are a few ways to identify possible cancer-specific molecular targets. One way is to look at the relative abundance of certain proteins in a cancer cell compared to a healthy cell. For example, HER2, a cell surface epidermal growth factor receptor, is overexpressed in aggressive forms of breast cancer and has been targeted by chemotherapeutic agents.[22] A comparable example, folate receptor α (FRα), is overexpressed in epithelial ovarian tumors at a level 10- to 100-fold higher than normal expression.[23] This presents an intriguing target for chemotherapeutics. One application of targeting FRα comes in the imaging of tumors. Gallium 67–chelator complexes have been fused to folic acid to enhance the selectivity of radio-imaging tumors.[24] Many examples of folate targeted therapeutics are found in the literature.[25] Folic acid has been conjugated to protein toxins to inhibit protein synthesis,[26] attached to chemotherapeutics,[27] used for immunotherapies,[28] and conjugated to liposomes[29] and nanoparticles.[30]

Another way to target cancer is to see if mutations in cancer cells result in modified protein function, which ultimately increases proliferative phenotypes. p53, which normally acts as a tumor suppressing protein, is known to be mutated in many types of cancer.[31] p53 can activate DNA repair proteins to repair damaged DNA, arrest cell growth allowing for time for DNA repair, and initiate apoptosis. If one or all of these functions of p53 is altered by a mutation, the result may be a proliferating cell that is unable to regulate DNA repair or initiate cell death. These are some of the main

ingredients in the recipe for cancer. As a result, drugs that target p53 mutants and downstream pathways have been developed.[32]

Lastly, genetic alterations of genes that normally code for two different proteins can join and create fusion-proteins Many fusion-proteins, such as modified tyrosine kinase ROS1, have been shown to drive cellular proliferation.[33] Inhibiting the function of this fusion-protein through use of a small molecule ligand may be a viable approach to targeting cancers expressing this phenotype. For example, Gleevec, also known as Imantinib, is a small molecule inhibitor of BCR-Abl tyrosine kinase that is found exclusively in cancer cells.[34]

In targeting these characteristics of cancer cells we begin to tackle the issue of off-target toxicity through enhancing specificity.

1.3 Light Targeted Chemotherapeutics

Another interesting approach toward the specificity of chemotherapeutics comes through the use of light. There are a variety of ways that light has been used to specifically target cancer cells, but all focus on the idea that a drug or process that is detrimental to a cancer cell will only be activated where irradiated. Perhaps the most common form of light targeted cancer treatment comes with a technique known as photodynamic therapy (PDT).

1.3.1 Photodynamic therapy

Photodynamic therapy (PDT) utilizes a photosensitizer to create reactive oxygen species (ROS) which are toxic to cells (Figure 1.2). Initially, hematoporphyrin, a photosensitizer, was found to fluoresce under ultraviolet light irradiation.[35] In the 1970's hematoporphyrin was used to treat animal tumors as it was found to be preferentially retained in cancer tissue.[36] Since the first clinical trials around this time, a myriad of photosensitizers have been introduced. Some examples of photosensitizers include porfimer (Photofrin®), and Photogem® (Figure 1.3). They work by taking light energy and converting it to ROS through a photosynthetic process that involves the oxygen in the environment of the targeted tissue.[37] Therefore, three pieces are needed for PDT; light, photosensitizers, and oxygen. As the field of PDT has grown, so too have the photosensitizers and methods for delivering light. Because longer wavelength light passes more easily through tissue, photosensitizers that are sensitive to near-IR light, such as lutetium texaphyrin, have emerged.[38]

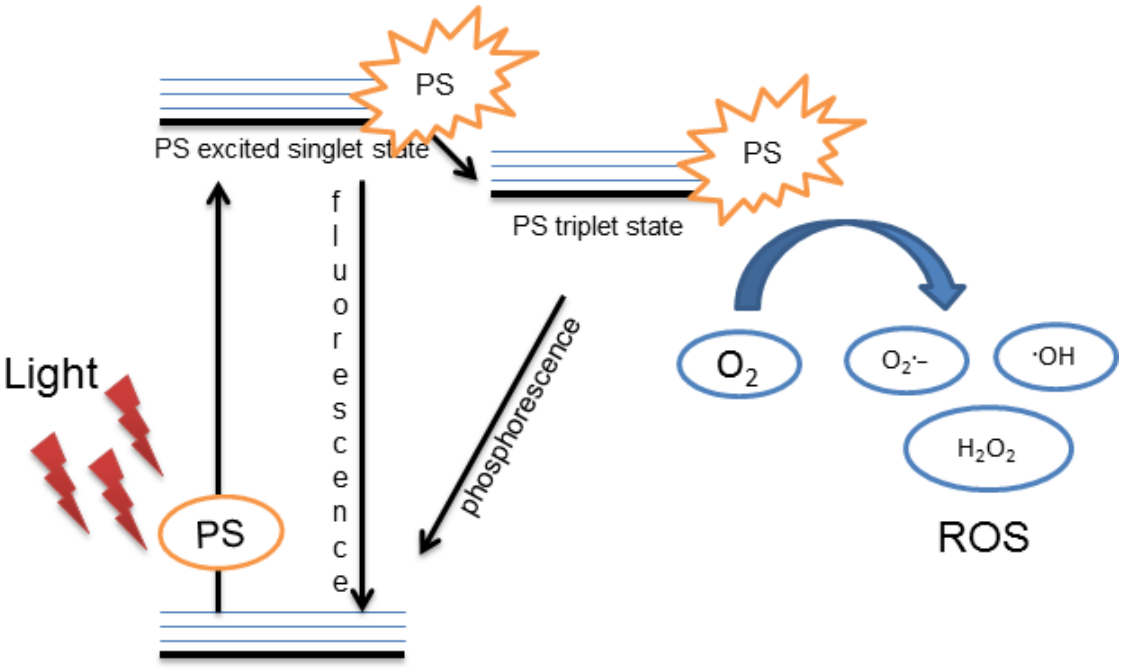

Figure 1.2. Pathway of creating reactive oxygen species through the use of photosensitizers.

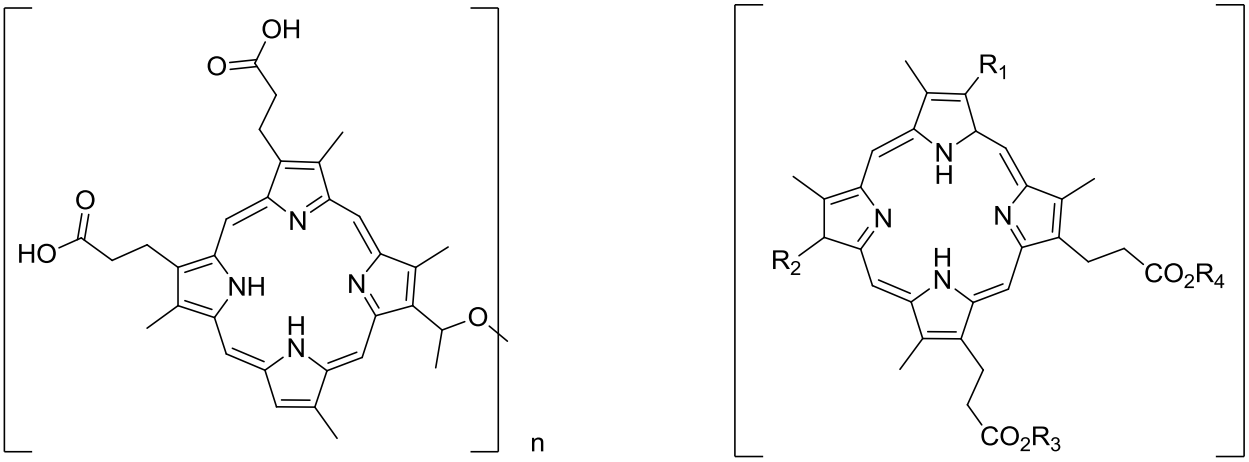

Photofrin

Photogem

Figure 1.3. Structures of clinically approved photosensitizers are shown above exhibiting similar porphyrin backbones.

1.3.2 Limitations of PDT

Photodynamic therapy (PDT) is an attractive way of targeting localized tumors because of its noninvasive nature. However, PDT has several drawbacks in clinical uses. One of the drawbacks is the requirement of an oxygen rich environment to be effective; yet tumors are often hypoxic.[39] In addition to this drawback, many photosensitizers, such as Photofrin®, absorb light in the 630 – 690 nm range.[40] These wavelengths can be absorbed by some of the chromophores found in tissue, such as melanin.[41] To measure treatment effectiveness, researchers define penetration depth of light as the depth where incident light intensity decreases to 37% because of scattering.[42] At 630nm, a wavelength relevant to Photofrin®, 37% of incident light is achieved after only 3-5mm. In addition, scattering of light in the tissue results in lower intensity light and a change in the direction of the light beam. A final drawback of PDT comes from administration of the photosensitizers. Photosensitizers must be allowed to achieve high enough concentrations at the tumor site before irradiation can occur.[43] It can be difficult to determine the best irradiation time as different patients metabolize photosensitizers at different rates. Also, sensitivity to ambient light can become an issue in the weeks and months following treatment.

1.4 Targeting the Acidic Environment of Cancer

Cancer cells, in general, exhibit a lower pH, both intracellularly and extracellularly, when compared to normal cells. Through a process known as the Warburg Effect, cancer cells use utilize glycolysis to produce adenosine triphosphate (ATP), the energy currency of the cell.[7] This aerobic glycolysis results in the production of lactic acid which results in the low pH environment of cancer cells.

Much of the research targeting the acidic phenotype thus far has focused on pH sensitive polymers or micelles that break up and release drugs in a lower pH environment.[44, 45] Early pH sensitive liposomes were constructed in part with a weakly acidic amphiphile which offers stability to a bilayer phase at neutral pH, but become protonated under acidic conditions, which ultimately destabilizes the liposome. An exception to these delivery methods is the pH low insertion peptide (pHLIP).[46] pHLIP is a water soluble peptide at physiological pH. However, under acidic microenvironments the C-terminus of pHLIP forms an alpha-helix and inserts itself in to the lipid bilayers.[47] However, drug delivery with pHLIP is limited as the peptide stays in the lipid bilayer.

The hydrophobicity of the cellular membrane has evolved to protect the cell from exogenous biomolecules. However, certain peptides, similar to pHLIP, are able to overcome this obstacle. Cell penetrating peptides (CPP's) were originally designed around the HIV TAT translocating factor and Antennapedia transcription factor.[48, 49] These peptides have been refined to include only the residues that are responsible for cell permeability, which are largely positively charged and arginine containing. In

chapter 3, we investigate the possibility of pH sensitive versions of CPPs for pH sensitive delivery.

1.5 Dual Targeting Chemotherapeutics

One way to increase specificity for cancer is through the method of dual targeting. The idea of dual targeting introduces a concept of attacking cancer from two different angles to decrease off-target toxicity. Many of the methods for dual targeting have centered on targeting an oncogenic pathway, targeting an overexpressed protein or receptor, or a combination of the two. For example, folic acid has been conjugated to micelles containing doxorubicin.[50] Doxorubicin preferentially targets cancer cells and by loading cancer-specific, folic acid coated micelles with Dox, dual targeting becomes realized. Nanoparticles are easily functionalized and present good scaffold for dual-targeting. For example, Folic acid decorated nanoparticles containing moieties to release Dox in a low pH environment have been developed.[51]

CHAPTER 2. Photoswitchable Anticancer Activity via *trans-cis* Isomerization of a Combretastatin A-4 Analog

I would like to acknowledge Charles E. Lyons and John C. Hackett for their contribution.

Org. Biomol. Chem., 2015, DOI: 10.1039/c5ob02005k.

2.1 Introduction

Off-target toxicity persists as a challenge in the development and improvement of cancer chemotherapeutics. The use of light is one means to target therapy at the tumor site. In photodynamic therapy (PDT), a photosensitizer is employed to create cytotoxic reactive oxygen species (ROS) at a point of irradiation.[52, 53] One of the clinical challenges involving PDT is that hypoxic tumor microenvironments can limit the ability to create sufficient ROS for therapy.[54, 55] As an alternative, researchers have used light to trigger drug activation or drug delivery. Examples include the release of anti-cancer drugs from a negatively charged, cell-impermeable small molecule along with release from cancer-targeting dendrimers, nanoparticles and liposomes.[5, 56-63] Although these methods for targeted drug delivery are promising, in all cases the drug activation is irreversible upon illumination. Very recently, Presa and coworkers have developed Pt(II) complexes with ligands that can be switched between more toxic and less toxic forms depending on the wavelength of light used.[64] One potential problem for the clinical application of each of these light-activated drug systems is that the activated drug can diffuse away from the illuminated site of the tumor, causing unwanted damage to the tissues it encounters. An ideal light-activated drug would automatically revert to a less potent form over time in order to limit this off-target toxicity.

2.2 Combretastatin A-4

Combretastatin A-4 was first extracted from *Combretum Caffrum*, an African Bushwillow tree, and shown to inhibit tubulin polymerization in 1989.[65] CA4 (Figure 2.1) is an anticancer drug that exhibits selective cytotoxicity toward tumor

vasculature.[66, 67] A variety of cancer cells are highly sensitive to CA4 treatment. GI_{50} values are often under 10 nM.[68, 69] A prodrug of CA4 (CA4-phosphate) is currently being tested in clinical trials in combination with existing chemotherapy agents.[70, 71] CA4 contains a cis-stilbene structure (Figure 2.1), which is known to be 60-fold more potent than the trans isomer.[72] We reasoned, therefore, that an analog of CA4 that could reversibly switch from the trans to the cis form with light would have novel photoactivatable properties. Although stilbenes themselves are photoswitchable, this process requires <300 nm UV light which is toxic to cells.[73]

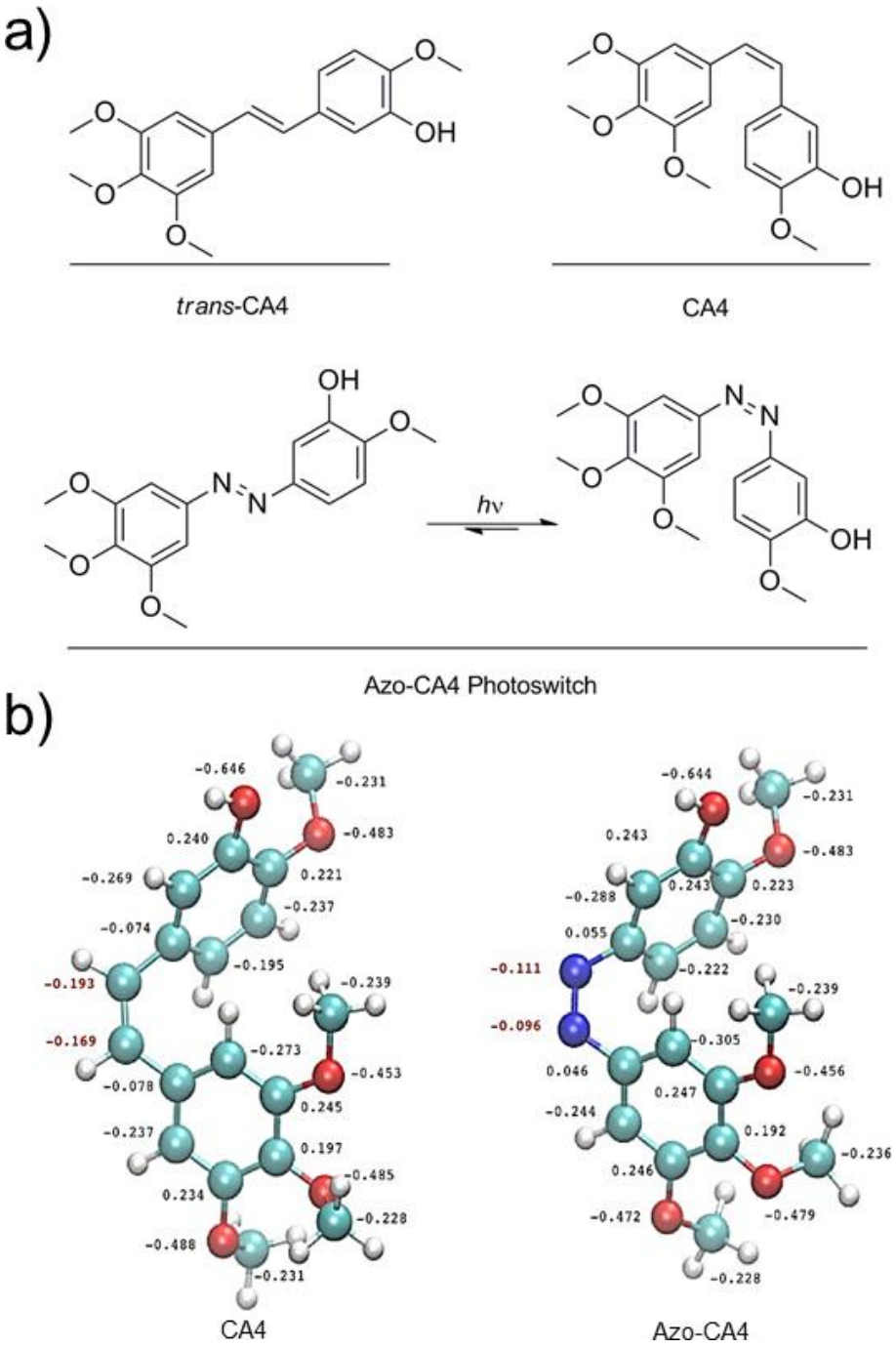

Figure 2.1. a) Design of Azo-CA4, a photoswitchable analog of CA4. b) RI-MP2/def2-TZVP derived[80] electronic structure of CA4 (left) and Azo-CA4 (right). Labeled charges for non-hydrogen atoms were computed using the natural population analysis method. Computational experiments were performed by John C. Hackett.

2.3 Photoswitches and Azobenzene

Azobenzene, a molecule that undergoes *trans-cis* isomerization under irradiation, has a growing number of applications in polymer chemistry,[74] peptide secondary structure,[75] and for controlling drug activation.[76]

2.4 Combretastatin A-4 on an Azobenzene Scaffold

Azobenzenes contain a molecular backbone that resembles the stilbenoid backbone of CA4, with the olefinic carbon atoms replaced with nitrogens (Figure 2.1). Yet, unlike stilbenes, azobenzenes are able to be switched from the trans to cis form with low intensity light that is compatible with cells.[77] Moreover, when irradiation is terminated, the cis form of azobenzenes relaxes back to the thermodynamically stable trans form with a half-life that ranges from milliseconds to hours.[76, 78, 79] In principle, therefore, an azobenzene analog of CA4 (Azo-CA4, Figure 1a) will exhibit the dual properties we desired: enhancement in potency with light and automatic turn-off over time.

To verify that our Azo-CA4 was, indeed, highly similar in structure to CA4, we performed a computational study (Figure 2.1). Both molecules were fully optimized at the RI-MP2/def2-TZVP level of theory and natural population analyses were performed.[80] The optimized geometries are quite similar and the natural charges calculated for non-hydrogen atoms are almost identical with the exception of the nitrogens on the azo bridge.

2.5 Retrosynthetic Analysis of Azo-CA4

To build a combretastatin analog on an azobenzene scaffold, we decided to work on the two aryl substituents separately. In searching the literature, we found a one-step synthesis of asymmetric azobenzenes and discovered the starting materials for this synthesis, 3,4,5-trimethoxyaniline and 2-methoxy-4-nitrophenol, were commercially available.

2.6 Failed Synthetic Routes

2.6.1 Route 1

For our first attempt we tried a one-step synthesis between the nitrophenol and the Trimethoxyaniline (Scheme 2.2).[81] However, no reaction occurred. The proposed mechanism of this reaction is shown (Scheme 2.3).

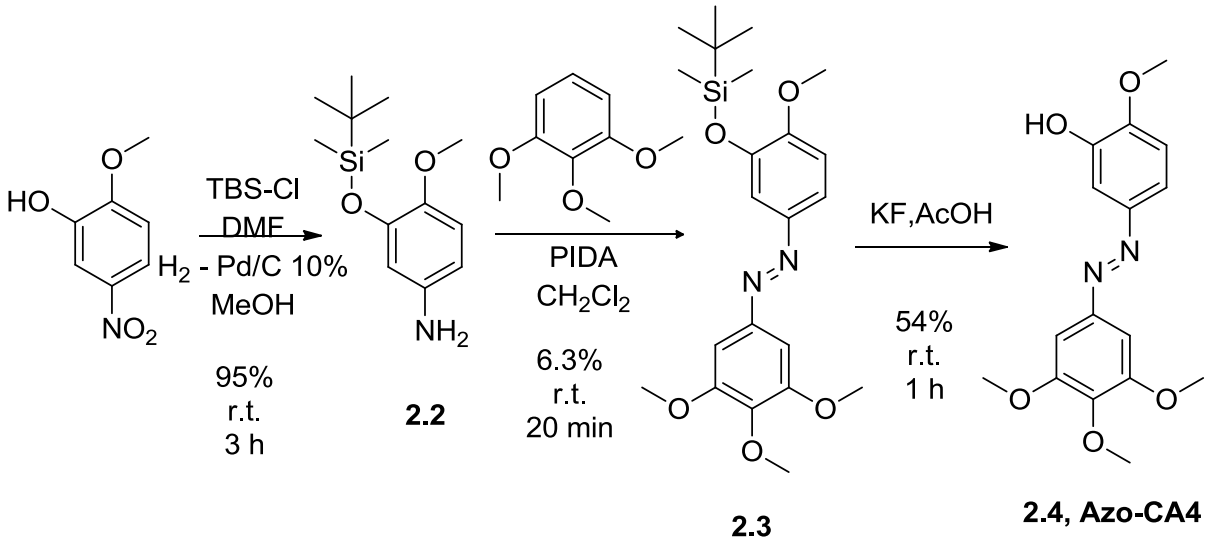

Scheme 2.1: Synthesis of Azo-CA4.

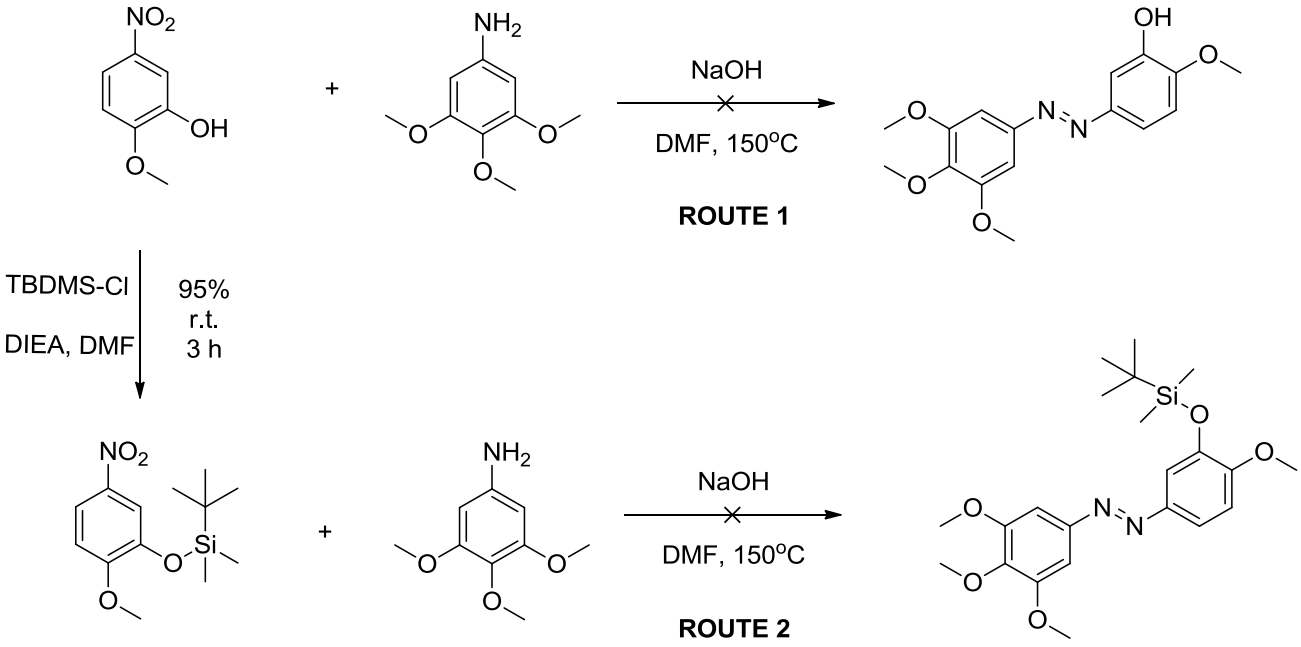

Scheme 2.2. Shown are the failed synthetic schemes for route 1 and route 2.

2.6.2. Route 2

After the failed reaction the first thing that was tried was a microwave assisted synthesis. Similar results were obtained. The literature[81] that we were studying at the time showed poor yields when starting materials were extremely electron-rich, specifically on the nitroaromatic compound. This is consistent with the proposed mechanism (Scheme 2.3) which begins with nucleophilic attack on the aromatic nitro group. "Electron rich," refers to the substituents on the rings besides the nitro moiety. We thought that under the current reaction conditions the phenolic moiety would be deprotonated, making the nitroaromatic compound extremely electron rich. We, therefore, decided to use a silyl protecting group (TBDMS-Cl) to protect the phenolic moiety of the nitroaromatic compound that we could later remove with a fluorine anion (Scheme 2.2). After protection of the phenolic moiety, the coupling step was carried out under similar conditions. No product formation was observed.

We hypothesized that making the nitro aniline more reactive might be an option moving forward. We attempted to convert the amine of trimethoxyaniline to a nitroso group to be reacted with the other half of our molecule. However, reaction of trimethoxyaniline with diphenyl diselenide did not yield nitroso compound. We hypothesize that the nitroso compound was too reactive to be isolated.

2.7 Synthesis of Azo-CA4

To synthesize Azo-CA4 (Scheme 2.1), we first protected the phenolic oxygen of nitroaniline 1 with a TBDMS group to give **2.2**. Compound **2.2** was coupled to 3,4,5-trimethoxyaniline with diacetoxyiodobenzene[82] to yield azobenzene **2.3** which was separable from homo-aniline coupling side products. Finally, **2.3** was deprotected with fluoride ion to yield Azo-CA4, **2.4**.

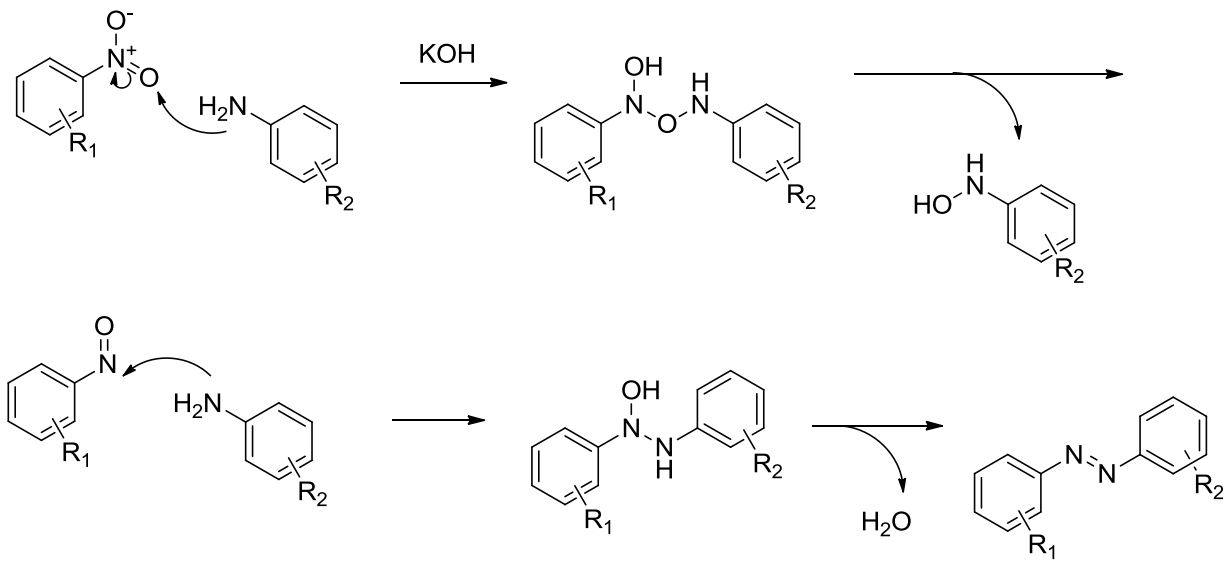

Scheme 2.3. The proposed mechanism of an asymmetric azobenzene formation between nitrophenol and aniline in the presence of strong base.[81]

2.8 Kinetics of Photoswitching and thermal relaxation

The first step in assessing Azo-CA4 was to analyze the kinetics of photoswitching. We analyzed the photoswitching properties of Azo-CA4 (Figure 2.2). The absorbance spectrum of trans azo-CA4 showed a λmax of 379 nm and an extinction coefficient that is in accordance with other electron-rich *trans* azobenzenes (Figures 2.2a, 2.3, and 2.4).[83] After 30 seconds of irradiation with 380 nm light, the compound's absorption pattern had dramatically shifted toward an absorption profile that is characteristic for cis azobenzenes[84, 85] (Figure 2.2a). Over time Azo-CA4 reverted back to the trans form with a half-life of 84 min at 37°C (Figure 2.2b and c, and 2.4). Multiple cycles of switching and relaxation could be performed over 24 h without degradation (Figure 2.2d).

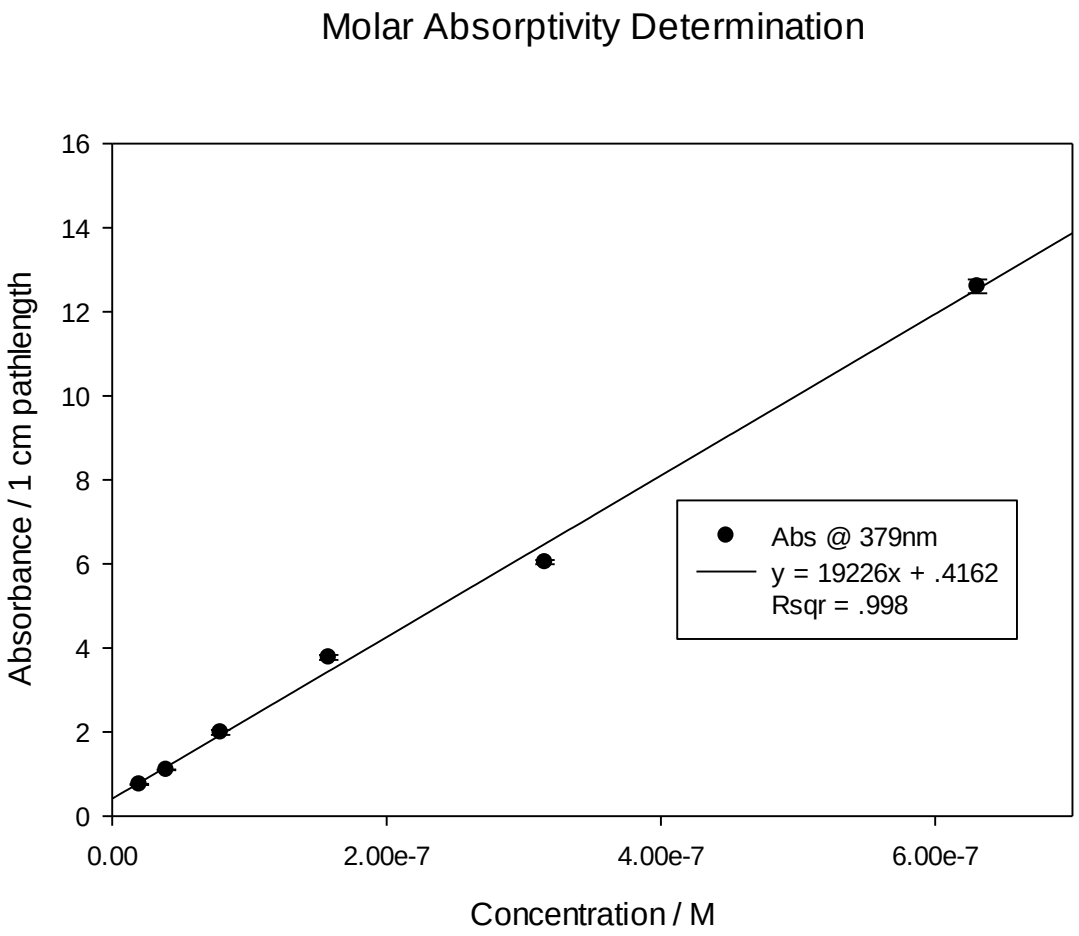

Figure 2.2. Determination of the molar absorptivity of Azo-CA-4 on a NanoDrop spectrophotometer with a 0.1 cm pathlength.

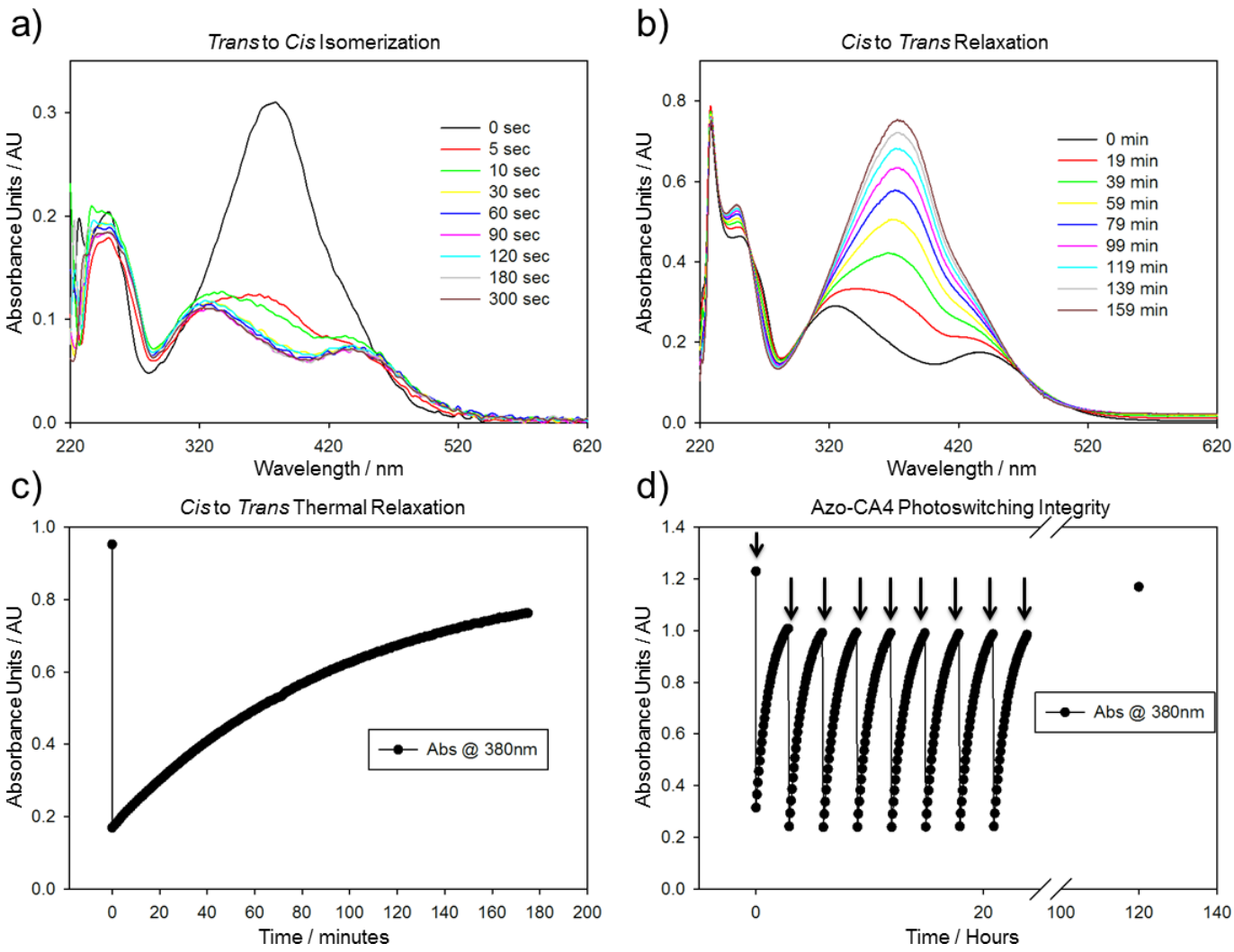

Figure 2.3. Absorption experiments performed on Azo-CA4. a) Absorption spectra of Azo-CA4 (157 μM) after exposure to 380 nm light (4.4 mW/cm^2) for various amounts of time. b) Absorption spectra demonstrating thermal relaxation over time of Azo-CA4 in the dark at 37°C. Prior to placing in the dark, Azo-CA4 was treated for 1 minute with 380 nm light (4.4mW/cm^2). c) Time course of Azo-CA4 relaxation monitored by absorbance at 380 nm. d) Time course of 380 nm absorbance of Azo-CA4 over time. The sample was irradiated with 380nm light (4.4mW/cm^2) for 1 minute every 3 hours at 37°C (arrows). The final point indicates a fully dark-adapted Azo-CA4 left in the dark for 100 hours after the last irradiation.

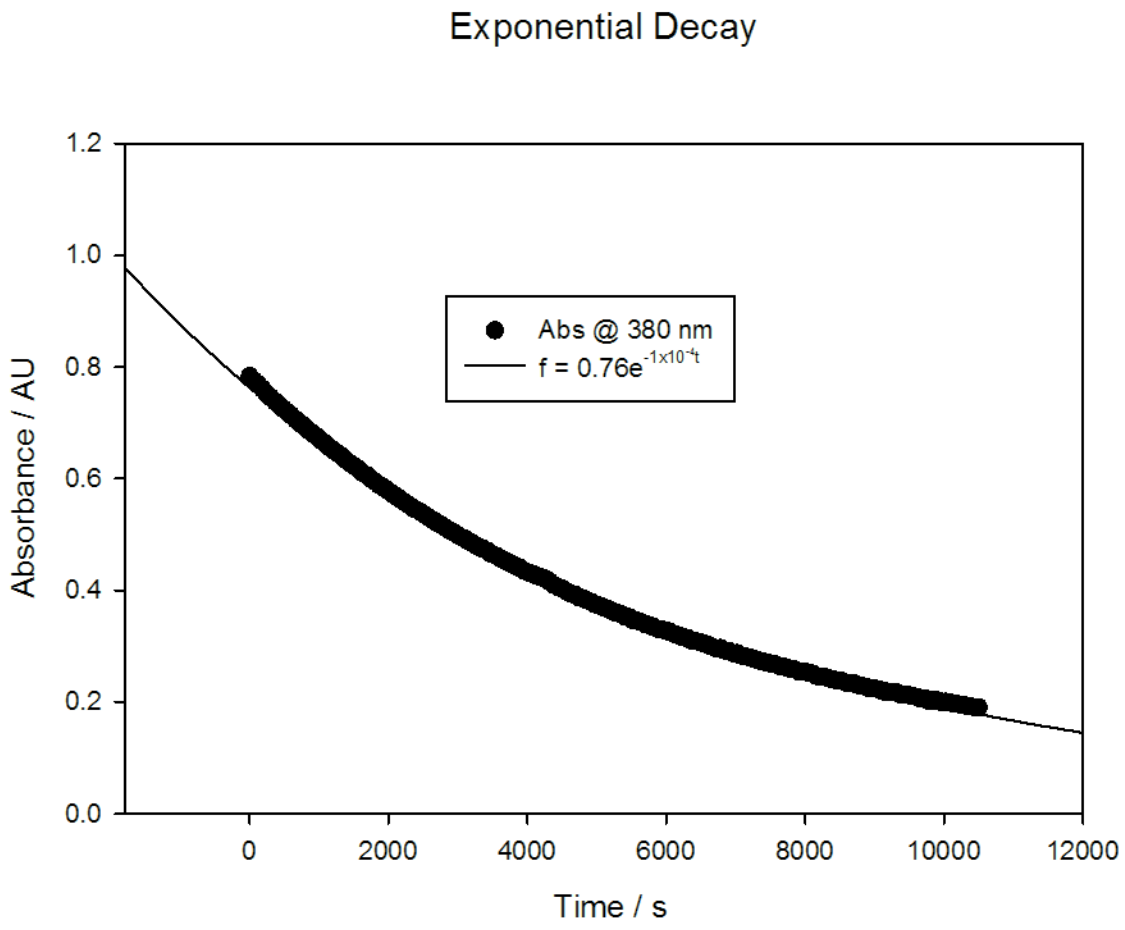

Figure 2.4. Exponential decay of absorbance of Azo-CA4 at 380nm. Azo-CA4 was irradiated with 380nm light for 1 minute. Absorbance readings were taken every 60 seconds for ~3hr and subtracted from the initial absorbance reading.

2.9 Tubulin polymerization assays

The first big test in the possible use of Azo-CA4 as a cancer drug was to test its ability to inhibit tubulin polymerization *in vitro*. We then sought to demonstrate that Azo-CA4 would inhibit tubulin polymerization in a similar manner to CA4 (Figure 2.5 and 2.6). *In vitro* experiments were carried out in the light using a fluorescent tubulin polymerization assay. We sought to show that Azo-CA4 was a more potent inhibitor of tubulin polymerization when irradiated with light. We compared our findings with the same experiments done with a negative vehicle control and combretastatin A4 (Figure 2.6) As expected, in the light, Azo-CA4 was a more potent inhibitor of tubulin polymerization than in the dark; light activated Azo-CA4 had an IC_{50} of 5.1 μM (Figure 2.6), similar to the IC_{50} of CA4 (1.9 μM).[2]

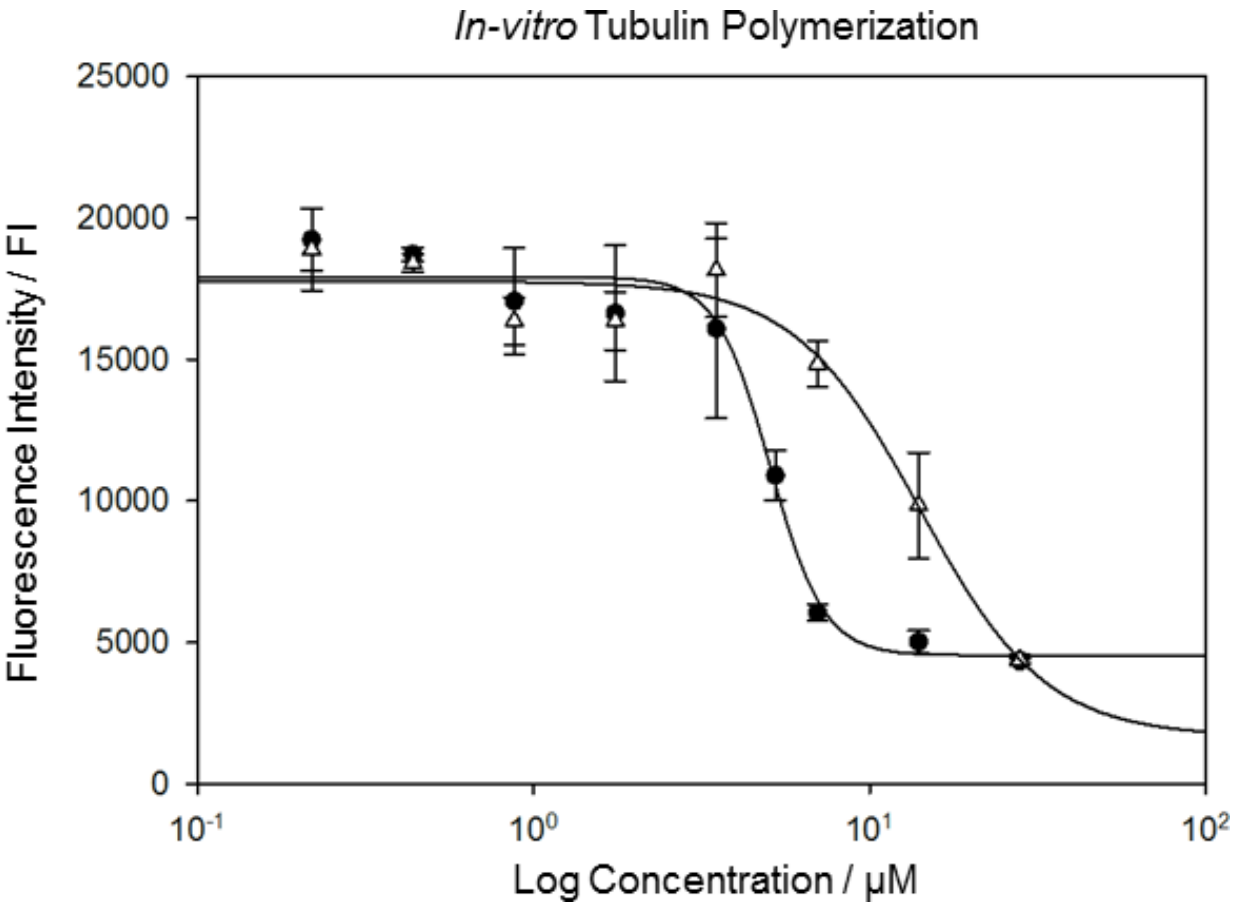

Figure 2.5. *In-vitro* tubulin polymerization inhibition assay. Tubulin fluorescence was monitored every minute for 1 hour. Closed circles represent tubulin containing wells irradiated with light (4.4 mW/cm^2) for 1 min in the presence Azo-CA4 prior to the start of the assay. Open triangles represent tubulin exposed to Azo-CA4 without illumination.

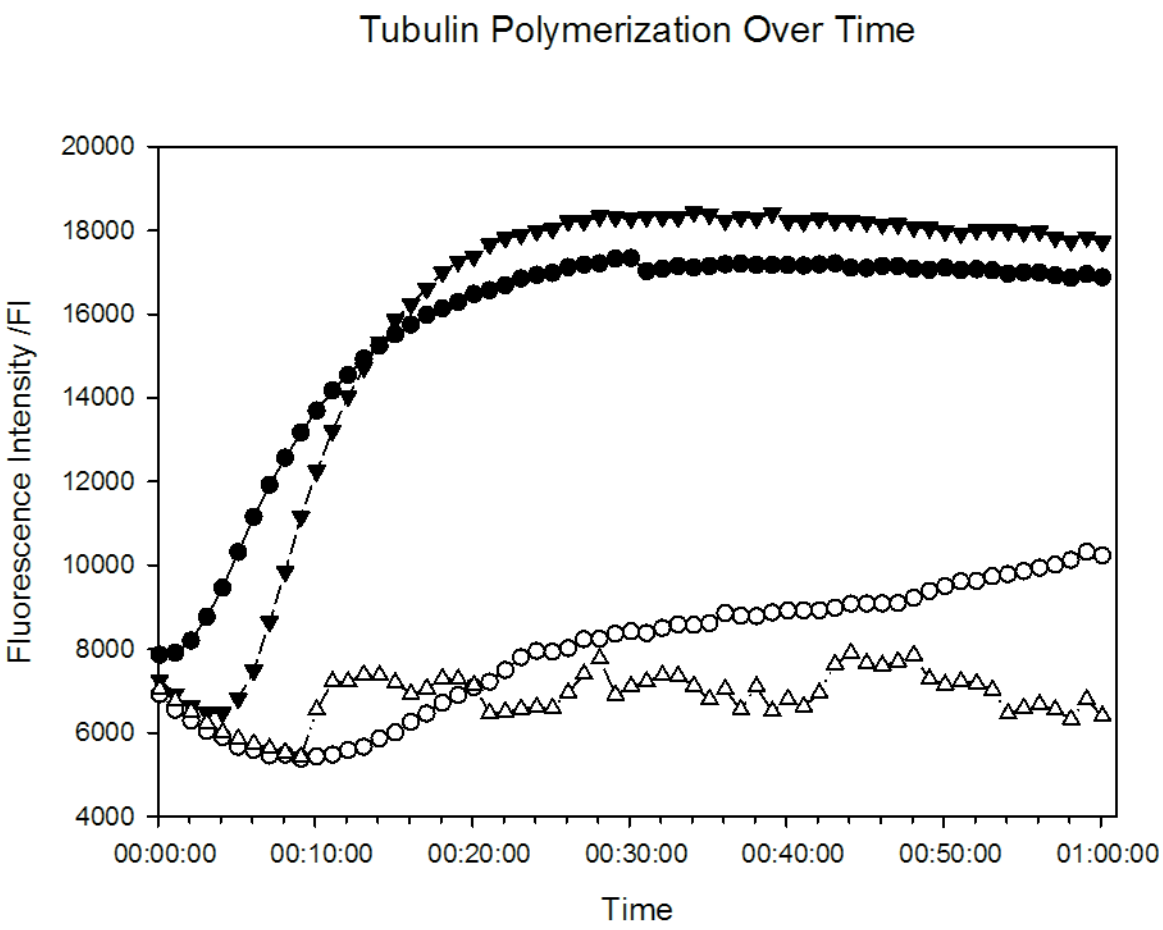

Figure 2.6. Tubulin polymerization represented as fluorescence of a binder of tubulin heterodimer (Cytoskeleton, Inc, CO, USA). Vehicle control (6.2% DMSO in H_2O, closed triangles), Azo-CA4 in the absence of light (20μM, closed circles), Azo-CA4 irradiated with 4.4mW/cm^2 light at 380nm immediately prior to the experiment (20μM, open circles), and CA4 (20μM, open triangles). Experiments were performed in triplicate in a BioTek Synergy H1 Hybrid plate reader.

2.10 Cell viability assays

To investigate if the trend in tubulin polymerization inhibition would translate to potency in living cells, we performed cell viability assays on human umbilical vein endothelial cells (HUVEC), as CA4 is known to be especially potent towards tumor vasculature.[86][87] We also evaluated the effects of Azo-CA4 on a breast adenocarcinoma epithelial cell line (MDA-MB-231) that has shown sensitivity to CA4[88] and was used as a model for cancer. Assays with CA4 itself in these cell lines showed the expected growth inhibitory profile and a GI_{50} in the low nM range, consistent with other reports (Figure 2.7).[3] With Azo-CA4, we observed significant enhancement of growth inhibition in the presence of light vs. untreated controls for both cell lines (Figure 2.8). In HUVEC cells, light treatment led to a 13-fold decrease in the GI_{50} from 9.5 μM to 720 nM (Table 1). In MDA-MB-231 cells, the GI_{50} was 601 nM in the light, a 35-fold enhancement. Light alone at the same dose was not growth inhibitory for either cell line (Figure 2.9). When we increased the interval between light pulses, we observed diminished potency, consistent with the ability of Azo-CA4 to automatically turn off its activity over time (Figure 2.10).

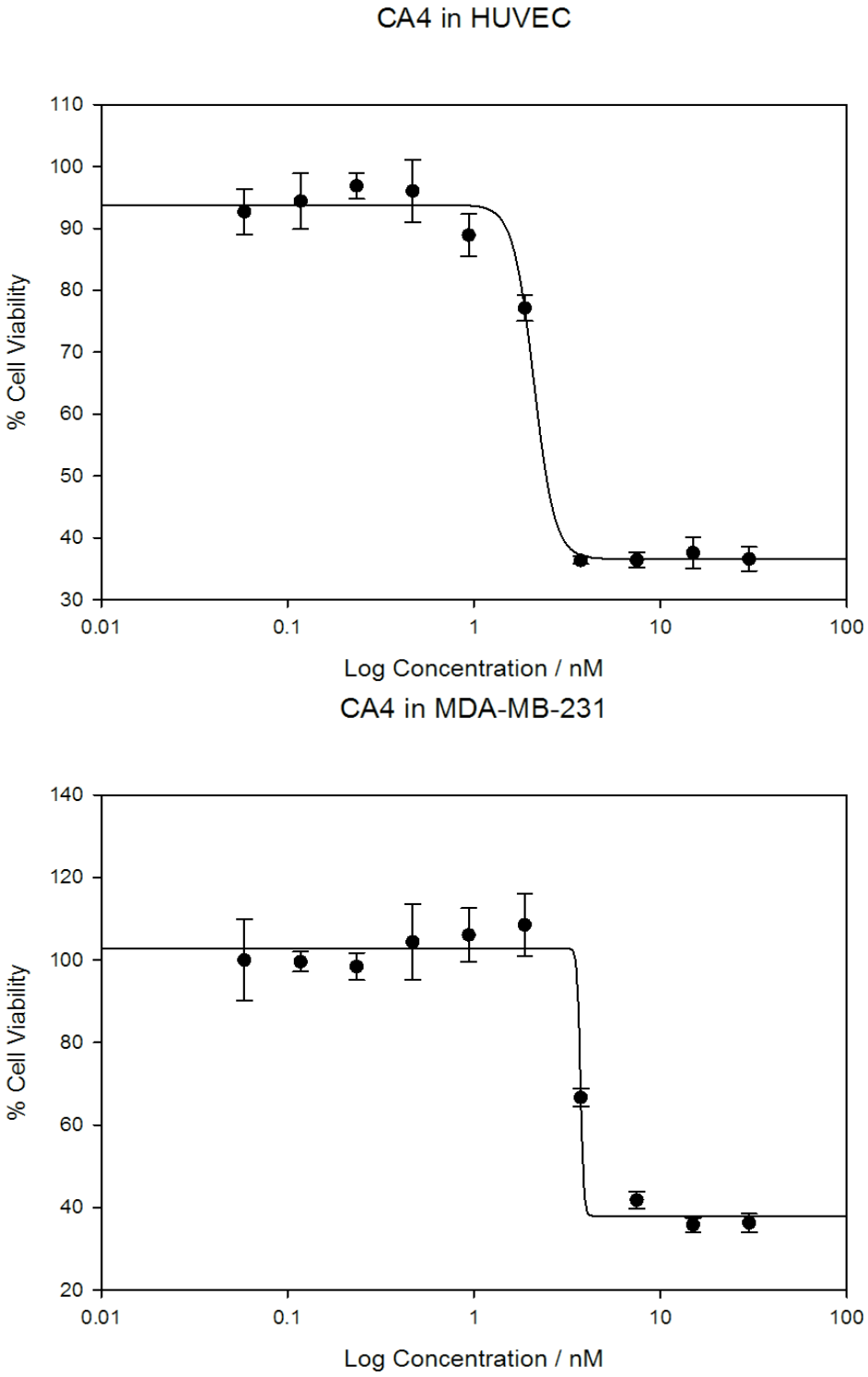

Figure 2.7. Cell viability assays performed using Cell TITER Blue (CTB) fluorescent reagent. HUVECS were seeded at 1500 cells per well (left) and MDA-MB-231 were seeded at 10,000 cells per well (right) for six hours. Combretastatin A4 (Sigma) was added to the wells in concentrations from 30 - 0.06 nM (0.25% DMSO) and incubated at 37°C for 48 hours. At the end of the incubation period 20µL CTB was added to the wells and incubated for an additional 2 hours. Fluorescence was normalized against controls.

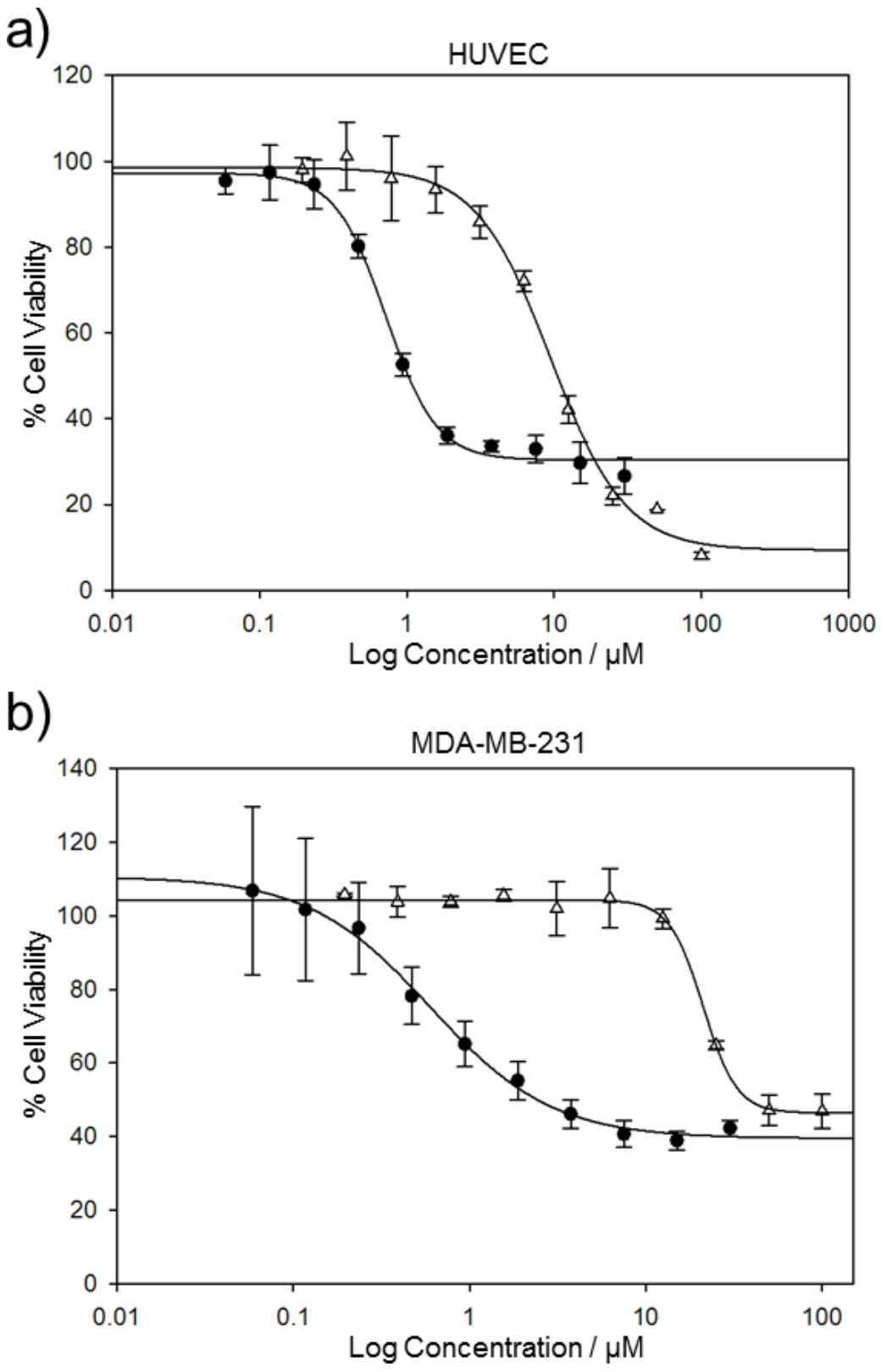

Figure 2.8. Cell viability assays reported as a percentage of vehicle controls. Cells were treated with varying concentrations of Azo-CA4 for 48 hours and were either exposed to 380 nm light (4.4 mW/cm^2) for 1 minute every hour (closed circles) or kept in the dark (open traingles).

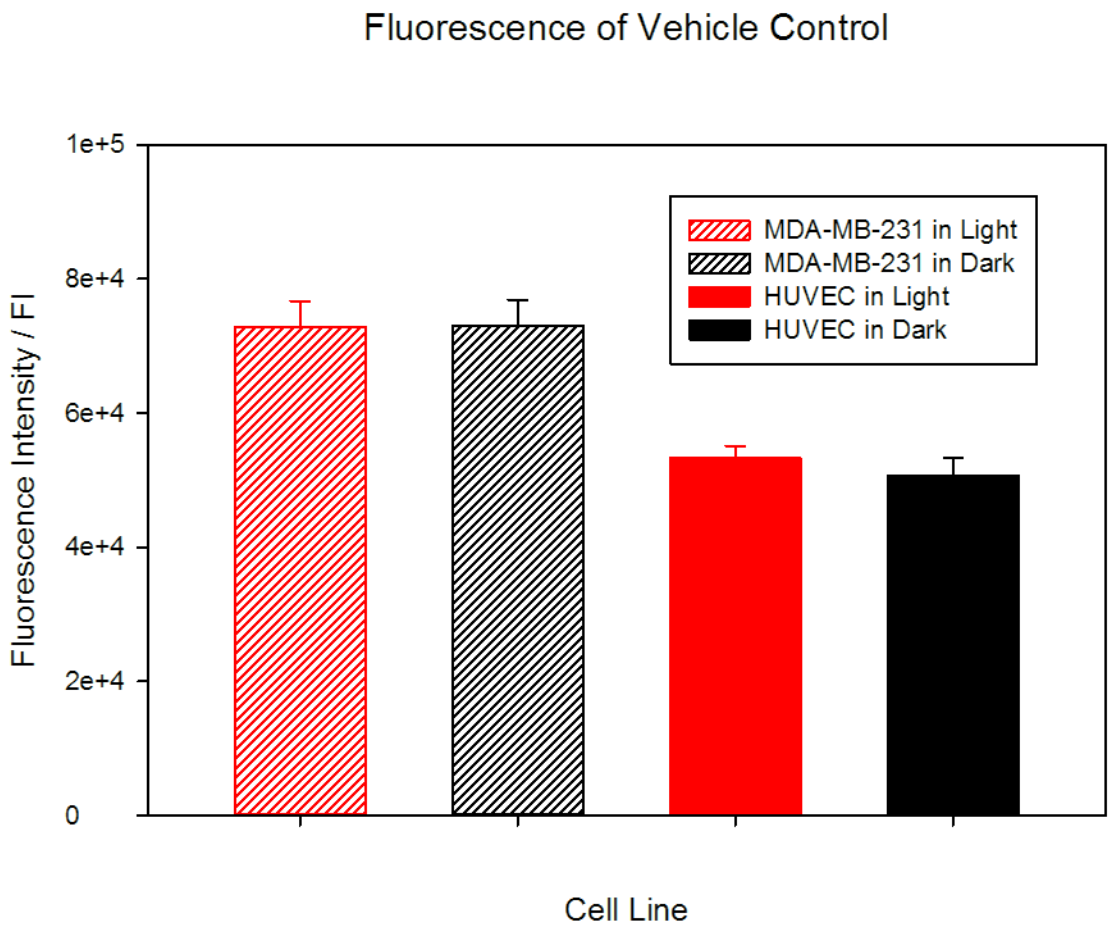

Figure 2.9. Experiments performed to show that light alone is not responsible for cell death. Fluorescence intensity of vehicle control wells after 48 hours of light exposure (1 minute pulse every hour, 4.4mW/cm^2, shown in red) and vehicle control wells kept in the dark (black). At the end of the 48 hour growing period, cells were incubated with CTB for 2 hours and read on the BioTek Hybrid S1 plate reader. Experiments were performed in triplicate.

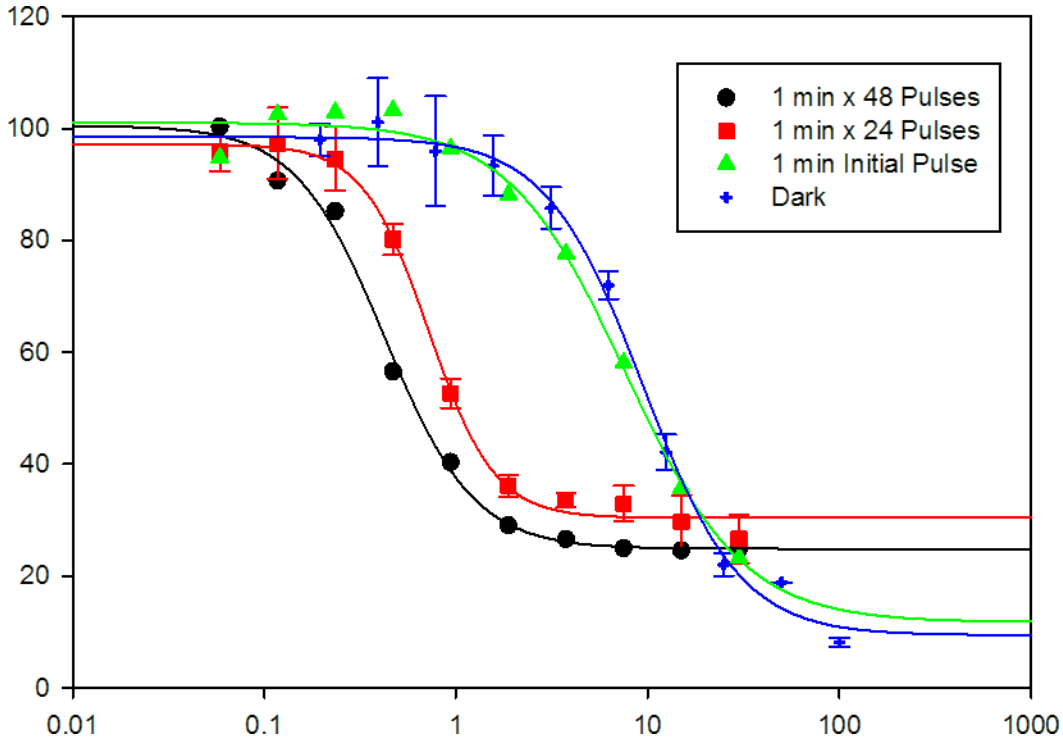

Figure 2.10. Cell viability assays conducted to probe the effects of increasing light dosage. HUVEC were either treated with drugs in 5 replicated wells and shielded from light (black circles) or irradiated with 380nm light (4.4mW/cm^2) for one minute at the beginning of the experiment (green triangles), irradiated for 1 minute every 2 hours (red squares), or irradiated for 1 minute every hour (blue crosses). The GI_{50} values are shown in parentheses in the legend.

2.11 Bladder Cancer Assays

In addition to the HUVEC and MDA-MB-231 cell lines, a third cell line was assayed. A transitional cell carcinoma cell line (T24) was screened against varying concentrations of Azo-CA4. We chose a bladder cancer cell line because the thin nature of the tumors and accesibility of a scope to to irradiate the tumors in a clinical setting. Although there was a clear effect of the drug and an IC_{50} could be determined, cells were surviving at a very high level (~70%) compared to the other cell lines assayed (Figure 2.11). T24 cell lines grew extremely slowly, and the dynamic range of the growth inhibitory assay was therefore diminshed.

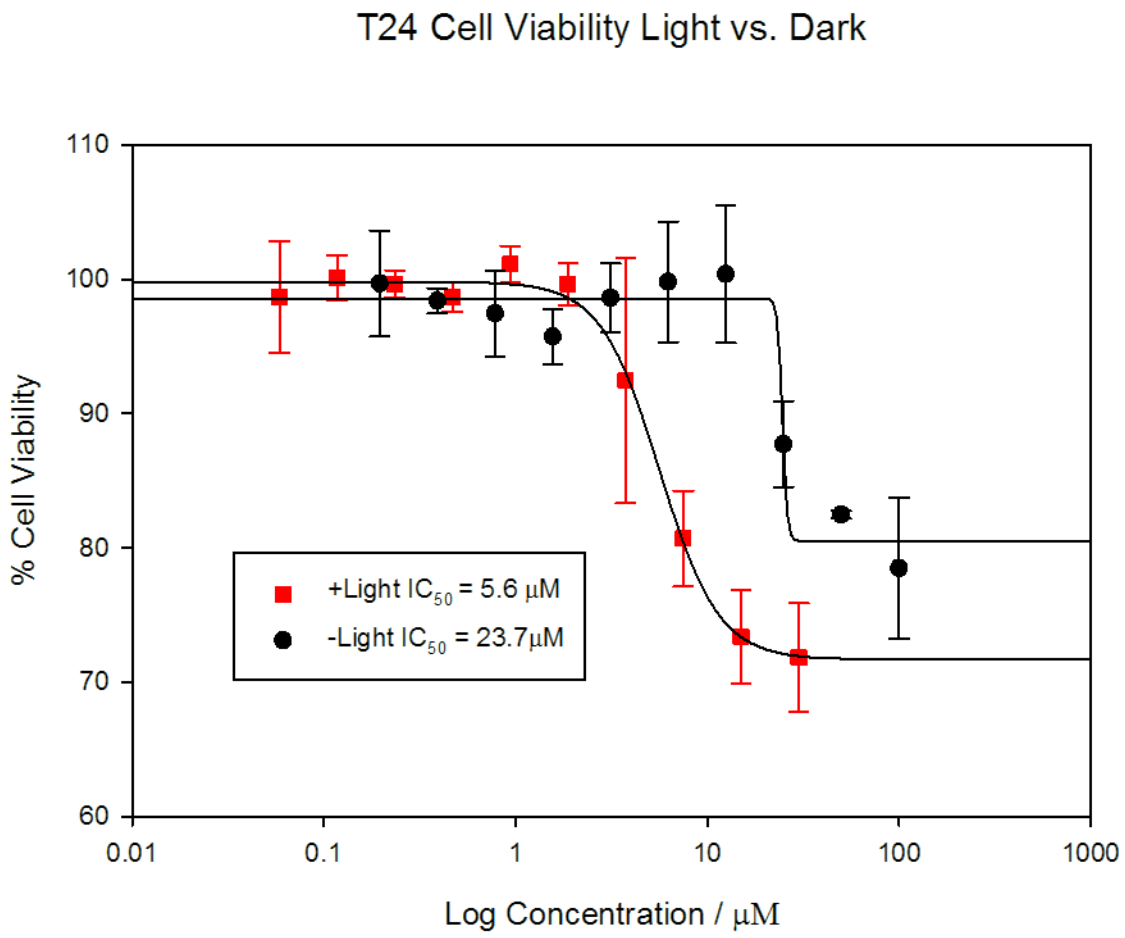

Figure 2.11. Cell viability assays reported as a percentage of vehicle controls. Cells were treated with varying concentrations of Azo-CA4 for 48 hours and were either exposed to 380 nm light (4.4 mW/cm^2) for 1 minute every hour (red square) or kept in the dark (black circles).

2.12 Glutathione Reduction Assays

The significant gap between the cytotoxicity of CA4 and Azo-CA4 in these cell lines suggested that Azo-CA4 may be unstable. Since azobenzenes are known to react with glutathione (GSH),[89, 90] we evaluated the extent to which GSH could inactivate Azo-CA4 (Figure 4). Both forms of Azo-CA4 were degraded by GSH over the course of several hours. Interestingly, the light-activated *cis*-Azo-CA4 compounds were degraded more rapidly than *trans*-Azo-CA4 (Figure 2.12).

To investigate this further, we treated our compound with light and GSH and followed the course of the reaction by LC-MS/MS (Figure 2.13 and Figure 2.14). As expected, the peak corresponding to the *cis*-Azo-CA4 decreased over time (Figure 2.13). Surprisingly, a new peak of the same mass was formed during the reaction. This peak did not co-elute with *trans*-Azo-CA4 (Figure 2.13), and therefore must be due to a rearrangement product or products. (Note also that the samples were irradiated with light immediately prior to injection which would have eliminated the majority of the *trans* isomer even if was present beforehand). Additionally, transient formation of a peak of 624 Da was observed during the reaction. The MS-MS fragmentation of this peak showed neutral loss peaks of 307, 275, and 129, all of which are characteristic for GSH adducts (Figure 2.15).[91] The 624 peak was not present in a control reaction lacking Azo-CA4 (Figure 2.16), lending credence to the fact that this species is an adduct of glutathione and Azo-CA4.

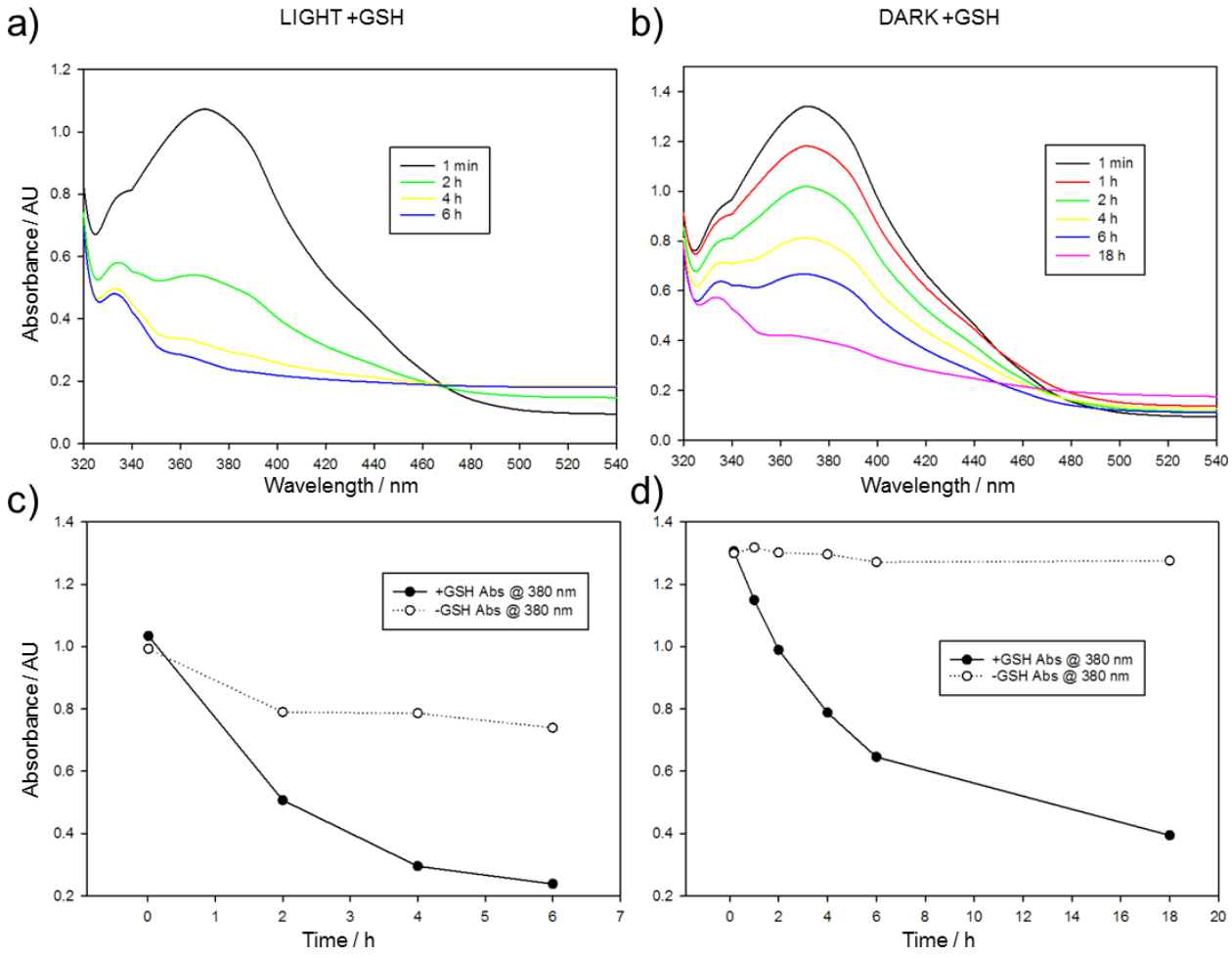

Figure 2.12. Glutathione exposure in light. Azo-CA4 (300 μM in 5.7% DMSO / PBS pH 7.2) in the presence of fully reduced glutathione (10 mM in PBS pH 7.2) and TCEP (5 mM in PBS pH 7.2) was placed in 3 separate wells (100 μL / well) of a 96 well plate at 37°C and (a) exposed to light (380 nm, 4.4 mW/cm^2) for 1 min every 2 h. Absorbance spectra were taken at different time points directly preceding exposure to light and are expressed as an average of triplicate readings. (b) is identical to (a) except the reaction was kept in the dark, and the Azo-CA4 concentration was 400 μM. (c) and (d) plot the change absorbance of 380 nm over time of the data in (a) and (b) compared to identical reactions lacking glutathione. The decrease in absorbance of the minus GSH control in (c) is due to incomplete relaxation back to the *trans* state.

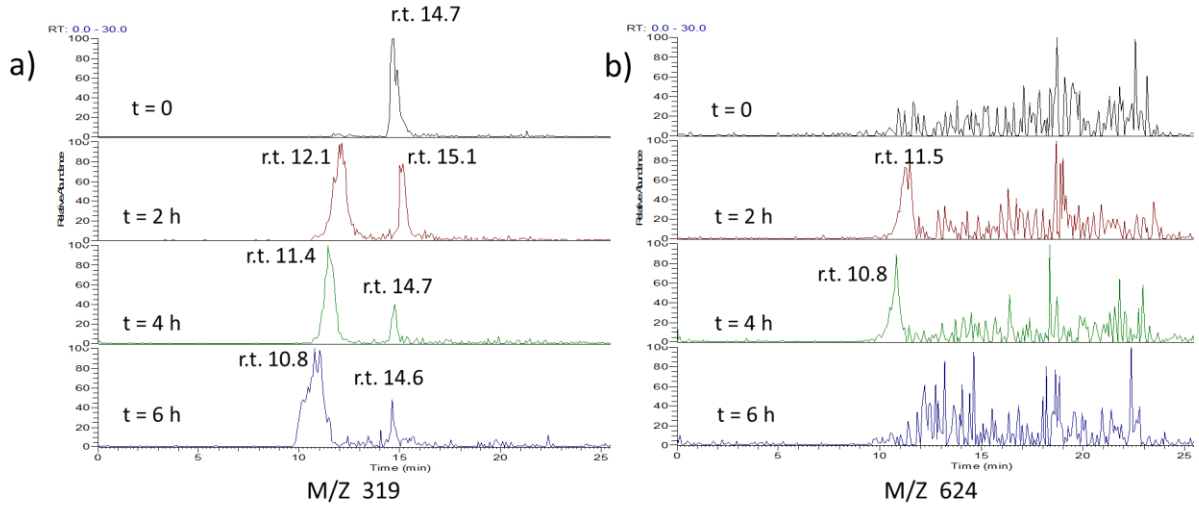

Figure 2.13. Azo-CA4 (300 μM in 5.7% DMSO / PBS pH 7.2) in the presence of fully reduced glutathione (10 mM in PBS pH 7.2) and TCEP (5 mM in PBS pH 7.2) was placed in 3 separate wells (100 μL / well) of a 96 well plate at 37°C and exposed to light (380 nm, 4.4 mW/cm^2) for 1 min every 2 h immediately preceding analysis. At the times given, a sample was removed and injected onto an analytical column containing 5um phenyl C-18 YMC and analyzed by ESI-MS. (a) Traces for ions of M+H identical to Azo-CA4 (319 Da). (b) Traces corresponding to M/Z of 624 Da. Slight retention time drifts are expected due to manual loading of the capillary containing sample onto the instrument.

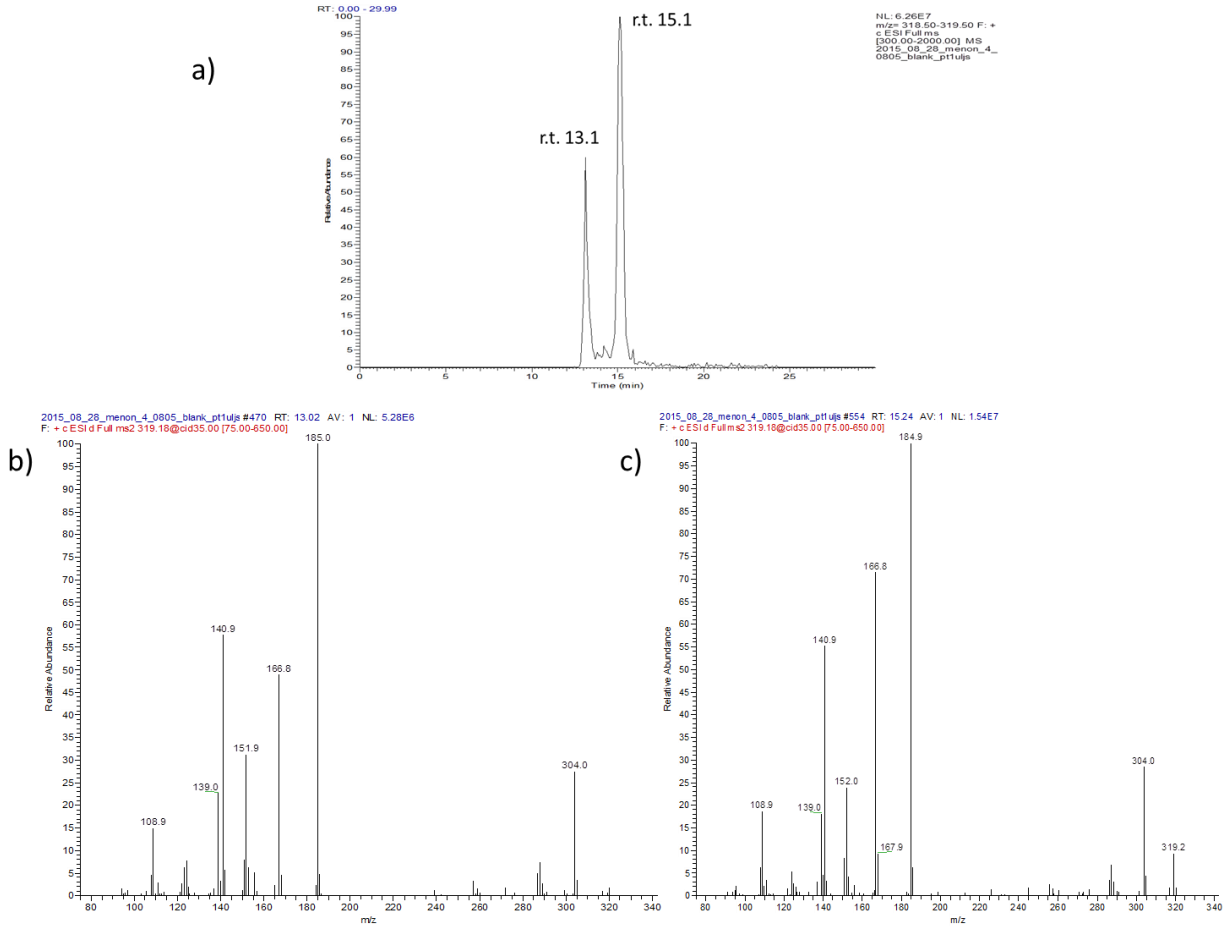

Figure 2.14. (a) LC-MS chromatogram of a mixture of *cis* and *trans* Azo-CA4. Peaks of corresponding to a mass of 319 Da are shown. Based on comparisons with other LC-MS experiments, the *trans* isomer has a retention time of 13.1 and the *cis* isomer has a retention time of 15.1. (b) MS/MS spectrum of the 319 Da peak with retention time of 13.1 min. (c) MS/MS spectrum of the 319 Da peak with retention time of 15.1 min.

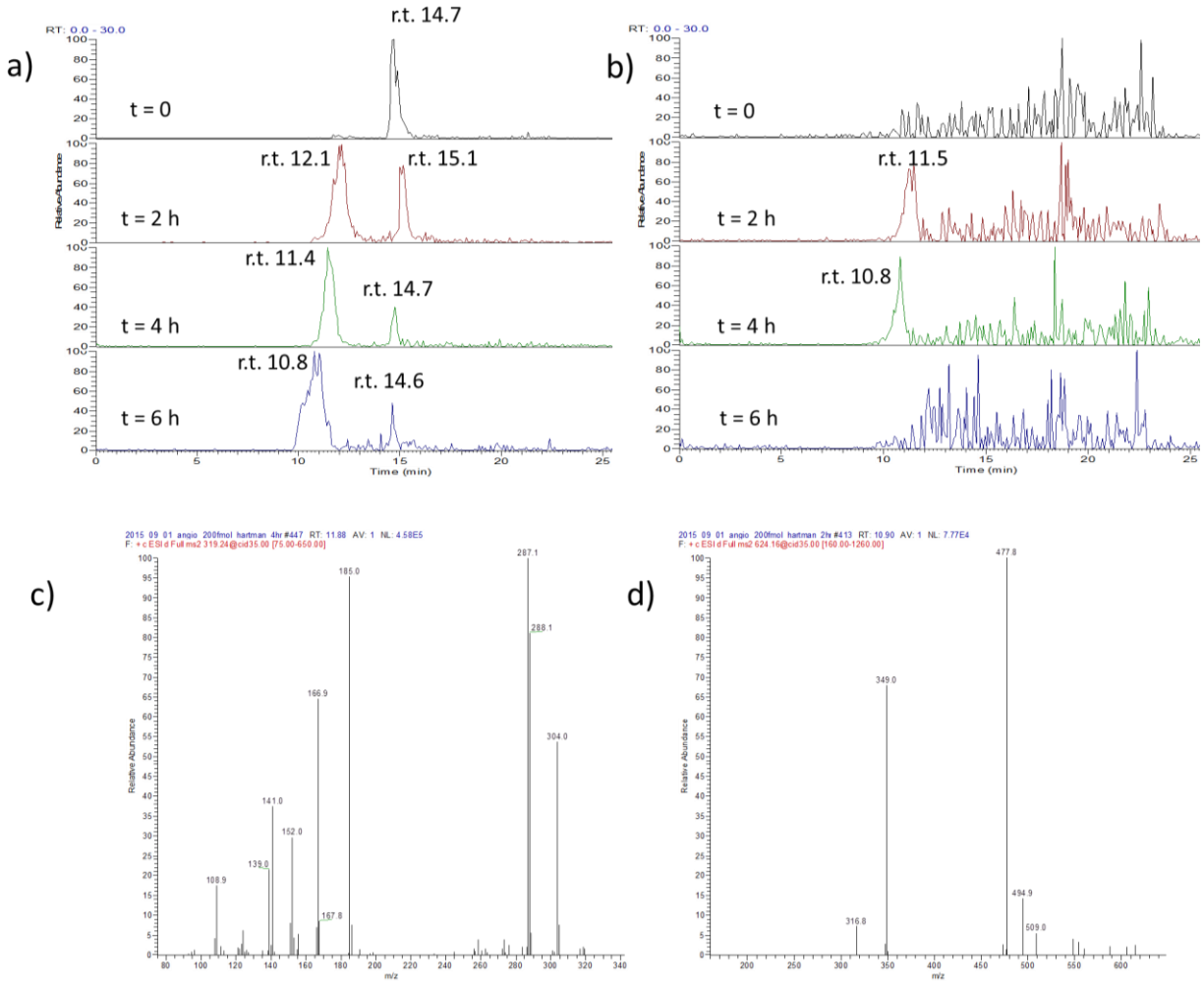

Figure 2.15. (a) and (b) repeated from Figure 2.14 above and highlight the 319 and 614 Da peaks respectively. (c) MS/MS spectrum of the 319 Da peak sampled at 11.88 min (t = 4 h). (c) MS/MS spectrum of the 624 Da peak sampled at 10.90 min (t = 2 h). Peaks at 317 (neutral loss of 307), 349 (neutral loss of 275), and 495 (neutral loss of 129) are all characteristic for glutathione adducts.

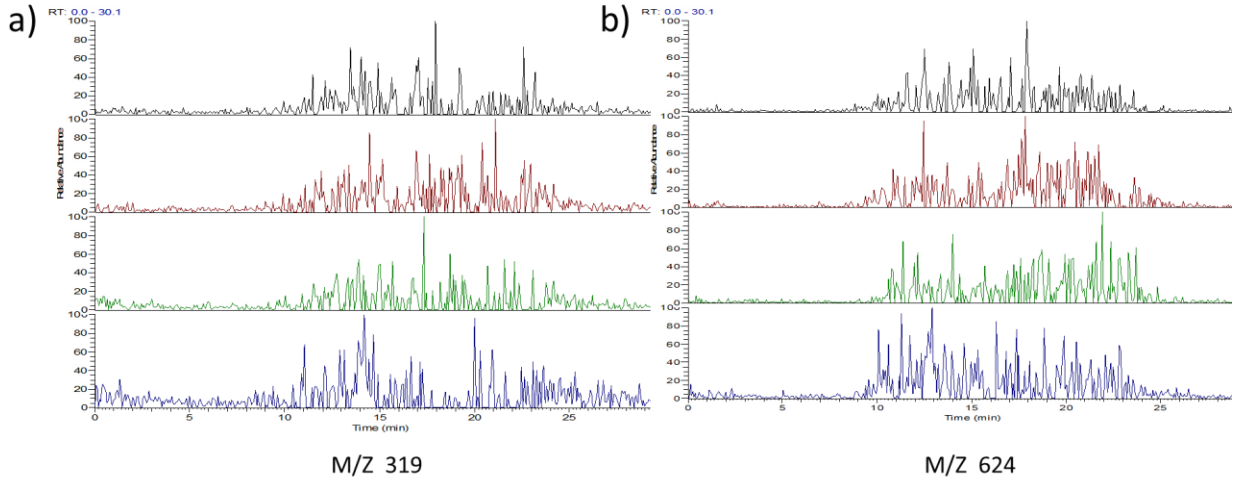

Figure 2.16. Evidence that the 319 and 624 Da peaks require Azo-CA4. Reactions were identical to those described in Figure 5, except they lacked Azo-CA4. No significant peaks at 319 or 624 nm were observed.

2.13 Discussion

During he preparation of our manuscript Borowiak et. al.[92] Published a paper in which Azo-CA4 was synthesized and assayed in a similar manner to the work we had done. It was necessary for us to differentiate our work from Borowiak so we began to focus on an explanation for diminishing activity of Azo-CA4 over time in cells. Shortly after shifting our focus, a second publication focusing on the synthesis of Azo-CA4 was released.[93]

The half-life of thermal reversion of Azo-CA4 and its future analogs is a critical piece of their potential use as automatic turn-off drugs and tools.[94] It is therefore significant that our values for the half-lives of Azo-CA4 vary significantly from those determined by Borowiak et. al. under the same conditions; our value is about 14-fold longer (85 min vs. 6.2 min).[95] Although in cells the half-life of Azo-CA4 can be altered by thiols, the cellular environment,[94] and by tubulin binding itself, all of our cell culture data supports the longer half-life value. For example, our measured EC_{50} values for Azo-CA4 with MDA-231 cells are very similar to those determined by Borowiak et. al. on this cell line,[95] yet we pulsed with light once per hour, and they pulsed every 15 seconds. If the half-life was 6.2 minutes as reported,[95] we should have observed significantly weaker potency with our pulse regimen.

Glutathione reactions with azobenzenes have been studied on a number of systems. For most azobenzenes, nucleophilic attack of GS^- anion on the diazo nitrogen gives the intermediate sulfenylhydrazide[96] (Figure 2.17). The sulfenyl hydrazide is then either attacked by a second glutathione anion to displace the reduced hydrazide or is hydrolyzed by water to give back the azobenzene plus a sulfenic acid (Figure 2.17).

The hydrazide is easily oxidized back to the azobenzene, and therefore, the net result of each of these reactions is re-formation of the original *trans*-azobenzene. By a similar mechanism, glutathione catalyzes the relaxation of *cis*-azobenzenes back into their *trans* form.[94, 97] With Azo-CA4; however, our data shows that reaction with glutathione leads to the destruction of the azobenzene structure. This has been observed before by Woolley with other electron rich methoxy-substituted azobenzenes.[88-90] Woolley proposed that the enhanced basicity of the electron rich azo nitrogens leads to protonation which primes the compound for nucleophilic attack by GSH. However, this proposed mechanism leads to the production of the same sulfenyl hydrazide (Figure 2.17) that would be expected to result in reversion back to the azobenzene. We measured the pKa of Azo-CA4, and it is below 4.6 (Figure 2.18), so it will not be protonated at physiological pH. Moreover, we did not see any ions corresponding either to the mass of the phenylhydrazide or the sulfenylhydrazide during the course of the reaction. Instead, our LC-MS data shows that a transient adduct of Azo-CA4 and GSH with a mass of 624 is formed during the GSH reaction. This mass is two less than would be expected for the sulfenyl hydrazide. The formation of this 624 Da species could potentially be explained by nucleophilic attack of the azo nitrogen onto GSSG to form the sulfenyl diazo cation. To test this, we incubated Azo-CA4 with GSSG, but no reaction was observed over 18 h (data not shown) which rules out this potential mechanism. One could envision other possibilities for formation of the sulfenyl diazo cation, or loss of the two hydrogens via a mechanism involving electrocyclization of the two rings. More work needs to be done to distinguish between these and other possibilities. Importantly, to our knowledge, this type of degradation has only been

observed with electron-rich azobenzenes, which suggests that addition of electron withdrawing substituents would eliminate or slow the degradation pathway.

In summary, Azo-CA4 exhibits remarkable enhancements in potency against HUVEC cells that are consistent with its ability to switch into the more toxic *cis* form in the presence of light. Moreover, over time, Azo-CA4 automatically converts back to its less toxic form. Provided the glutathione reactivity issue can be solved, Azo-CA4 and future, similar compounds offer the potential for automatic turn-off of drug activity in sites distal from the site of activation and thus present a novel means for tightly controlling drug potency and antitumor activity.

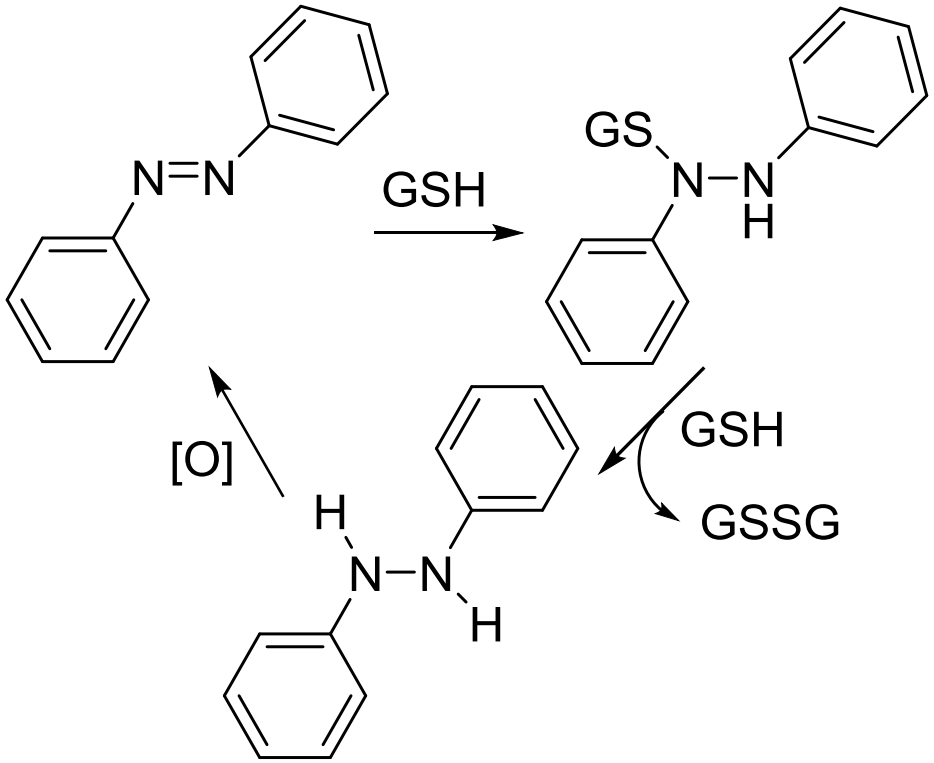

Figure 2.17. Reactions of azobenzenes with glutathione. Reported reaction cycle of azobenzenes with glutathione.

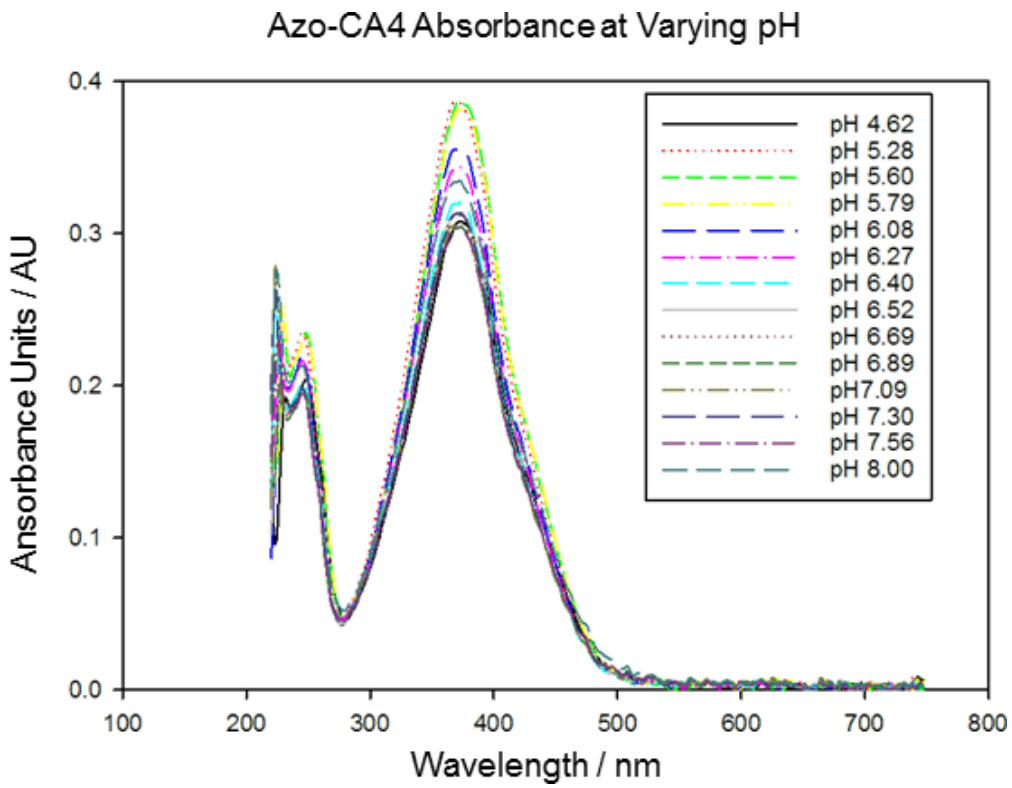

Figure 2.18. Absorbance of Azo-CA4 at different pH values. Absorbance spectra from 200-700 nm at different pH values (left). Absorbance spectra at 380 nm versus pH (right). All experiments were done in duplicate.

2.14 Experimental Section

All reagents and solvents were purchased from Sigma-Aldrich, VWR, or Fisher Scientific. Reagents for cellular assays were purchased from ATCC, Invitrogen-Gibco, or VWR. Tubulin polymerization assay kit was purchased from Cytoskeleton Inc. ^{1}H NMR spectra and ^{13}C spectra were recorded at room temperature on a Bruker 400 MHz Ultrashield Plus. Proton and Carbon chemical shifts are expressed in parts per million (ppm, δ scale) and are referenced to the solvent peak. UV-Vis experiments were carried out on either NanoDrop ND-1000 Agilent 8453 UV/Vis. Cell Titer Blue (CTB) fluorescence was measured on BioTek Synergy H1 Hybrid plate reader. Samples were loaded on a self-packed fused silica (Polymicro Technologies) trap column (360 micron o.d. X 100 micron i.d.) with a Kasil frit packed with 5-15 micron irregular phenyl C-18 YMC packing. The trap column was connected to an analytical column (360 micron o.d. X 50 micron i.d.) with a fritted tip at 5 micron or less (New Objective) packed with 5um phenyl C-18 YMC packing. Peptides were trapped and then eluted into a Thermo Finnigan LCQ deca XP max mass spectrometer with an acetonitrile gradient from 0 % to 80 % over one hour at a flow rate of between 50-150 nl/minute.

UV Lamp Specifications

The UV lamp used in all studies consisted of a simple aquarium light fixture containing two Philips PL-S 9W/2P BLB bulbs. Light was shined, in all experiments, at a consistent distance of 5 cm from the top of plate and was measured to be 4.4mW/cm^2.

UV-Vis Absorption Spectroscopy experiments:

Molar extinction coefficient determination. A 3.14 mM stock solution of Azo-CA4 was prepared in 23% DMSO in water. The solution was stirred vigorously and kept in the dark. 400 µL of the solution was placed in the each of three tubes and diluted to 1 mL with water to give a final concentration of 1.26 mM Azo-CA4. 2-fold serial dilutions were made and the absorption of each solution was measured on a NanoDrop ND-1000 spectrophotometer. The molar absorptivity, based on three independent trials, was found to be 19,150 $L * mol^{-1} * cm^{-1}$.

Half-Life of thermal relaxation determination. A 2 mL solution of 49.8 µM Azo-CA4 was prepared in 0.25% DMSO in water. An initial absorbance reading was taken before the solution was exposed to light. The cuvette was illuminated for 1 min and the absorbance (380 nm) was measured every minute for 175 minutes thereafter. Each reading was subtracted from the initial reading, and the resulting data was fit an exponential decay algorithm.

Azo-CA4 photoswitching integrity assay. A 63.7 µM solution of Azo-CA4 in DMSO was placed in a cuvette in an Agilent 8453 UV/VIS at 37°C for 23 hours. The sample was illuminated for 1 min every 3 hours and the absorbance was measured every 5 minutes.

pH sensitivity experiments. A 183 µM solution of Azo-CA4 in 3.2% DMSO in 50 mM phosphate buffer (pH 8.0) was prepared. The absorption spectrum and pH were measured after multiple additions of concentrated HCl.

Glutathione reduction assay. Azo-CA4 (1.05mM) was incubated in the presence of Glutathione (GSH, 10mM) and Tris(2-carboxyethyl)phosphine hydrochloride (TCEP, 5mM in 9.5% DMSO in PBS. Azo-CA4 samples were exposed to light for 1 minute every hour for 20 hours or were kept in the dark. Absorption spectra were taken at various time points on a NanoDrop. All experiments were done in triplicate.

***In-vitro* Tubulin Polymerization.** A fluorescence *In*-vitro tubulin polymerization assays using porcine tubulin were conducted using a fluorescence based polymerization assay kit (Cat. #BK011P; Cytoskeleton, Denver, CO) and following the manufacturers protocol. A 96 well plate was warmed to 37°C for 30 min prior to beginning the experiment. Tubulin polymerization buffer was prepared at 4°C by mixing 750 µL General Tubulin Buffer (80 nM PIPES ph 6.9, 2mM $MgCl_2$, 0.5 mM EGTA as final concentrations) with 250 µL Tubulin Glycerol Buffer (15% glycerol in General Tubulin Buffer at final concentration), and 10 µL GTP stock (1 mM final concentration). 500 µL of Tubulin Polymerization buffer was warmed to room temperature and one 200 µL tubulin vial was thawed for 1 min in a water bath and then placed on ice. Tubulin was mixed with 420 µL of tubulin polymerization buffer and placed in each of five wells contains drug and control.

Each assay was exposed to varying concentrations of Azo-CA4 (80 µM - 800 nM) prepared in tubulin polymerization buffer. Samples were either exposed to light (380 nm, irradiated for 1 minute) or kept in the dark. Irradiated samples of Azo-CA4 were added to tubulin containing wells directly after exposure to light. Azo-CA4

samples kept in the dark were added at the same time and the kinetic assay was started immediately and proceeded for 1 hour at 37°C (Ex. 350nm, Em. 435nm). IC_{50} values were calculated as a percentage of assays lacking Azo-CA4 by fitting the points to the four parameter logistic equation using SigmaPlot software.

Cell culture experiments:

Cell lines and culture conditions. The HUVEC line was cultured in the recommended BASAL media supplemented with VEGF growth factors, 5% Fetal Bovine Serum (FBS, Life Technologies), 2% L-glutamine and 1% of a 10,000 Units/mL Penicillin and 10,000 µg/mL Streptomycin solution. The MDA-MB-231 line was cultured in DMEM media with supplemented with 10% FBS and 1% of a 10,000 Units/mL Penicillin and 10,000 µg/mL Streptomycin solution. The T24 line was cultured in McCoy's 5a Medium (ATCC) and supplemented with 10% FBS and 1% of a 10,000 Units/mL Penicillin and 10,000 µg/mL Streptomycin solution.

Cell viability assays. Cells (18,750 cells/mL for HUVEC, 125,000 cells/mL for MDA-MB-231 and T24 125,000 cells/mL) were seeded in dark, flat bottom 96 well plates with clear lids for > 2 hours in 80 µL. After the growing period, Azo-CA4 and CA4 were added at varying concentrations in 20µL 0.25% DMSO in media. Differing concentrations of Azo-CA4 (30µM – 58.6nM for experiments in the light and 100µM – 195nM for experiments in the dark) and CA4 (30nM – 0.059nM) were replicated 5 times on each plate. Cells were incubated with drug for 48 hours with one 96 well plate undergoing irradiation at 380nm every hour for 1 minute for the duration of the experiment and the kept in the absence of light. 5 wells in each experiment were devoted to media with no cells or cells with vehicle. At the end of the 48 hour time period cells were incubated for 2 hours with 20µL Cell Titer Blue reagent (CTB)[98] at which time fluorescence was measured on a BioTek Synergy H1 Hybrid plate reader (Ex. 560nm, Em. 590nm). Cell viability was expressed as a percentage of maximum

(cells with vehicle) and corrected for background fluorescence of the media and data is shown as an average ± S.D. of three independent experiments. GI_{50} values were calculated using SigmaPlot software using a four parameter logistic equation.

2.15 Chemical Synthesis

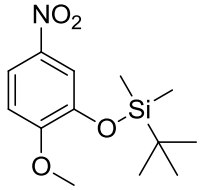

3-((*tert*-butyldimethylsilyl)oxy)-4-methoxynitrobenzene, 2.1. To a solution of 2-methoxy-5-nitrophenol (5 g, 29.6 mmol) in DMF (120 mL), TBDMS-Cl (4.90 g, 32.5 mmol) was added in one portion. The reaction mixture was stirred vigorously for 3 hours until TLC showed disappearance of 2-methoxy-5-nitrophenol. The mixture was evaporated and water (80 mL) was added. This solution was extracted 3 times with DCM (80 mL) and the combined organic layers were washed with brine, dried over Na_2SO_4, and evaporated to yield 7.73 g (92.3%) of a brown solid.

^{1}H NMR (400 MHz, $CDCl_3$) δ 7.89 (dd, *J* = 9.0, 2.8 Hz, 1H), 7.71 (d, *J* = 2.7 Hz, 1H), 6.89 (d, *J* = 9.0 Hz, 1H), 3.92 (s, 3H), 1.01 (s, 9H), 0.19 (s, 6H).

^{13}C NMR (101 MHz,$CDCl_3$) δ 156.76, 145.01, 141.42, 118.40, 116.06 , 110.48 , 55.87 , 25.60, 18.44, 17.39 , -4.63, -4.92.

HRMS ESI-MS (M + H^+) $C_{13}H_{22}NO_4Si^+$ calc. 284.1313 obsd. 284.1314.

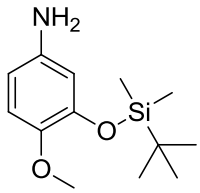

3-((*tert*-butyldimethylsilyl)oxy)-4-methoxyaniline, 2.2. Compound **2.1** (2 g, 7.1 mmol) was dissolved in an anhydrous 1:1 mixture of MeOH and EtOH (24 mL) in the presence of 10% Pd/C (400 mg, 0.38 mmol) under Ar. The reaction vessel was purged for 20 minutes with H_2 gas, sealed, and stirred for 3 h. The reaction was filtered through Celite and evaporated to yield 1.69 g (94.5%) of a dark brown oil.

^{1}H NMR (400 MHz, $CDCl_3$) δ 6.68 (d, *J* = 8.4 Hz, 1H), 6.28 (d, *J* = 2.8 Hz, 1H), 6.25 (dd, *J* = 8.4, 2.7 Hz, 1H), 3.72 (s, 3H), 3.30 (s, 2H), 0.99 (s, 9H), 0.15 (s, 6H).

^{13}C NMR (101 MHz, $CDCl_3$) δ 146.12, 144.32, 140.65, 114.43, 109.49, 108.20, 56.62, 25.76, 18.43, -4.36, -4.64.

HRMS ESI-MS ($M + H^+$) $C_{13}H_{24}NO_2Si^+$ calc. 254.1571. obsd 254.1566.

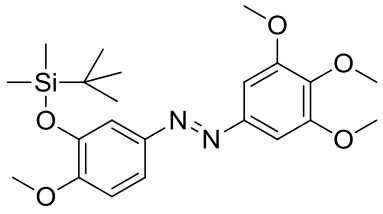

(*E*)-1-(3-((*tert*-butyldimethylsilyl)oxy)-4-methoxyphenol)-2-(3,4,5-trimethoxyphenyl)diazene, 2.3. Compound **2.2**. (1 g, 3.9 mmol) and 3,4,5-trimethoxyaniline (723 mg, 3.9 mmol) were stirred in freshly distilled CH_2Cl_2 under Ar. (Diacetoxyiodo)benzene (2.54 g, 7.9 mmol) was added in one portion. The reaction was allowed to proceed until the disappearance of compound 2 via TLC (20 minutes). The reaction mixture was rotary evaporated and was purified by flash column chromatography (100% Hexanes to 20% EtOAc in Hexanes) to yield 107 mg (6.3%) of an orange solid.

^{1}H NMR (400 MHz, $CDCl_3$) δ 7.58 (dd, *J* = 8.6, 2.4 Hz, 1H), 7.45 (d, *J* = 2.4 Hz, 1H), 7.21 (s, 2H), 6.96 (d, *J* = 8.6 Hz, 1H), 3.97 (s, 6H), 3.92 (s, 3H), 3.90 (s, 3H), 1.03 (s, 9H), 0.20 (s, 6H).

^{13}C NMR (101 MHz, $CDCl_3$) δ 153.82, 153.51, 148.69, 146.99, 145.53, 140.16, 119.41, 113.35, 111.20, 100.16, 61.02, 56.22, 55.59, 29.71, 25.74, 18.50, 1.03, -4.56.

HRMS ESI-MS (M + H^+) $C_{22}H_{33}N_2O_5Si^+$ calc. 433.2153. obsd 433.2149.

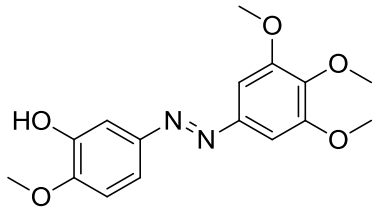

(*E*)-2-methoxy-5-((3,4,5-trimethoxyphenyl)diazenyl)phenol, 2.4. To a solution of compound **2.3** (53.5 mg, 0.12 mmol) in DMF (4 mL) potassium fluoride hydrate (81.6 mg, 1.4 mmol) and AcOH (20 µL, 0.35 mmol) were added. The reaction was complete after 1 hour as monitored via TLC. The reaction mixture was evaporated to yield an orange powder. The powder was dissolved in 5 mL DCM and washed with H_2O (3 x 5 mL), once with brine, and dried over Na_2SO_4. The organic layer was purified by flash column chromatography (100% Hexanes to 20% EtOAc in Hexanes) to yield 20.6 mg (53.9%) of a waxy orange solid.

^{1}H NMR (400 MHz, $CDCl_3$) δ 7.56 – 7.51 (m, 2H), 7.22 (s, 2H), 6.98 (d, *J* = 8.3 Hz, 1H), 5.72 (s, 1H), 3.98 (s, 3H), 3.96 (s, 6H), 3.93 (s, 3H).

^{13}C NMR (101 MHz,$CDCl_3$) δ 153.53, 149.20, 148.56, 147.44, 146.23, 140.32, 118.92, 110.09, 106.16, 100.26, 61.02, 56.20.

HRMS ESI-MS (M + H^+) $C_{16}H_{19}N_2O_5$ calc. 319.1288. obsd 319.1299.

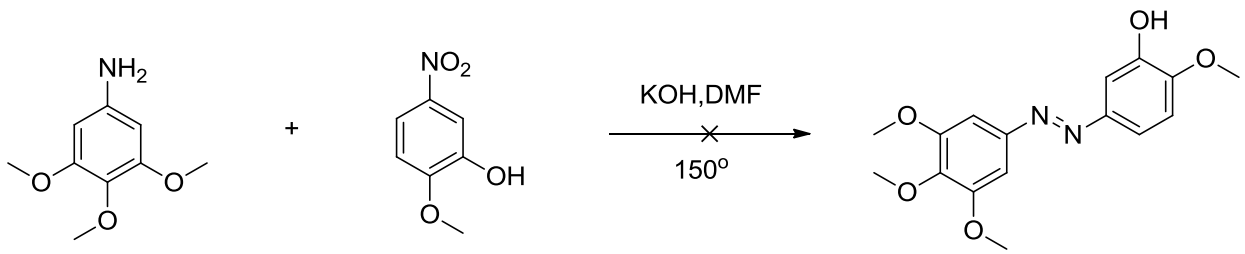

Failed Synthesis, Route 1. 2,4,5-trimethoxyaniline (3eq) was dissolved in DMF. KOH (10eq) was added to the reaction mixture and it was stirred until all of the solid dissolved. To the reaction mixture was added 2-methoxy-5-nitrophenol (1eq). The reaction mixture was attached to a reflux condenser and heated at 150^{o}C for 24 hours. After 24 hours the reaction was checked by TLC. No new products were seen. The reaction was allowed to continue for 6 days and monitored by TLC. No new product was observed.

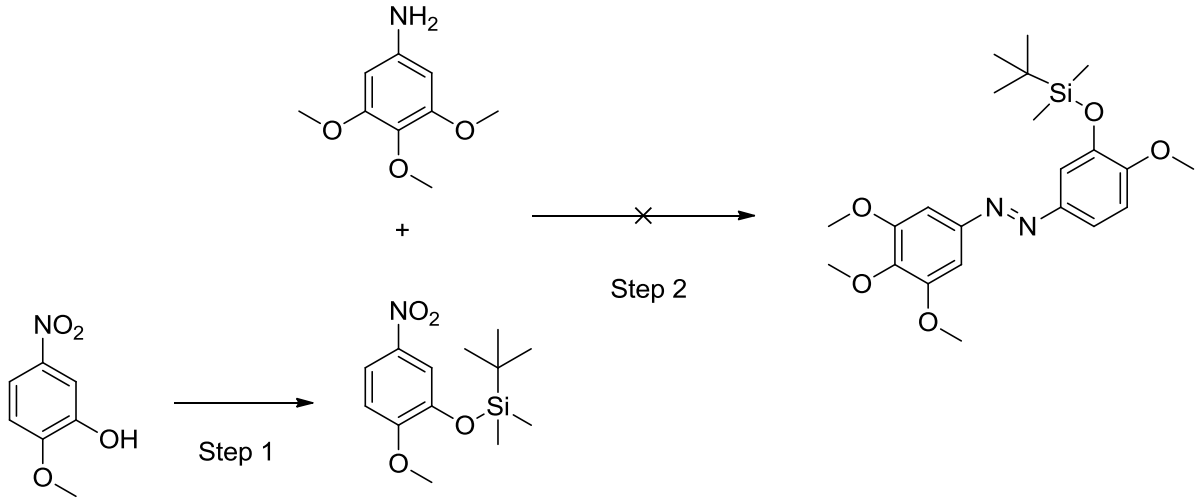

Failed Synthesis, Route 2.

Step 1: 2.1 was prepared in the same way as reported above.

Step 2: 2,4,5-trimethoxyaniline (3eq) was dissolved in DMF. KOH (10eq) was added to the reaction mixture and it was stirred until all of the solid dissolved. To the reaction mixture was added 2-methoxy-5-nitrophenol-TBDMS (1eq). The reaction mixture was attached to a reflux condenser and heated at 150^{o}C for 24 hours. After 24 hours the reaction was checked by TLC. No new products were observed. The reaction was allowed to continue for 6 days and monitored by TLC. No new product was observed.

2.16 Summary

In summary, a novel photoswitching drug with reversible photoactivation and GI_{50} values in the mid-nM range has been prepared. In the future, it may be possible to control the amount of glutathione in the cell by administration GSH synthesis inhibitor. Also, we may be able to increase the toxicity of Azo-CA4 by coadministration with another mitotic inhibitor such as paclitaxel or by creating an electron withdrawing derivative.

CHAPTER 3. FOLATE RECEPTOR-α MEDIATED AND PHOTOCLEAVABLE DRUG DELIVERY

3.1 Introduction

There are a number of ways that light has been used to specifically deliver a payload to a cancer cell. One of these ways involves the use of micelles, containing a cargo, with some type of chromophore that disrupts electrostatic interaction of the amphiphilic block copolymers, which is necessary for micelle formations, upon absorption of a specific wavelength.[99] When these micelles are decorated with a cancer specific ligand, dual targeting is achieved. Azobenzene is an example of these chromophores that can change conformation to destabilize micelle structure. Similar to light-responsive micelles are liposomes, which consist of concentric bilayers containing phospholipids. Liposomes, like micelles, can carry a cargo such as doxorubicin. Research is being conducted in to destabilizing the lipid bilayer, usually decorated with a targeting ligand, through an outside energy source (irradiation) to trigger drug release in the vicinity of a target.[100] Light-activated drug delivery through conjugation to light sensitive nanomaterials is also being researched. For example, silica nanoparticles expressing targeting ligands are biocompatible and contain light sensitive functionalities for the controlled release of drugs.[101] Finally, direct conjugation of a drug through a photocleavable linker to a cancer specific ligand is being researched.

3.2 Designing Dual Specificity Drug Conjugates

Our dual-specificity drug delivery system uses three parts (Figure 3.1). First and foremost, a cancer specific ligand is needed. Next, you need a drug. Lastly, a photocleavable linker molecule between the drug and ligand (or cell impermeable molecule) is required. The cancer-specific ligand has affinity for some phenotype of cancer cells. Usually this is the overexpression of cell-surface receptors. When we attach this to Doxorubicin through a light cleavable molecule, we now have a drug conjugate that is not only specific for the cancer cell through the ligand, but also cannot offer toxicity without the introduction of some external radiation source.

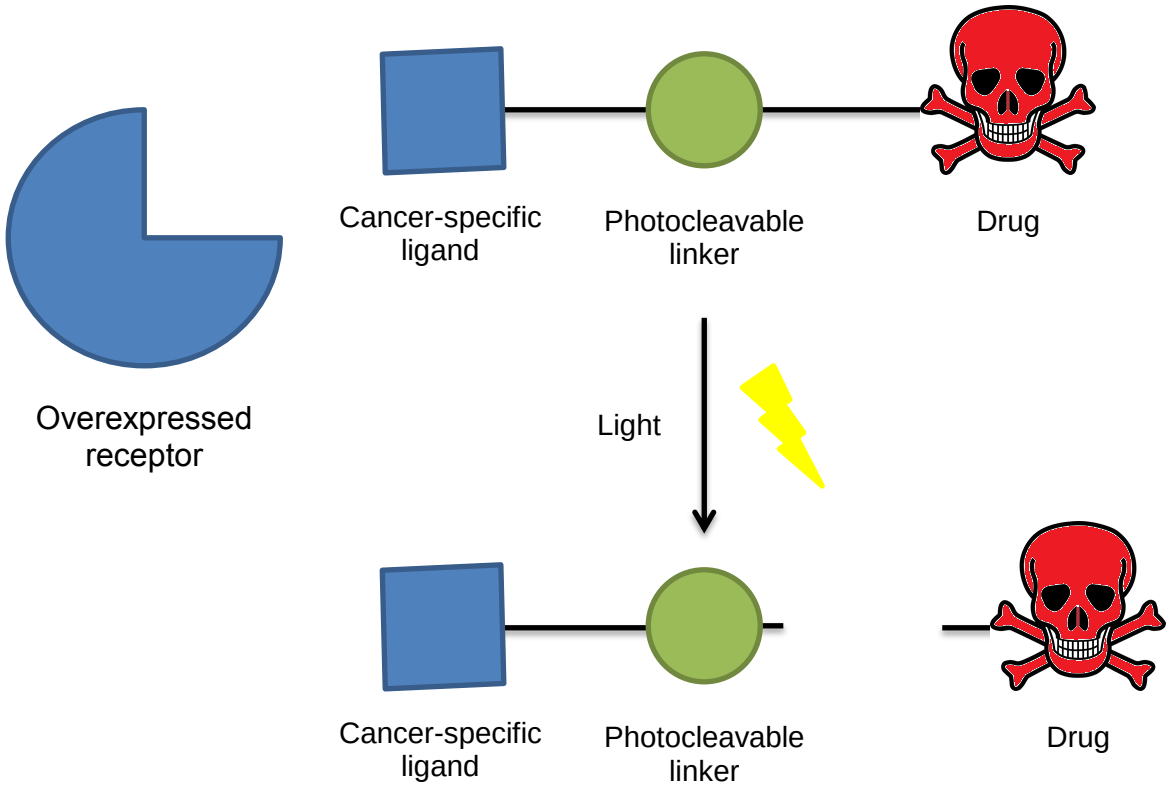

Figure 3.1. Ligand targeted, photocleavable drug release allowing for passive diffusion in the vicinity of the target.

3.2.1 Cancer Specific Ligand-Folic Acid Conjugates

Many types of cancers over express folate receptor-α (FR-α) on the cell surface.[6] For this reason we hypothesized that conjugation of folic acid to doxorubicin through a photocleavable linker would present a novel way to achieve dual targeting of cancer cells.

During our literature searches for the synthesis of folic acid conjugates, we discovered what we thought was an nonselective way to synthesize these conjugates, usually through a carbodiimide coupling.[102-104] Folic acid contains a pteroic acid moiety attached to a glutamic acid moiety. The glutamic acid moiety contains two carboxylic acid units, which are both reactive to carbodiimide coupling methods. Because it is known that the alpha carboxylic acid unit is important in binding FRα, wanted a method for selective attachment at the gamma-carboxylic acid.[105] Therefore, we decided to synthesize folic acid in two pieces (Scheme 3.1 and 3.2). The first piece is the glutamic acid moiety of folic acid and the second piece is a pteroyl azide. We started by functionalizing the γ-carboxylic acid of glutamic acid with **3.3**. We achieved the chemoselectively with Boc protection at off-target carboxylic acids. After deprotection of the propargyl functionalized glutamic acid we were able to attach it to pteroyl azide.

Pteroyl azide was prepared in a multistep synthesis. We started with cyclicaztion of the glutamic acid moiety with trifluoroacetic anhydride (**3.4**). Subsequently, we used a hydrolysis step to yield **3.5** and nucleophilic attack by hydrazine to remove the glutamic acid moiety and yield **3.6**. *tert*-Butyl nitrite and isothicyanate were employed to yield pteroyl aizde, **3.7**.

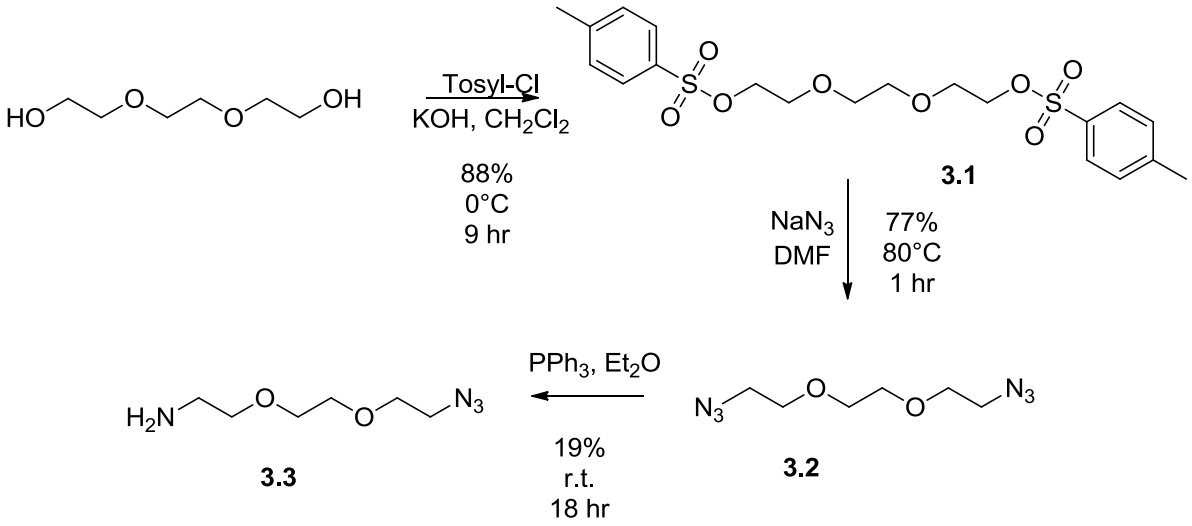

Scheme 3.1. Total synthesis of a folic acid analog for click chemistry.

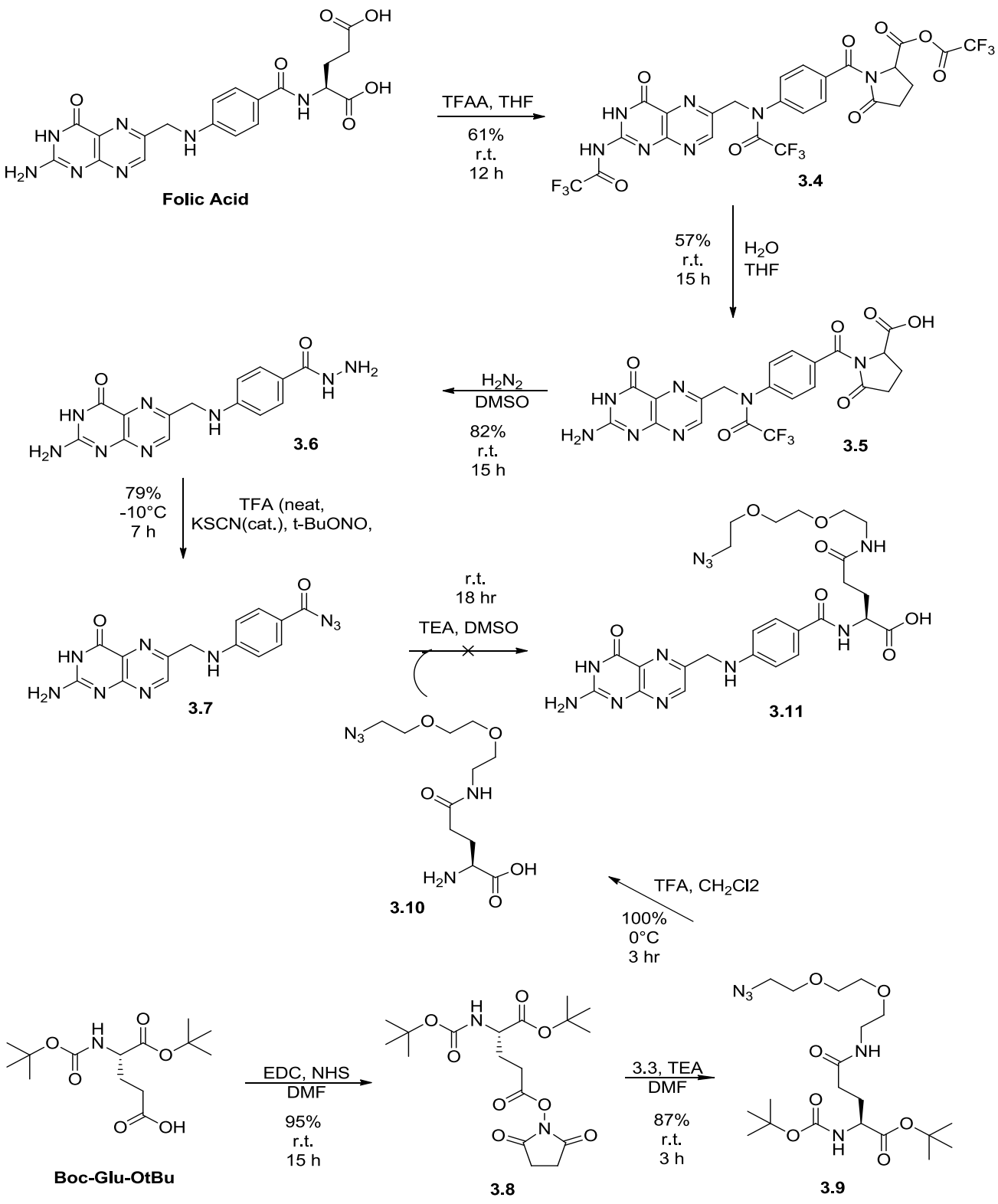

Scheme 3.2. Total synthesis of a folic acid analog for click chemistry.

3.2.2 EDANS Conjugates

Negatively charged molecules struggle to cross cellular membranes. Negative-negative electrostatic interactions between phospholipids in a cellular membrane and the sulfonic acid moiety of Ethylenediaminonapthalenesulfonic acid (EDANS) molecule will keep EDANS and anything attached to it from entering a cell. However, upon irradiation of a photocleavable linker, a payload may passively diffuse through the cell. This work has been reported previously[5] and in this work the synthesis was optimized and scaled up in order to perform experiments with mouse tumor xenografts.

My main goal during the synthesis of this previously reported compound was to enhance yields during each step. Improved yields were recorded for each step of the multi-step synthesis. Mostly, improved yields were achieved by carefully transferring between glassware during extractions and other purification steps. However, during the reaction with Bis-PNP, going from **3.13** to **3.14**, yields were improved by changing the order of addition. Originally, Bis-PNP was added to a stirring solution of **3.13**, but yields were improved by adding **3.13** to a concentrated stirring solution of Bis-PNP.

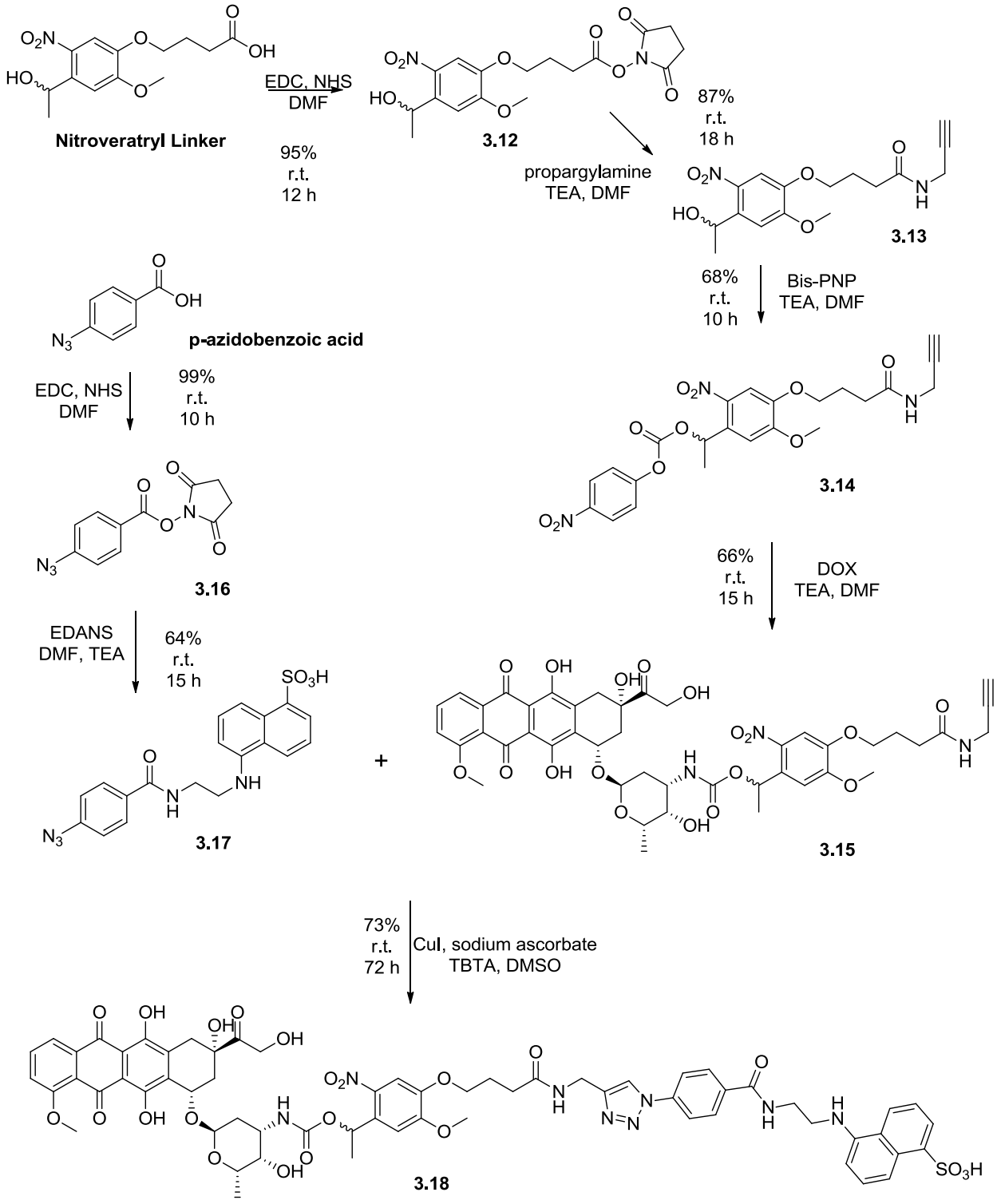

Scheme 3.3. Total synthesis of Dox-EDANS

3.3 Discussion

We anticipate that the effectiveness of photocaged permeability will translate to mouse xenografts. The carefully synthesized EDANS-DOX conjugate was prepared with improved yields at every step of the synthesis.

3.4 Experimental Section

All reagents and solvents were purchased from Sigma-Aldrich, VWR, or Fisher Scientific. ^{1}H NMR spectra and ^{13}C spectra were recorded at room temperature on a Bruker 400 MHz Ultrashield Plus. Proton and Carbon chemical shifts are expressed in parts per million (ppm, δ scale) and are referenced to the solvent peak (DMSO) or TMS ($CDCl_3$).

3.5 Chemical Synthesis[106]

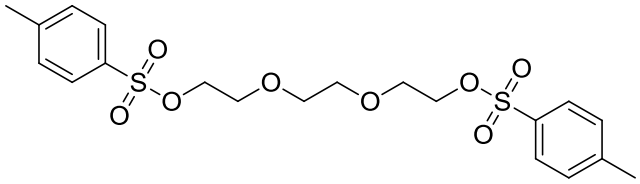

Bis-p-tosyltriethylene glycol, 3.1. Triethylene glycol (1.68 g, 11 mmol) and p-tosyl chloride (4.26 g, 22 mmol) were dissolved in CH_2Cl_2 (25 mL) and stirred. The reaction mixture was cooled on ice and KOH (5.37 g, 96 mmol, powdered) was added in portions over a period of 5 minutes. After 4 hours, 150 mg of additional p-tosyl chloride was added. After 5 hours, the reaction appeared complete via TLC (1:1 / EtOAc:Hexanes). The reaction mixture was added to a separatory funnel along with H_2O (30 mL). The aqueous layer was washed twice with CH_2Cl_2 (30 mL) and dried over sodium sulfate to yield 4.5g (87.7%) of a white solid. ^{1}H NMR is in agreement with previous reports.[107]

^{1}H NMR (400 MHz, DMSO-d_6) δ 7.80 – 7.75 (m, 4H), 7.47 (d, *J* = 8.1 Hz, 4H), 4.12 – 4.07 (m, 4H), 3.56 – 3.51 (m, 4H), 3.38 (s, 4H), 2.41 (s, 6H).

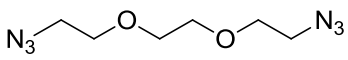

Bis-azidetriethylene glycol, 3.2. Compound **3.1** (4.437g, 10mmol) was suspended in DMF (15 mL) and NaN_3 (1.3g, 20mmol) was added to it. The reaction mixture was stirred in an oil bath at 80°C for 1 hour at which time TLC (3:2 / Hexanes:EtOAc) with PPh_3 and ninhydrin stain indicated that only the bis-azide was present. The DMF was evaporated on high vacuum overnight. The white solid was suspended in diethyl ether, filtered, and evaporated to yield 1.5 g (77.3%) of colorless oil. ^{1}H NMR is in agreement with previous reports.[108]

^{1}H NMR (400 MHz, DMSO-d_6) δ 3.65 – 3.58 (m, 4H), 3.58 (s, 4H), 3.39 (dd, *J* = 5.6, 4.3 Hz, 4H).

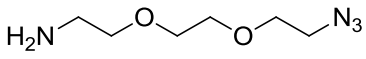

2-(2-(2-azidoethoxy)ethoxy)ethanamine, 3.3. Compound **3.2** (500mg, 2.5mmol) was dissolved in a 10 mL solution (5:1:4 / Et_2O:THF:1.5M HCl) in an argon environment sustained by pressure from a balloon. A solution of PPh_3 (655.1mg, 2.5mmol) in Et_2O (5 mL) was added via syringe over a period of 5 minutes. The reaction mixture was stirred at room temperature for 18 hours. 4M HCl (3 mL) was added and the aqueous layer was extracted 7 times with CH_2Cl_2 (20 mL) until no UV absorbing spots were observed on TLC. 10 pellets of KOH were added the raise the pH to ~14 and the aqueous layer was extracted 3 times with CH_2Cl_2 (20 mL). The organic layer was evaporated to yield 82.4 mg (18.8%) of a colorless oil. ^{1}H NMR is in agreement with previous reports.[108]

^{1}H NMR (400 MHz, Chloroform-*d*) δ 3.67 (m, *J* = 12.9, 7.3, 6.1, 3.3 Hz, 6H), 3.52 (m, *J* = 5.2, 2.0 Hz, 2H), 3.39 (t, *J* = 5.1 Hz, 2H), 1.61 (s, 2H).

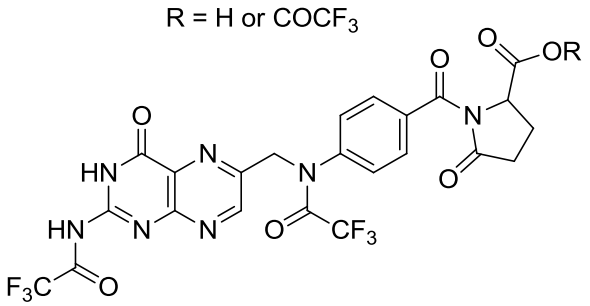

N [2,10]-Bis(trifluoroacetyl)pyrofolic acid/anhydride, 3.4. To a stirred suspension of folic acid (2g, 4.53mmol) in anhydrous THF (20 mL) was slowly added trifluoroacetic anhydride (5.12mL, 36.8mmol) at 0 °C. The reaction was warmed to room temperature and stirred overnight (12 h). The solution was concentrated by rotary evaporation and the thick, brown oil was added to a stirring solution of toluene (200 mL) with the aid of THF (2 mL). The yellow precipitate was collected by vacuum filtration (water aspirator). The solid was washed with Et_2O (10mL) to yield 1.85g (61.2%) of a yellow solid. ^{1}H NMR is in agreement with previous reports.[106]

^{1}H NMR (400 MHz, DMSO-d_6) δ 9.30 (s, 1H), 8.62 (s, 2H), 7.58 (d, *J* = 8.7 Hz, 2H), 7.11 (s, 4H), 6.86 (t, *J* = 6.1 Hz, 1H), 6.61 (d, *J* = 8.7 Hz, 2H), 4.46 (d, *J* = 6.0 Hz, 3H).

^{19}F NMR (d^6-DMSO) δ -66.13, -74.3, -75.02

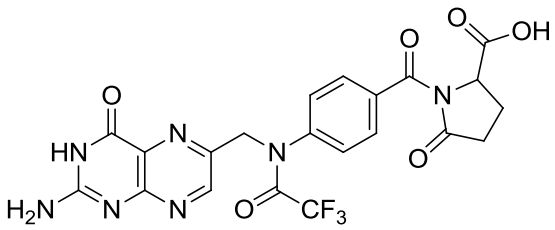

N^{10}-(Trifluoroacetyl)pyrofolic acid, 3.5. To a stirring solution of **3.4** (1.6 g, 2.6mmol) in THF (10 mL) was added ~10 g of crushed ice. The solution was allowed to warm to room temperature and stirred overnight (15 h). The mixture was slowly added to stirred Et_2O (40 mL). The precipitate was collected by vacuum filtration (water aspirator), washed with Et_2O (10 mL) and dried overnight under high vacuum to yield 1.23g (57% from folic acid) of a yellow powder. ^{1}H NMR is in agreement with previous reports.[106]

^{1}H NMR (400 MHz, DMSO-d_6) δ 8.64 (d, *J* = 3.6 Hz, 1H), 7.63 (s, 4H), 7.04 (s, 2H), 5.13 (s, 2H), 4.73 (dd, *J* = 8.9, 4.2 Hz, 1H), 2.62 – 2.39 (m, 3H), 2.04 (dd, *J* = 10.5, 5.3 Hz, 1H).

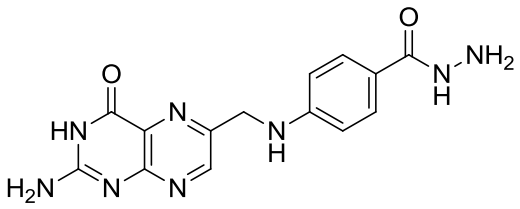

Pteroyl hydrazide, 3.6. Compound **3.5** (1g, 1.92mmol) was dissolved in DMSO (20mL) and hydrazine monohydrate (1.46mL, 30.1mmol) was added dropwise via syringe pump with stirring while maintaining the reaction temperature at 25 °C with the aid of an external water bath. The reaction was stirred overnight at room temperature (15 hours). MeOH (28 mL) was slowly added to the stirring reaction mixture. The precipitate was collected by vacuum filtration, washed with MeOH (15mL x 3) and Et_2O (15 mL x 3), and dried under high vacuum overnight to yield 515.1 mg (82%) as a yellow solid. ^{1}H NMR is in agreement with previous reports.[106]

^{1}H NMR (300 MHz, d^6-DMSO): δ 9.30 (s, 1H), 8.62 (s, 1H), 7.58 (d, J = 8.7 Hz, 2H), 7.11 (s, 3H), 6.86 (t, J = 6.1 Hz, 1H), 6.61 (d, J = 8.7 Hz, 2H), 4.46 (d, J = 6.0 Hz, 2H).

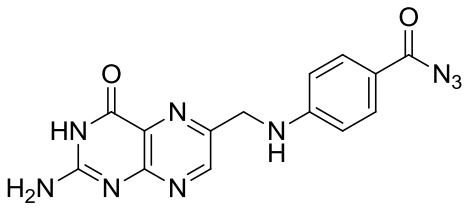

Pteroyl azide, 3.7. Compound **3.5** (250mg, 0.77mmol) was placed in a round bottom flask with cat. KSCN (3.8mg, 0.04mmol). The flask was cooled to -10°C via brine and ice and ice cold TFA (2 mL) was added to the round bottom. The reagents were allowed to dissolve and tBuONO (91.1µL, 0.77mmol) was added dropwise via syringe pump. The reaction was stirred at -10 °C for 7 h and allowed to warm to room temperature. 2-propanol (4 mL) was slowly added to afford an orange precipitate that was collected by centrifugation (30 min x 5,000 rpm). The pellet was washed with H_2O (4 mL),acetonitrile (4 mL), and Et_2O (4 mL), centrifuging after each wash (30 min x 5,000 rpm). The pellet was dried under high vacuum for 24 hours to give 204.3 mg (79%) of an orange solid. ^{1}H NMR is in agreement with previous reports.[106]

^{1}H NMR (300 MHz, d^6-DMSO): δ 8.69 (s, 1H), 7.69 (d, J = 8.8 Hz, 2H), 7.29 (s, 3H), 6.71 (d, J = 8.9 Hz, 2H), 4.56 (s, 2H).

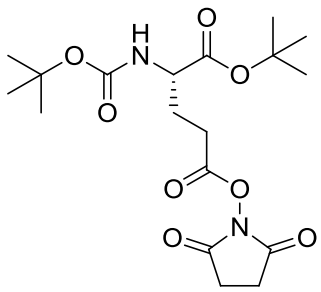

Boc-Glu-OtBu-NHS, 3.8. Boc-Glu-OtBu (100mg, 0.33mmol) was dissolved in DMF (5 mL). EDC (95mg, 0.50mmol) and N-hydroxysuccinimide (57mg, 0.50mmol) were added to the reaction mixture and stirred vigorously overnight (15 h). The reaction mixture was rotary evaporated. EtOAc (10 mL) was added and subsequently washed with H_2O (4 x 10mL). The organic layer was evaporated to yield 126 mg (95%) of a white solid. ^{1}H NMR is in agreement with previous reports.[109]

^{1}H NMR (400 MHz, Chloroform-*d*) δ 5.23 (d, *J* = 8.6 Hz, 1H), 2.83 (s, 4H), 2.70 (dd, *J* = 16.0, 9.9, 6.1 Hz, 2H), 2.27 (td, *J* = 9.2, 4.9 Hz, 1H), 2.08 – 1.98 (m, 1H), 1.48 (s, 9H), 1.45 (s, 9H).

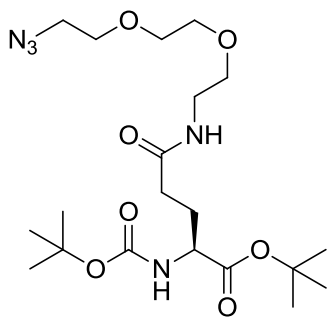

Boc-Glu-OtBu-TEG-azide, 3.9. Compound **3.8** (80mg, 0.20mmol) was dissolved in DMF (2 mL). Triethylamine (28µL, 0.20mmol) and compound **3.3** (31.4mg, 0.18mmol) were added and the reaction mixture was stirred for 3 h. The reaction mixture was rotary evaporated and EtOAc (10 mL) was added. The organic layer was washed with H_2O (3 x 10mL), citric acid (10 mL), brine solution (10 mL), and dried over sodium sulfate. The organic layer was then rotary evaporated to yield 80mg (87%) of a white solid.

^{1}H NMR (400 MHz, DMSO-d_6) δ 7.82 (s, 1H), 7.06 (d, *J* = 7.7 Hz, 1H), 3.77 (d, *J* = 4.7 Hz, 0H), 3.59 (d, *J* = 5.2 Hz, 2H), 3.54 (d, *J* = 7.5 Hz, 2H), 3.43 – 3.36 (m, 4H), 3.31 (s, 2H), 3.19 (d, *J* = 5.8 Hz, 2H), 2.13 (t, *J* = 7.8 Hz, 2H), 1.92 – 1.81 (m, 1H), 1.77 – 1.65 (m, 1H), 1.38 (d, *J* = 4.3 Hz, 18H).

^{13}C NMR (101 MHz, DMSO-d_6) δ 171.51, 171.35, 155.43, 79.07, 69.41, 53.98 , 50.00, 38.49 , 31.60, 27.86, 26.63 .

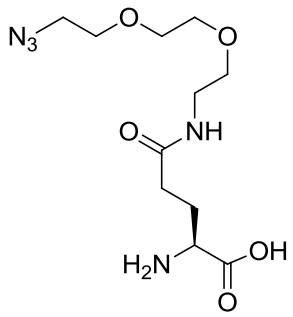

Glu-TEG-Azide, 3.10. Compound **3.9** (80mg, 0.17mmol) was dissolved in 30% TFA/CH_2Cl_2 (v/v) (2 mL) at 0°C. The reaction was stirred for 1 h and was then allowed to warm to room temperature and stirred for an additional 2 h at which point TLC (1:1 / EtOAc:Hexanes) with PPh_3/Ninhydrin stain indicated complete consumption of starting material. The reaction mixture was rotary evaporated to yield 53mg (100%) of a white solid. ^{1}H NMR is in agreement with previous reports.[110]

^{1}H NMR (400 MHz, DMSO-d_6) δ 8.02 (t, *J* = 5.6 Hz, 1H), 3.84 (t, *J* = 6.4 Hz, 1H), 3.62 – 3.47 (m, 4H), 3.47 – 3.30 (m, 3H), 3.20 (d, *J* = 5.8 Hz, 1H), 2.28 (ddd, *J* = 14.1, 8.6, 6.4 Hz, 1H), 1.98 (ddd, *J* = 12.8, 5.9, 2.6 Hz, 1H).

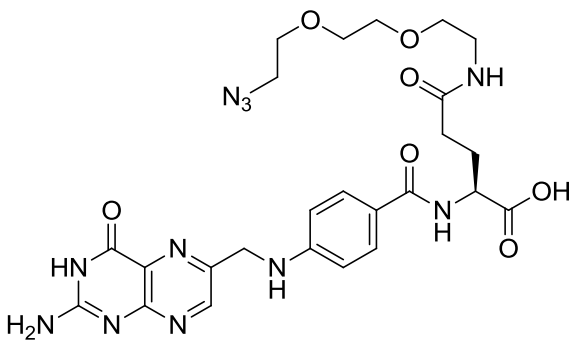

Failed synthesis of Folic-TEG-Azide, 3.11. Compound **3.10** (53mg, 0.17mmol) was dissolved in anhydrous DMSO (2 mL) and triethylamine (73µL, 0.51mmol) was added to the reaction mixture. The reaction mixture was stirred and compound **3.7** (65 mg, 0.19mmol) was added in one portion. The reaction was allowed to proceed overnight (18 h) with vigorous stirring. Acetonitrile (6 mL) was added and the yellow precipitate was collected by centrifugation (30min x 5,000 rpm). The pellet was washed with 1% HCl (6 mL), acetonitrile (6 mL), and diethyl ether (6 mL) with centrifugation after each wash. The resulting solid was dried under high vacuum overnight to yield 2.7 mg (2.5%). ^{1}H NMR was inconclusive as solvent peaks made visibility of the dilute product difficult to decipher.

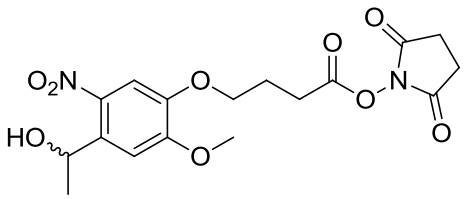

2,5-dioxopyrrolidin-1-yl 4-(4-(1-hydroxyethyl)-2-methoxy-5-nitrophenoxy)butanoate, 3.12. 4-(4-(1-hydroxyethyl)-2-methoxy-5-nitrophenoxy)butanoic acid (nitroveratryl photolinker, 400mg, 1.34mmol) was dissolved in DMF (20 mL) and shielded from ambient light with aluminum foil. The solution was cooled to 0°C and stirred for 10 min. EDC (312mg, 2.00mmol) and NHS (230mg, 2.00mmol) were added and the reaction mixture was stirred overnight (12 h), slowly warming to room temperature. DMF was rotary evaporated and EtOAc (10 mL) was added to the reaction vessel. The organic layer was washed with H_2O (4 x 20mL),brine (20 mL), dried over sodium sulfate, and rotary evaporated to yield 502mg (95%) of a yellow solid. ^{1}H NMR is in agreement with previous reports.[5]

^{1}H NMR (400 MHz, DMSO-d_6) δ 7.55 (s, 1H), 7.37 (s, 1H), 5.46 (t, *J* = 4.2 Hz, 1H), 5.26 (dd, *J* = 6.3, 3.5 Hz, 1H), 4.13 (t, *J* = 6.4 Hz, 2H), 3.91 (s, 3H), 2.82 (s, 6H), 2.61 – 2.57 d(m, 2H), 2.09 (t, *J* = 6.9 Hz, 2H), 1.37 (d, *J* = 6.3 Hz, 4H).

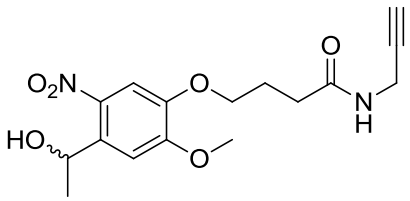

4-(4-(1-hydroxyethyl)-2-methoxy-5-nitrophenoxy)-N-(prop-2-yn-1-yl)butanamide, 3.13. Compound **3.12** (400mg, 1.0mmol) was dissolved in DMF (8 mL) and stirred at room temperature. In a separate vessel, propargylamine (129µL, 2.0mmol) and TEA (281µL, 2.0mmol) were dissolved in DMF (1 mL). The propargylamine/TEA solution was added dropwise to the reaction mixture containing 3.12 over a period of 10 min. The reaction mixture was shielded from ambient light via aluminum foil and stirred overnight (18 h). DMF was rotary evaporated and EtOAc (30 mL) was added to the flask and washed with H_2O (4 x 20mL),brine (20 mL), dried over sodium sulfate, and rotary evaporated to yield 296mg (87%) of a yellow solid. ^{1}H NMR is in agreement with previous reports.[5]

^{1}H NMR (400 MHz, DMSO-d_6) δ 8.33 – 8.28 (m, 1H), 7.53 (s, 1H), 7.37 (s, 1H), 5.47 (s, 1H), 5.27 (q, *J* = 6.2 Hz, 1H), 4.05 (t, *J* = 6.4 Hz, 2H), 3.92 (s, 3H), 3.86 (dd, *J* = 5.5, 2.5 Hz, 2H), 3.07 (t, *J* = 2.5 Hz, 1H), 2.28 (t, *J* = 7.4 Hz, 2H), 1.96 (p, *J* = 6.8 Hz, 2H), 1.38 (d, *J* = 6.2 Hz, 3H).

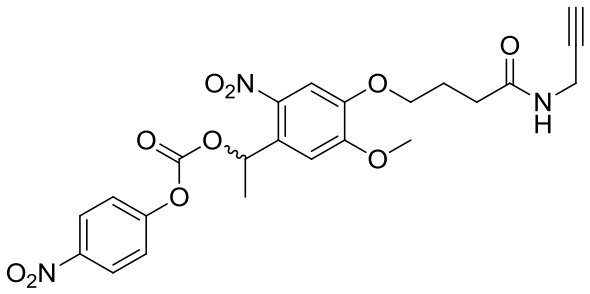

1-(5-methoxy-2-nitro-4-(4-oxo-4-(prop-2-yn-1-ylamino)butoxy)phenyl)ethyl (4-nitrophenyl) carbonate, 3.14. Bis(4-nitrophenyl) carbonate (543mg, 1.78mmol) was dissolved in DMF (5 mL) and stirred at room temperature. In a separate vessel, compound **3.13** (200mg, 0.59mmol) and TEA (166µL, 1.19mmol) were dissolved in DMF (5 mL) and added dropwise over a period of 30 min to the solution containing bis(4-nitrophenyl) carbonate. The reaction mixture was allowed to stir overnight (10 h), shielded from the light via aluminum foil. DMF was rotary evaporated and 1% HCl (20 mL) was added to the resulting oil. The mixture was extracted with EtOAc (30 mL). The organic layer was collected and washed with a saturated $NaHCO_3$ solution (3 x 20 mL), brine (20 mL), dried over sodium sulfate, and rotary evaporated to yield 198 mg (68%) of a yellow solid. ^{1}H NMR is in agreement with previous reports.[5]

^{1}H NMR (400 MHz, DMSO-d_6) δ 8.29 (d, *J* = 9.2 Hz, 2H), 7.59 (s, 1H), 7.53 (d, *J* = 9.2 Hz, 2H), 7.19 (s, 1H), 6.28 (q, *J* = 6.4 Hz, 1H), 4.08 (t, *J* = 6.4 Hz, 2H), 3.96 (s, 3H), 3.85 (dd, *J* = 5.5, 2.6 Hz, 2H), 3.06 (t, *J* = 2.5 Hz, 1H), 2.27 (t, *J* = 7.4 Hz, 2H), 1.96 (t, *J* = 7.0 Hz, 2H), 1.72 (d, *J* = 6.4 Hz, 3H).

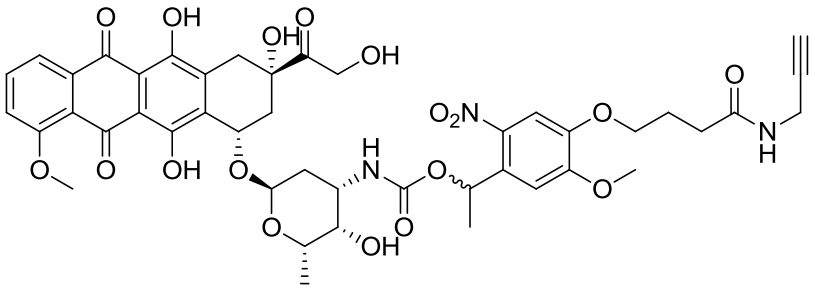

Dox-NV-alkyne, 3.15. Doxorubicin (104mg, 0.18mmol) was dissolved DMF (3 mL) containing TEA (56µL, 0.76mmol) and stirred in a foil-covered flask. Compound **3.14** (100mg, 0.20mmol) was added to the reaction mixture in one portion and allowed to stir overnight (15 h). DMF was rotary evaporated and EtOAc (30 mL) was added to the vessel. The organic layer was washed with H_2O (4 x 20 mL), brine (20 mL), dried over sodium sulfate, and rotary evaporated. The oil was dissolved in a minimal amount of EtOAc and purified by silica flash column chromatography (100% EtOAc → 1:9 / MeOH:EtOAc) to yield 107 mg (66%) of a deep red oil. ^{1}H NMR is in agreement with previous reports.[5]

^{1}H NMR (400 MHz, DMSO-d_6) δ 14.01 (d, *J* = 18.5 Hz, 2H), 13.25 (d, *J* = 7.6 Hz, 2H), 7.90 (t, *J* = 5.8 Hz, 4H), 7.64 (q, *J* = 5.4 Hz, 2H), 7.53 (s, 1H), 7.48 (s, 1H), 7.16 (s, 1H), 7.12 (s, 1H), 6.09 – 6.02 (m, 1H), 5.38 (d, *J* = 5.1 Hz, 1H), 5.21 (d, *J* = 8.0 Hz, 1H), 4.94 (s, 1H), 4.81 – 4.73 (m, 2H), 4.62 (d, *J* = 5.8 Hz, 1H), 4.55 (d, *J* = 5.7 Hz, 3H), 4.14 – 3.76 (m, 25H), 2.30 – 2.06 (m, 8H), 2.02 – 1.78 (m, 6H), 1.52 – 1.43 (m, 7H), 1.11 (dd, *J* = 9.2, 6.3 Hz, 6H).

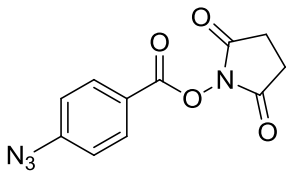

2,5-dioxopyrrolidin-1-yl 4-azidobenzoate, 3.16. 4-azidobenzoic acid (500mg, 3.06mmol) was dissolved in DMF (15 mL). EDC (881mg, 4.60mmol) and NHS (529mg, 4.60mol) were added to the reaction mixture and stirred overnight (10 h). DMF was rotary evaporated and EtOAc (20 mL) was added to the reaction vessel. The organic layer was washed with H_2O (4 x 20 mL), brine (20 mL), dried over sodium sulfate, and rotary evaporated to yield 796mg (99%) of an off-white solid. ^{1}H NMR is in agreement with previous reports.[5]

^{1}H NMR (300 MHz, DMSO-d_6) δ 8.13 – 8.07 (m, 2H), 7.38 – 7.30 (m, 2H), 2.88 (s, 4H).

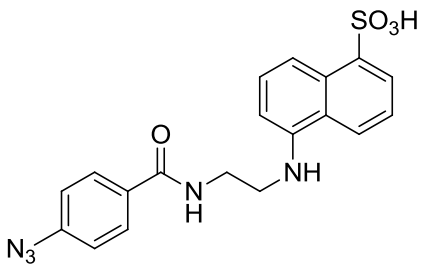

5-((2-(4-azidobenzamido)ethyl)amino)naphthalene-1-sulfonic acid, 3.17. To a stirred solution of **3.16** (53.7mg, 0.21mmol) in 5mL DMF, TEA (39.2µL, 0.28mmol) was added. EDANS (50mg, 0.19mmol) was then added to the reaction mixture and stirred overnight (15 h). DMF was rotary evaporated and CH_2Cl_2 (10 mL) was added to the resulting oil. The organic layer was washed with H_2O (3 x 10 mL), brine (10 mL), dried over sodium sulfate and rotary evaporated. The product was redissolved in a minimal amount of $CHCl_3$ and purified by silica flash column chromatography (15:85 / MeOH:$CHCl_3$) to yield 50mg (64%) of a brown solid. ^{1}H NMR is in agreement with previous reports.[5]

^{1}H NMR (400 MHz, DMSO-d_6) δ 8.79 (t, 1H), 8.16 (d, 2H), 7.95 (d, *J* = 8.7 Hz, 2H), 7.31 (ddd, *J* = 23.7, 8.6, 7.4 Hz, 3H), 7.22 (d, *J* = 8.6 Hz, 2H), 6.67 – 6.63 (m, 1H), 3.61 (d, *J* = 6.2 Hz, 2H), 3.48 – 3.29 (m, 5H), 3.07 (dd, *J* = 7.3, 4.8 Hz, 2H).

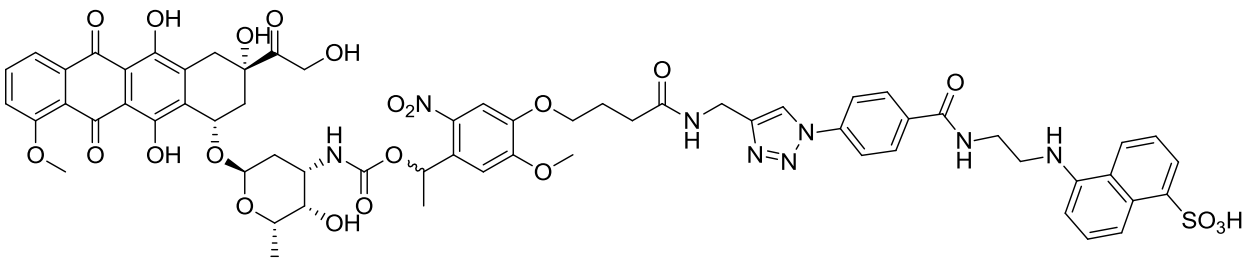

Dox-NV-EDANS, 3.18. Stock solutions of all reagents were freshly prepared immediately before the experiment. 500µL of compound **3.17** (100mM in DMSO), 500µL compound **3.15** (100mM in DMSO), and 500µL TBTA ligand (10mM in DMSO) were stirred at room temperature in a round bottom flask protected from ambient light via aluminum foil. 500µL sodium ascorbate (100mM in water) and 500µL copper sulfate (20mM in water) were then added to the reaction mixture. The reaction was stirred for 72 hours until TLC indicated completion (1:4 / MeOH:$CHCl_3$). The reaction mixture was concentrated, filtered and purified on RP-HPLC using 20% acetonitrile (0.1% TFA in H_2O) for 10 minutes followed by a gradient of acetonitrile concentration from 20% to 70% over 30 minutes at 6mL/min. The fractions (~15mL each) were collected in to tubes containing 500 µL of ammonium bicarbonate (2mg/mL) to quench TFA. A mixture of diastereomers eluted at 26.5 and 28.5 min) comparable to the literature.[5] The aforementioned fractions were collected, combined and lyophilized to yield 10mg (73%) of a deep red solid. ^{1}H NMR is in agreement with the previously reported compound.[5]

^{1}H NMR (400 MHz, DMSO-d6) δ 14.05 (s, 1H), 13.28 (s, 1H), 8.85 (t, J = 5.9 Hz, 2H), 8.71 (s, 1H), 8.45 (d, J = 5.4 Hz, 2H), 8.05 (d, J = 15.4 Hz, 5H), 7.92 (d, J = 6.5 Hz, 4H), 7.54 (s, 1H), 7.40 – 7.21 (m, 8H), 7.00 (d, J = 8.0 Hz, 1H), 6.65 (d, J = 7.6 Hz, 2H), 6.05 (d, J = 6.4 Hz, 1H), 5.22 (s, 1H), 4.95 (s, 1H), 4.54 (s, 3H), 3.96 (d, J = 29.1 Hz, 8H),

3.62 (d, J = 6.0 Hz, 3H), 3.43 (d, J = 6.3 Hz, 3H), 2.97 (s, 2H), 2.35 – 1.74 (m, 7H), 1.45 (d, J = 6.6 Hz, 5H), 1.09 (d, J = 6.5 Hz, 4H).

CHAPTER 4. TARGETING THE ACIDIC EXTRACELLULAR ENVIRONMENT OF CANCER

4.1 Introduction

Since the discovery of the translocation of the HIV-1 Tat protein, there have been many attempts to discover which parts of the protein are responsible for cell permeability.[48] It was later found that permeable, truncated portions of Tat contained a large number of positively charged residues, especially L-arginine. From there, it has been shown that arginine homopolymers are effective at entering cells.[111] Not only do these peptides enter cells, but they are able to bring a cargo such as nucleic acids, polymers, liposomes, nanoparticles, and small molecule drugs.[112]

In addition to L-arginine homopolymers, there are a variety of cell penetrating peptides exhibiting unique sequences and designs. CPP's are usually composed of less than 40 amino acids, but the sequences can vary greatly. One way of improving CPP's is to modify them by creating cyclic peptides,[113] dendrimers,[114] and helices.[115] However, most CPP's are not selective and will enter any cell, which is why there is a demand for specificity in CPP design. For example, CPP's with tumor-homing capabilities have been designed by attaching a peptide known to accumulate in breast cancer tissue to a well-studied CPP.[116] Almost all CPP's have a multitude of positively charged residues, such as arginine.

Many cell penetrating peptides rely on positively charged residues to facilitate cell permeability.[117] The reason for this is that the initial interaction between positively charged CPP's and phospholipids in the plasma membrane is electrostatic.[118] The positively-charged residues interact with negatively charged polysaccharides such as heparin sulfate. Furthermore, it has been shown that lysine is not as effective for cellular internalization as arginine.[111] Therefore, it is evident that internalization not

only comes from positive charges, but from the guanadine moiety of the arginine residue.

We hypothesized that an arginine analog, L-canavanine, may be a good substitute for the residues of a CPP. L-canavanine, an L-arginine analog, exhibits a side-chain residue with a lower pKa than its canonical counterpart. Synthesizing an L-canavanine homopolymer will allow for a poly-cationic peptide to form in a low pH environment, thus becoming cell permeable (Figure 4.2).

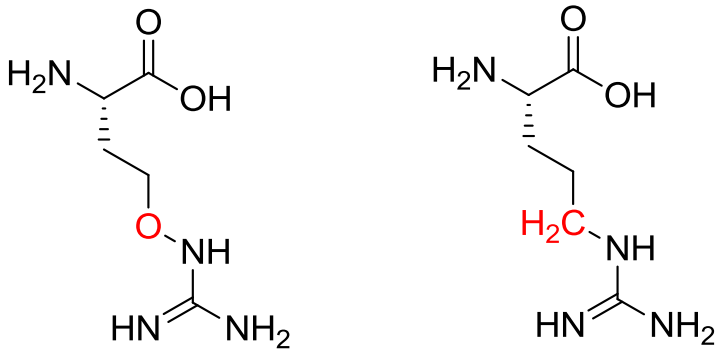

Figure 4.1: Structural differences between L-cav (left) and L-arg (right) highlighted in red.

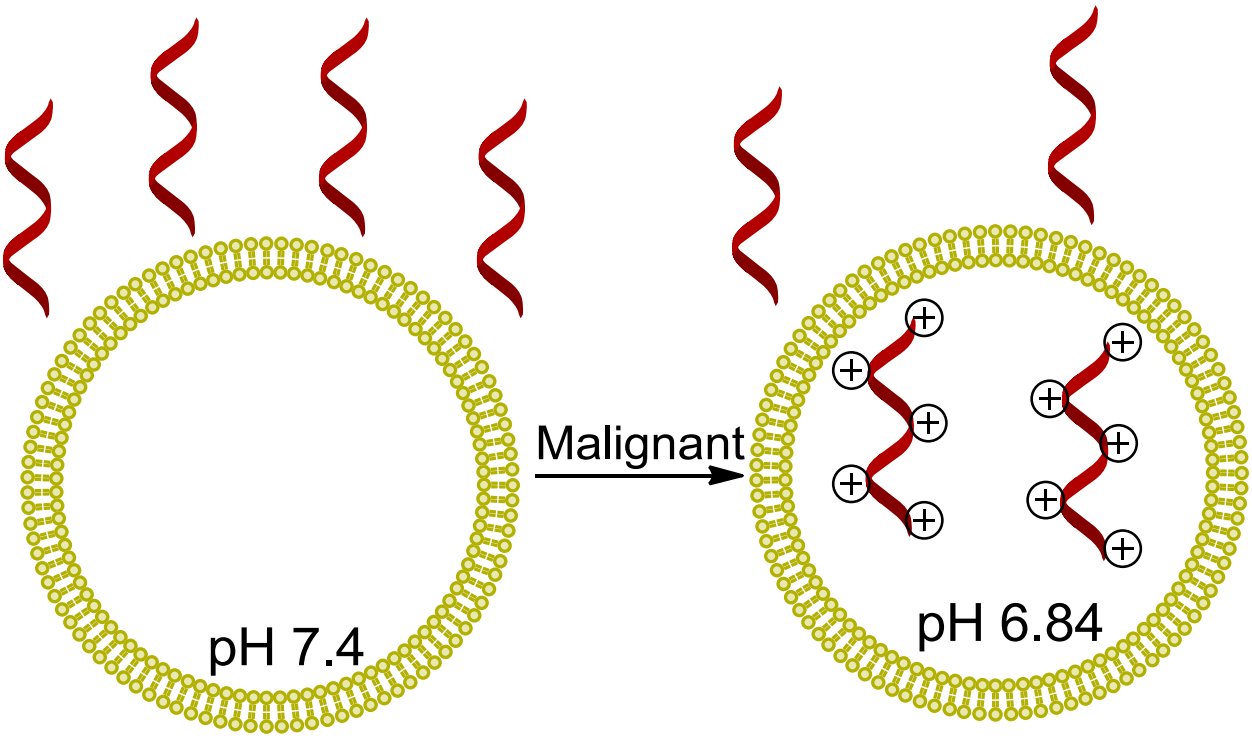

Figure 4.2: L-canavanine polypeptide becomes charged and permeable in the acidic extracellular environment of cancer cells.

4.2 L-Canavanine and Targeting Cancer

L-Canavanine, an L-arginine analog (Figure 4.1) exhibits a pKa of 7.04, which is significantly lower than the pKa of arginine (12.48).[119] A general average over a variety of cancer types shows a pH of 6.84 in the extracellular environment.[120] Regular physiological pH in the extracellular environment is generally ~7.4. The matched pH of the extracellular environment of tumors and the pKa of canavanine may introduce a way to selectively charge a peptide in the vicinity of tumors in turn enabling permeability.

4.3 Designing Poly-Canavanine Peptides

Peptides will be synthesized by a CEM Liberty microwave assisted peptide synthesizer. The optimal arginine peptide for cell permeability is the nonaarginine peptide (R_9).[117] Therefore, we hypothesize that nonacanavanine (Cav_9) should be the starting place for our experiments. It is known that pKa is transient in proteins and to correct for that we will vary our peptides by adding L-arginine residues in increasing quantities and positions (Table 4.1).[121]

Arg_9	5-FAM-RRRRRRRRR
Peptide 1	5-FAM-RRRRXXXXX
Peptide 2	5-FAM-XXXXXRRRR
Peptide 3	5-FAM-XRXRXRXRX
Cav_9	5-FAM-XXXXXXXXX

Table 4.1. Peptides and controls with 5-Fam at N-terminus

4.4 Attempted syntheses of Fmoc-Cav-Pbf-OH.

4.4.1 Route 1

L-canavanine is an L-arginine analog. Therefore, we decided to apply the same protecting group chemistry to L-canvanine as we used with L-arginine. The reason for protecting the side-chain of L-arginine is because lactam formation resulting from nucleophilic attack of the side chain on the carboxylic acid during peptide synthesis is known to occur.[122] During the attempted synthesis of Fmoc-Cav-Pbf, several synthetic routes were attempted. Initially, the straightforward route was followed (Scheme 4.1). In this route L-canavanine was reacted with N-(9-Fluorenylmethoxycarbonyloxy)succinimide (Fmoc-OSu) to afford the Fmoc-Cav-OH precursor in 69% yield. However, multiple attempts to attach the Pbf group failed to give the desired product. We believe that the oxyguanidine moiety on the residue of canavanine lacked the nucleophilicity to react with the sulfonyl chloride of Pbf-Cl. The reaction mixture showed as a streak of multiple spots on TLC which is assumed to coincide with instability of the Fmoc protecting group.

Route 1

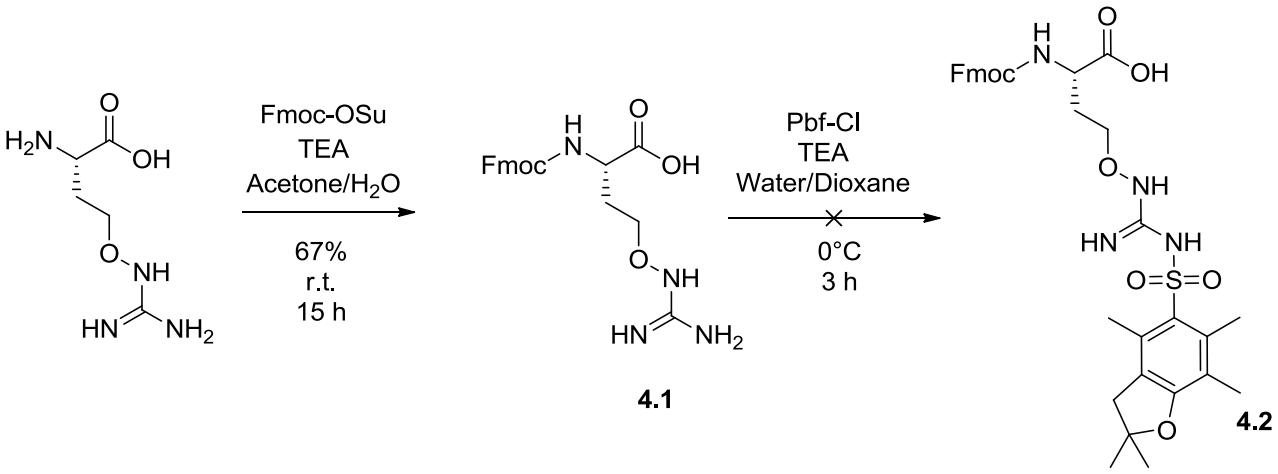

Scheme 4.1. Route 1 shows the first attempted synthesis of Fmoc-Cav-Pbf. Attachment of the Pbf protecting group was unsuccessful.

4.4.2 Route 2

We then sought to first protect the alpha-amine of L-canavanine with an orthogonal protecting group so that we could run the Pbf protection reaction in more basic conditions. We decided to use N-[2-(Trimethylsilyl)ethoxycarbonyloxy]succinimide (Teoc-OSu), a protecting group to be later cleaved with fluorine anion, to protect the alpha-amine of L-canavanine (Scheme 4.2). The next step was to protect the guanidine side-chain of L-canavanine with Pbf in the presence of NaOH. Following Pbf protection then we planned to deprotect the alpha amine and re-protect it with Fmoc to make it suitable for peptide synthesis. However, even under strongly basic conditions, the Pbf reaction continued to fail, even in the presence of a strong base. No change in starting material was observed.

Route 2.

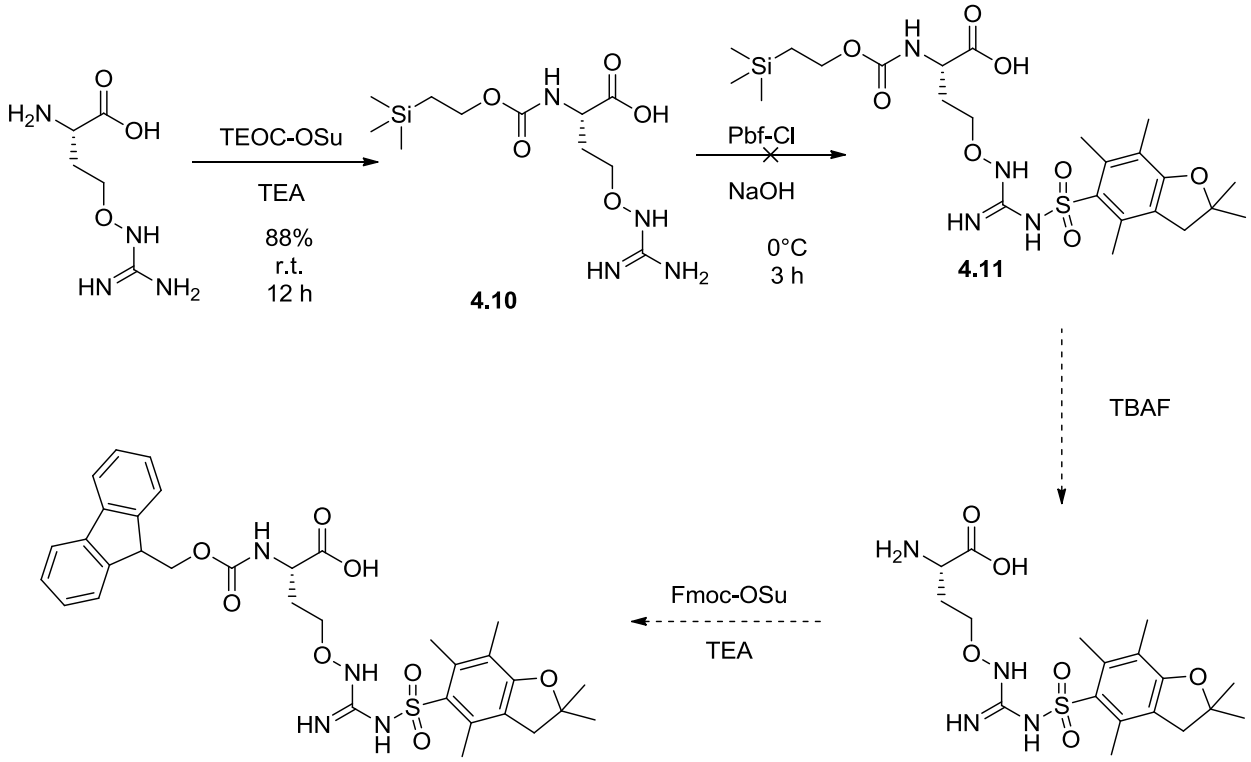

Scheme 4.2. Proposed synthesis of Fmoc-Cav-Pbf-OH through the use of an orthogonal protecting group for attachment of Pbf under more basic conditions.

4.4.3 Route 3

Although Pbf-protection of L-arginine is the preferred protection method, we hypothesized that we may be able to achieve peptide synthesis utilizing a different protecting group. We decided to move forward with a *tert*-butyloxycarbonyl (Boc) protecting group. This method does not work for arginine normally because of conversion to L-ornithine during solid phase peptide synthesis.[123] It was suspected that L-canavanine would be inert to this reaction. Initially, protection of Fmoc-Cav-OH with Boc-anhydride was unsuccessful (Scheme 4.3).

We then decided to try to synthesize Fmoc-Cav-$(Boc)_2$-OH in a series of smaller steps. The thought was that we could use an Fmoc-protected 2-amino-4-bromobutyric acid (Scheme 4.4), which would undergo nucleophilic attack from a Boc-protected hydroxylguandine. However, upon Fmoc-protection of the alpha-amine, irreversible lactone formation occurred. We attempted to open the ring with HBr in MeOH, but were unsuccessful.

From this point we found it necessary to protect the carboxylic acid of 2-amino-4-bromobutyric acid by synthesizing the methyl ester, followed by Fmoc protection and subsequent reaction with the Boc-protected hydroxylguanidine (Scheme 4.5). We were successful up to the point of connecting the Boc-protected hydroxylguanidine. Because of a lack of reaction as indicated by TLC, we hypothesized that the hydroxyl guanidine may be too sterically hindered to react. Certainly we could push this reaction with basic conditions, but sensitivity of the Fmoc prevented this approach.

Route 3

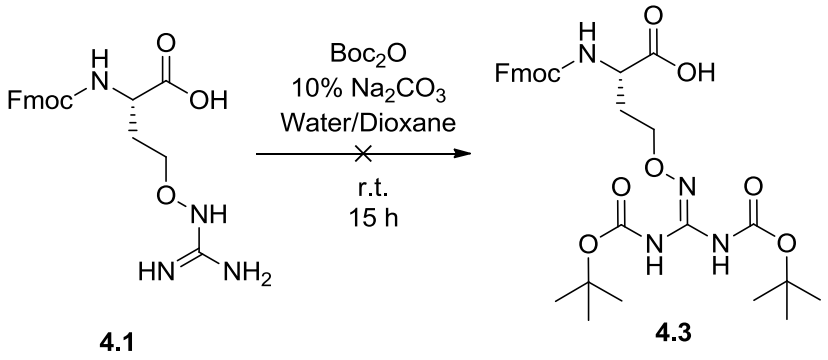

Scheme 4.3. Synthesis of Fmoc-Cav-$(Boc)_2$-OH utilizing Boc anhydride

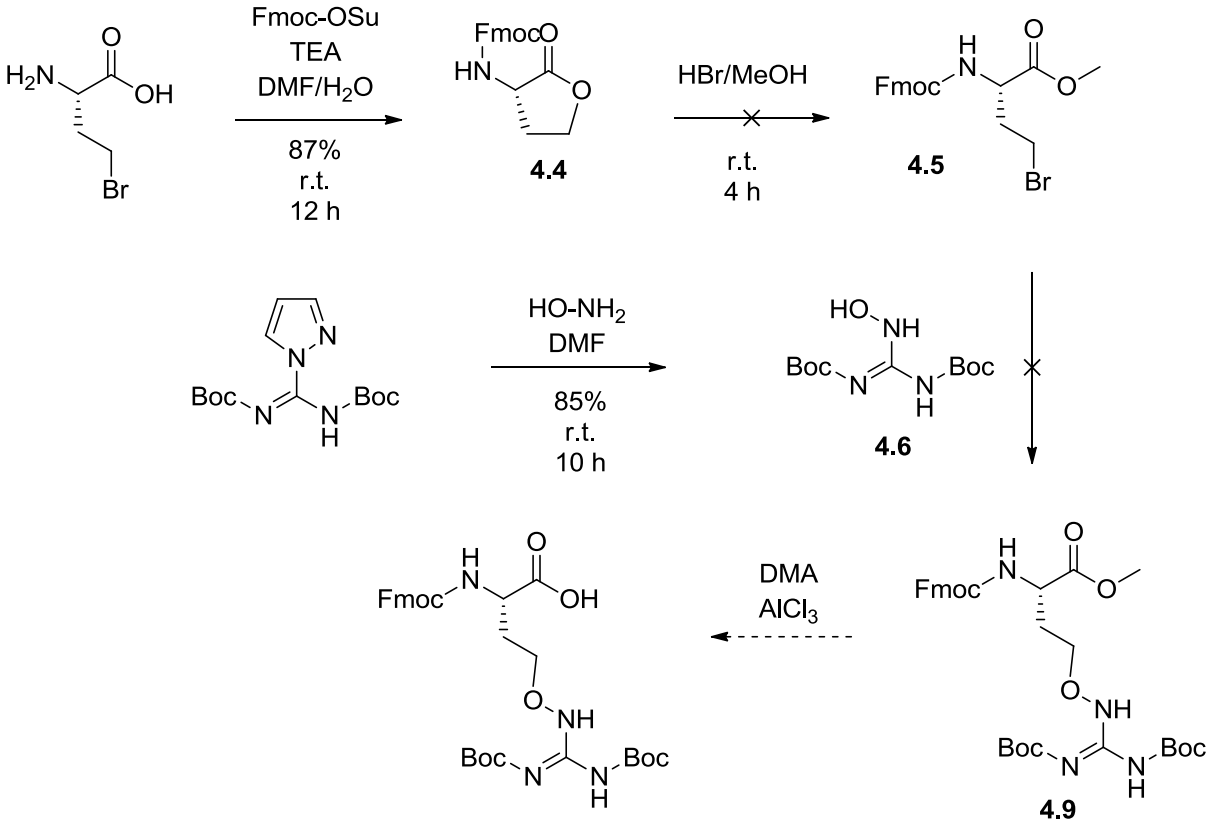

Scheme 4.4. Synthesis of Fmoc-Cav-$(Boc)_2$-OH using the Boc protected hydroxylguanidine.

Route 3

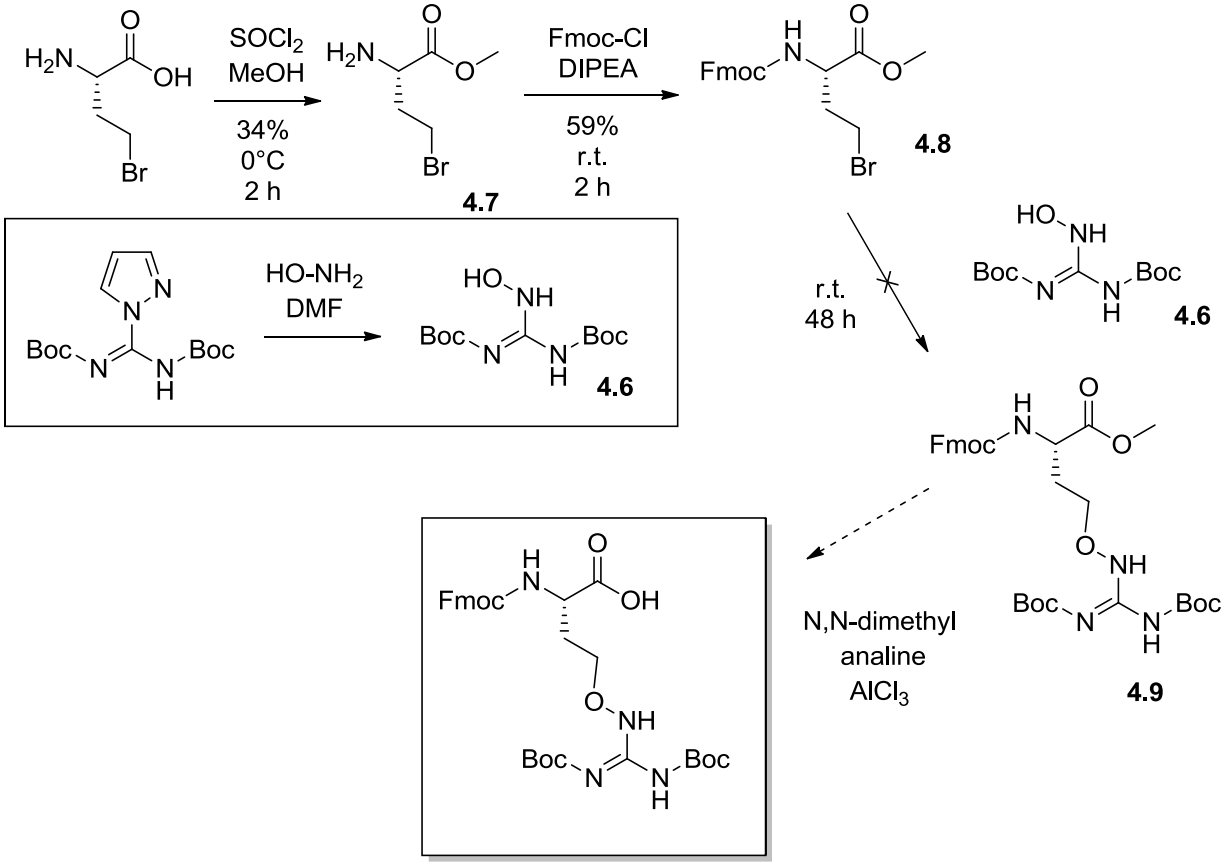

Scheme 4.5. Synthesis of Fmoc-Cav-$(Boc)_2$-OH using the Boc protected hydroxylguanidine. Initially, lactone formation is prevented by creating the methylester.

4.4 Discussion

Unfortunately, time restraints and failed synthetic progress have prevented this project from becoming fully realized. After considering the need for side-chain protection during the synthesis of Arginine peptides, we decided that the same necessity may not be present for the unreactive residue of Canavanine. We could try a synthesis of a Canavanine containing peptide without Pbf protection. In the future, we hypothesize that it may be possible to use an oxyguanidine moiety that is not necessarily a canavanine derivative. Guanidine-containing amino acids have been used before to mimic cell penetrating peptide and the same principles could be applied to oxyguanidine.[124]

4.5 Experimental Section

All reagents and solvents were purchased from Sigma-Aldrich, VWR, or Fisher Scientific. ^{1}H NMR spectra and ^{13}C spectra were recorded at room temperature on a Bruker 400 MHz Ultrashield Plus. Proton and Carbon chemical shifts are expressed in parts per million (ppm, δ scale) and are referenced to the solvent peak (DMSO) or TMS ($CDCl_3$).

4.6 Chemical Synthesis

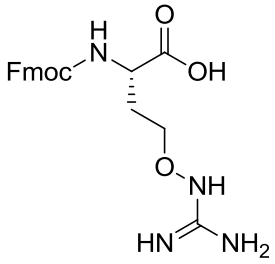

Fmoc-Canavanine-OH, 4.1. L-canavanine sulfate (250mg, 0.91mmol) was dissolved in H_2O (500 µL) in the presence of TEA (191µL, 1.36mmol). The solution was allowed to stir for 10 min. To the solution was added, dropwise, Fmoc-OSu (277mg, 0.82mmol) in Acetone (500 uL). TEA (10 µL aliquots) was added to keep the reaction at a pH of 8-8.5. A white precipitate formed and was collected and washed with H_2O (3 x 1 mL) to yield 244mg (67%) of a white solid. ^{1}H NMR is in agreement with previous reports.[125]

^{1}H NMR (400 MHz, Chloroform-*d*) δ 7.89 (d, J = 7.6 Hz, 2H), 7.72 (dd, J = 7.3, 3.4 Hz, 2H), 7.44 – 7.38 (m, 2H), 7.33 (td, J = 7.5, 1.2 Hz, 2H), 4.24 (d, J = 5.3 Hz, 2H), 3.94 (d, J = 5.8 Hz, 0H), 3.74 (s, 1H), 2.10 – 1.95 (m, 1H), 1.95 – 1.76 (m, 1H).

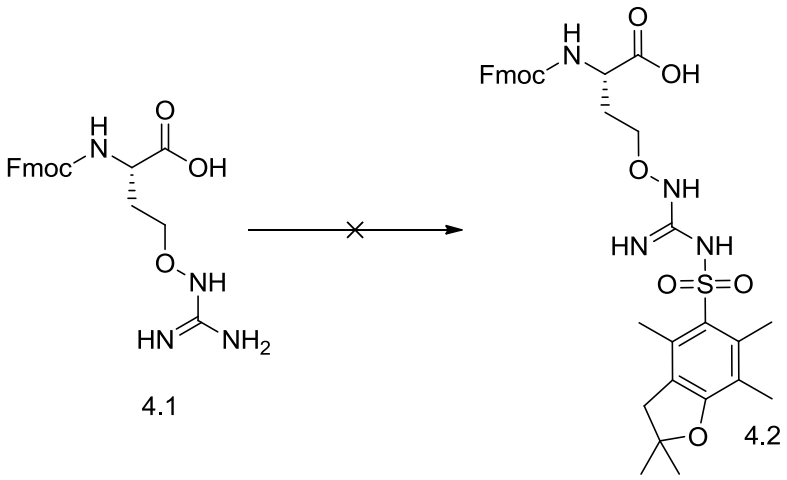

Failed synthesis of Fmoc-Cav-(Pbf)-OH, 4.2. Compound **4.1** (22.2mg, 55.7μM) was dissolved in a 1:1 mixture of Acetone:H_2O (600 μL). The mixture was stirred in an ice bath and TEA (14.6μL, 0.11mmol) was added. The solution was allowed to stir for 10 min. Pbf-Cl (32.2mg, 0.11mmol), dissolved in acetone, was added via syringe pump over 30 minutes. The pH was monitored and kept at ~8-8.5 by the addition of TEA. Once the addition of Pbf-Cl was complete, the reaction was allowed to warm to room temperature and react for an additional 2 h. Disappearance of Pbf-Cl was monitored by TLC (20% MeOH:DCM). Several new spots had formed and after separation by preparative TLC no desired product was isolated.

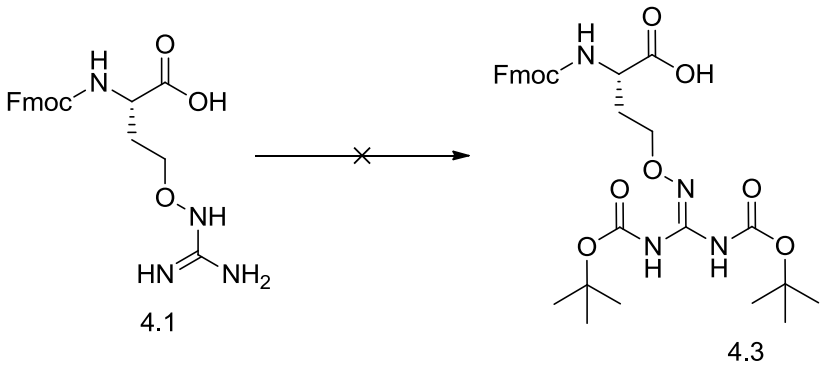

Failed synthesis of Fmoc-Cav-(Boc)$_2$-OH, 4.3. Compound **4.1** (37.4mg, 93.9μM) was dissolved in 10% Na_2CO_3 (350 μL) and stirred. Boc anhydride (27.3mg, 0.19mmol) in dioxane (350 μL) was added in one portion. The reaction was monitored for disappearance of starting material. After 3 h the starting material was still present by TLC and the reaction was allowed to go overnight. No disappearance of starting material was seen. However, a new spot on TLC was observed and collected via flash column. This new compound did not correspond to the product, and considerable starting material remained in the reaction.

Fmoc-(2-oxotetrahydrofuran-3-yl)carbamate, 4.4. 2-amino-4-bromobutyric acid (100 mg, 0.38 mmol) was dissolved in H_2O (2.4 mL) and stirred. TEA (53 µL, 0.37 mmol) was added to the solution. The solution was allowed to stir for 10 min and placed in an ice bath. To the reaction mixture was added Fmoc-OSu (142.5 mg, 0.42 mmol) dissolved in DMF (0. 8mL), dropwise via syringe pump. After 2 h the reaction mixture was allowed to warm to room temperature and allowed to run overnight (12 h). Disappearance of Fmoc-OSu was monitored by TLC and a new spot was seen forming. The new spot was separated by flash column chromatography (1:1 / EtOAc:Hexanes) to yield 138mg (87%) of a beige solid. ^{1}H NMR is in agreement with previous reports.[126]

^{1}H NMR (400 MHz, Chloroform-*d*) δ 7.77 (d, J = 7.5 Hz, 2H), 7.59 (d, J = 7.5 Hz, 2H), 7.44 – 7.38 (m, 2H), 7.35 – 7.30 (m, 2H), 4.44 (s, 4H), 4.23 (t, J = 6.5 Hz, 1H), 2.82 (d, J = 12.9 Hz, 1H), 2.27 – 2.14 (m, 1H).

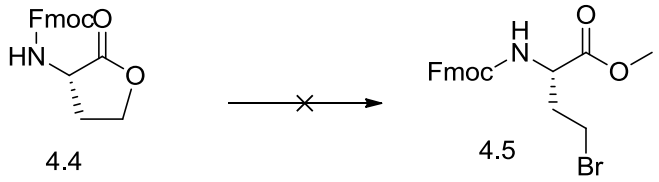

Failed synthesis of (S)-methyl 2-((((9H-fluoren-9-yl)methoxy)carbonyl)amino)-4-bromobutanoate, 4.5. This reaction was kept dry and all starting materials were lyophilized overnight before use. 2 mL HBr in MeOH (5-10%) was added to compound 4.4 (28.8mg, 68.9µmol) and stirred at room temperature until all the starting material had disappeared on TLC. Five new spots were observed on TLC and were separated by flash column (1:1 / EtOAc:Hexanes). All fractions were undecipherable on NMR.

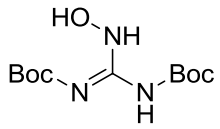

(Z)-tert-butyl(((tert-butoxycarbonyl)imino)(N-hydroxyl)methyl)carbamate, 4.6.

N,N'-Di-Boc-1H-pyrazole-1-carboxamidine (250mg, 0.81mmol) was dissolved DMF (6.4 mL) and a solution of hydroxylamine in H_2O (50% by wt, 45.6 µL, 0.82 mmol) in a dropwise fashion. The disappearance of starting material was monitored by TLC and the new spot was collected by flash column chromatography (4:1 / EtOAc:Hexanes). Fractions were lyophilized to yield 189 mg (85%) of a white solid. ^{1}H NMR is in agreement with previous reports.[127]

^{1}H NMR (400 MHz, Chloroform-*d*) δ 2.95 (s, 1H), 2.88 (d, *J* = 0.7 Hz, 1H), 2.17 (s, 1H), 1.49 (d, *J* = 5.3 Hz, 18H).

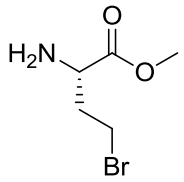

(S)-methyl 2-amino-4-bromobutanoate, 4.7. 2-amino-4-bromobutyric acid (51 mg, 0.19 mmol) was placed in an oven dried vessel with a stir bar and place in an ice bath. Anhydrous methanol (1 mL) was added and stirred. Thionyl chloride (28.1 µL, 0.39 mmol) was then added slowly and dropwise. The reaction was allowed to warm to room temperature, rotary evaporated, and a new spot on TLC (1:9 / MeOH:DCM) was collected by flash column chromatography to yield 18.3 mg (34%) of a beige solid. ^{1}H NMR is in agreement with previous reports.[128]

^{1}H NMR (400 MHz, Chloroform-*d*) δ 4.40 (s, 3H), 3.95 (dd, *J* = 8.1, 5.2 Hz, 1H), 3.80 (s, 3H), 3.69 – 3.56 (m, 2H), 2.49 – 2.37 (m, 1H), 2.29 (ddt, *J* = 14.4, 8.1, 6.1 Hz, 1H).

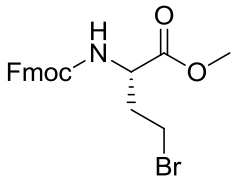

(S)-methyl-2-((((9H-fluoren-9-yl)methoxy)carbonyl)amino)-4-bromobutanoate, 4.8. Compound **4.7** (50mg, 0.18mmol) was dissolved in 606 µL (1:1 / dioxane:H_2O). DIPEA (32µL, 0.18mmol) was added and the solution was placed in an ice bath. To the stirring reaction mixture was added Fmoc-Cl (46.7mg, 0.18mmol) in dioxane (500 µL), dropwise. TLC was used to monitor disappearance of Fmoc-Cl and the reaction was complete after 2 h at which time the reaction mixture was rotovaporized and redissolved in a small amount of hexanes. Product was separated by flash column chromatography (4:1 / Hexanes:EtOAc) to yield 44.5mg (59%) of a beige solid.

^{1}H NMR (400 MHz, Chloroform-*d*) δ 7.80 – 7.72 (m, 3H), 7.63 – 7.56 (m, 3H), 7.44 – 7.36 (m, 3H), 7.34 – 7.28 (m, 3H), 5.41 (d, *J* = 8.3 Hz, 1H), 4.54 – 4.40 (m, 3H), 4.21 (t, *J* = 6.7 Hz, 1H), 3.76 (s, 3H), 3.38 (t, *J* = 7.0 Hz, 2H), 2.43 (ddd, *J* = 14.6, 10.0, 6.2 Hz, 1H), 2.23 (dq, *J* = 14.5, 7.2 Hz, 1H).

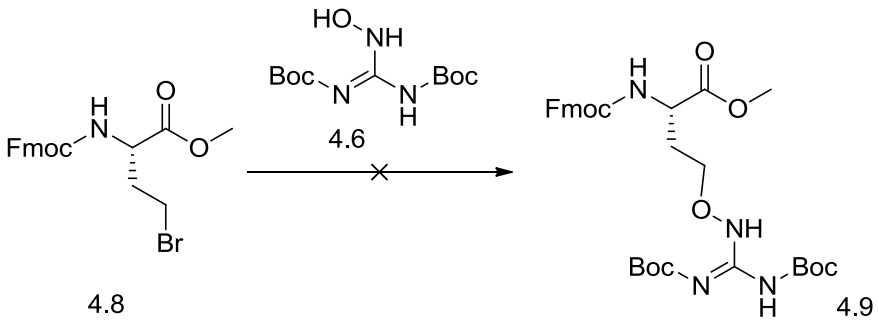

Failed synthesis of Fmoc-Cav-(Boc)$_2$-OMe, 4.9. Compound **4.8** (44.5mg, 0.11mmol) was dissolved in DMF (0.9 mL) and stirred in the presence of NaI (1.6mg, 1.01µmol). Compound **4.6** (20mg, 0.11mmol) was dissolved in DMF (0.5 mL) and added to the reaction mixture in a dropwise fashion. After two days no change in starting materials was observed on TLC.

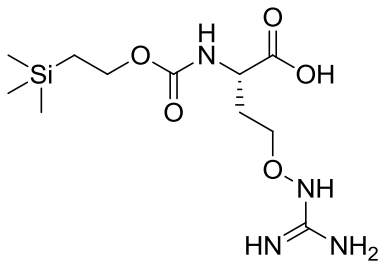

Teoc-Cav-OH, 4.10. L-canavanine sulfate (100mg, 0.36mmol) was dissolved in H_2O (1 mL). TEA (102µL, 0.73mmol) was added and the solution was allowed to stir for 10 min. Teoc-OSu (105mg, 0.40mmol) was added in dioxane (1 mL). The reaction was allowed to stir overnight (12 h). A white precipitate formed and was collected by vacuum filtration. The solid was washed with dioxane/H_2O (1:1 / 3 x 5 mL) and placed on high vacuum overnight to yield 103 mg (88%) of a white solid.

^{1}H NMR (400 MHz, DMSO-d_6) δ 6.79 (d, *J* = 7.2 Hz, 1H), 4.43 – 4.37 (m, 1H), 4.02 (t, *J* = 8.4 Hz, 2H), 2.05 – 1.75 (m, 2H), 0.94 – 0.88 (m, 2H), 0.02 (s, 9H).

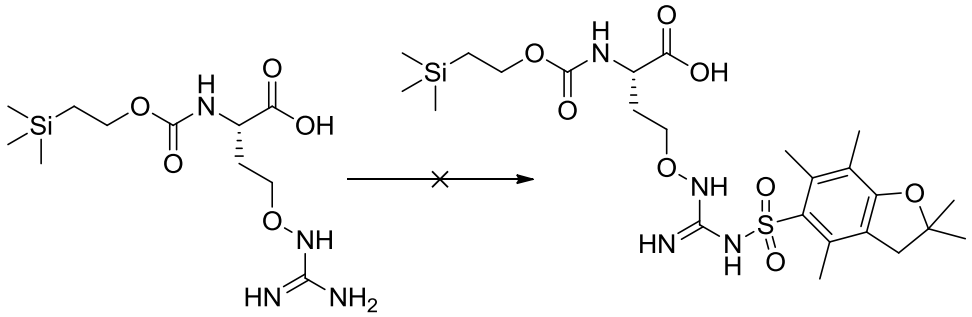

4.10 4.11

Failed synthesis of Teoc-Cav-Pbf-OH, 4.11. Compound **4.10** (27mg, 84.3µmol) was dissolved in 1mL (1:1 / H2O:Acetone) and placed on stir. 4M NaOH (100 µL) was added to the reaction mixture. Pbf-Cl (27mg, 93.5µmol) was added in one portion to the stirring mixture. A white precipitate formed, but was confirmed by NMR to be hydrolyzed Pbf starting material. No new spots were witnessed on TLC.

Chapter 5: Conclusion

Drug discovery and chemotherapy for cancer has had its ups and downs over the centuries. The main problem lies with the lack of specificity of chemotherapeutics and their propensity toward off-target toxicity. Therefore, it is not only important to find new drugs with enhanced specificity for cancer cells over normal cells, but importantly, to discover ways to take proven chemotherapeutics and increase their specificity. The latter is the focus of the Hartman Lab and I have focused this approach in to three distinct projects.

The first project, which dominated my research and ultimately proved the most fruitful in positive results, was turning combretastatin A4 into a photo activated drug. We were successful in showing that Azo-CA4 was not only a more potent inhibitor of tubulin polymerization in the light, but a more effective growth inhibitor in cancer cells in the light than in the dark. Importantly, we showed that Azo-CA4 lost potency when removed from the light, demonstrating its photoswitchable activity. It is important to continue shining light to sustain the activity of Azo-CA4.

The next two projects I worked on were very similar. These projects used a photocleavable appendage to attach Doxorubicin to either a cell targeting ligand or to a cell impermeable molecule. In the former project, Doxorubicin was linked to a folic acid through a nitroveratryl linker. This molecule allowed us to be specific for cancer cells in two ways: 1) by the affinity of folic acid for overexpressed folate receptor in many cancer cell lines an 2) the use of an external radiation source to cleave doxorubicin from the ligand. The important part of this project was to carefully construct this drug

conjugate so that we knew with complete certainty that the gamma-carboylic acid of folic acid was responsible for conjugation to the photocleavable linker. The latter project involved optimizing and scaling up the synthesis of EDANS-DOX. I began the synthesis of this molecule to test on mouse xenografts with the overall goal of improving the yield and synthetic methodology.

The final project that I worked on was similar to the first three in that we sought to take known chemotherapeutics and increase specificity. However, the project with poly-canavanine peptides did not utilize light to increase specificity. Instead, we focused on the unique oxy-guanadine side chain of canavanine to try to create a peptide with cell permeability optimized for low pH environments. Although, we did not get to construct a peptide with canavanine, the project presents a clearly promising project for future work.

Overall, the work achieved throughout the course of my graduate career will have a strong, positive impact on the field of cancer-specific chemotherapeutics. Through the continuance of my research we will further the fight against cancer and enhance the efficacy of existing drugs.

Appendix A: NMR Data

^{1}H NMR of 3-((*tert*-butyldimethylsilyl)oxy)-4-methoxynitrobenzene, 2.1.

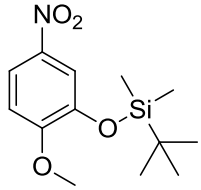

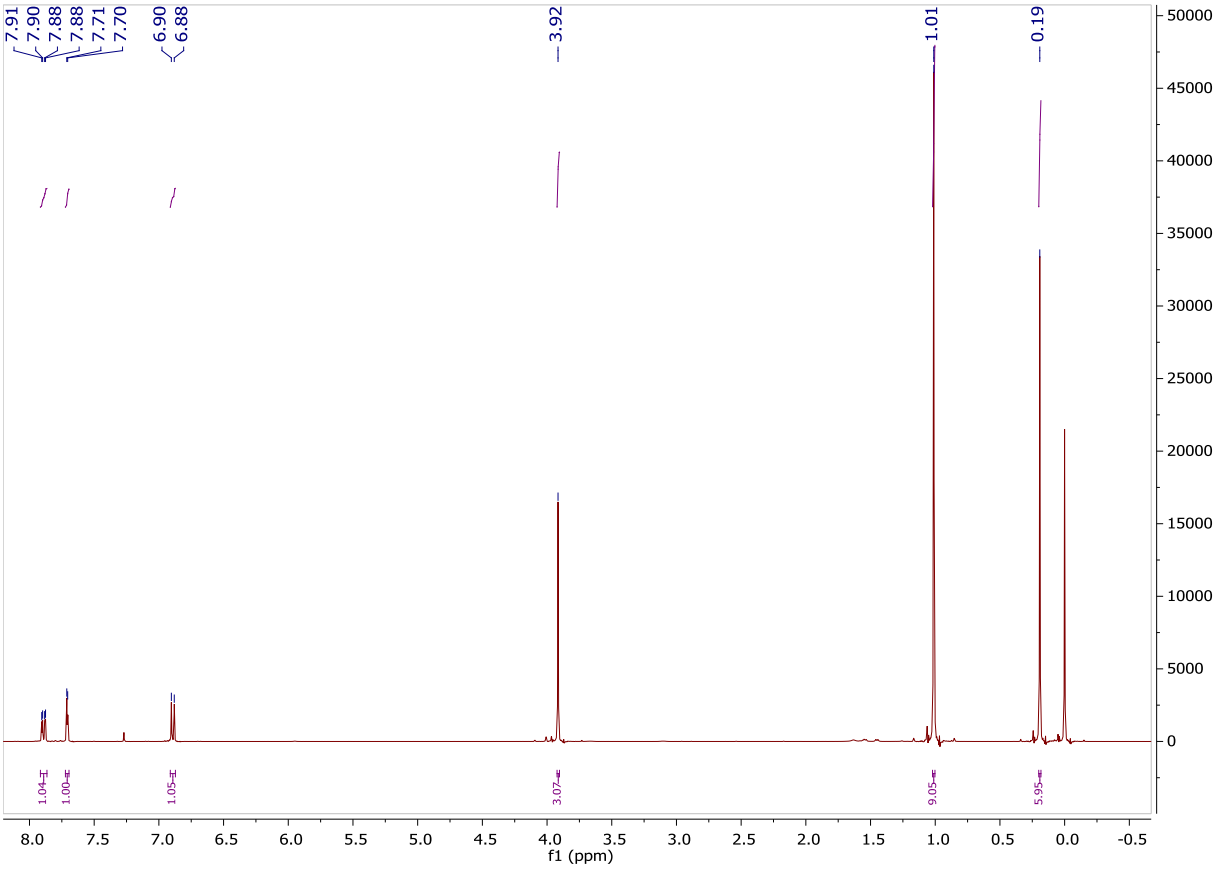

^{13}C NMR of 3-((*tert*-butyldimethylsilyl)oxy)-4-methoxynitrobenzene, 2.1.

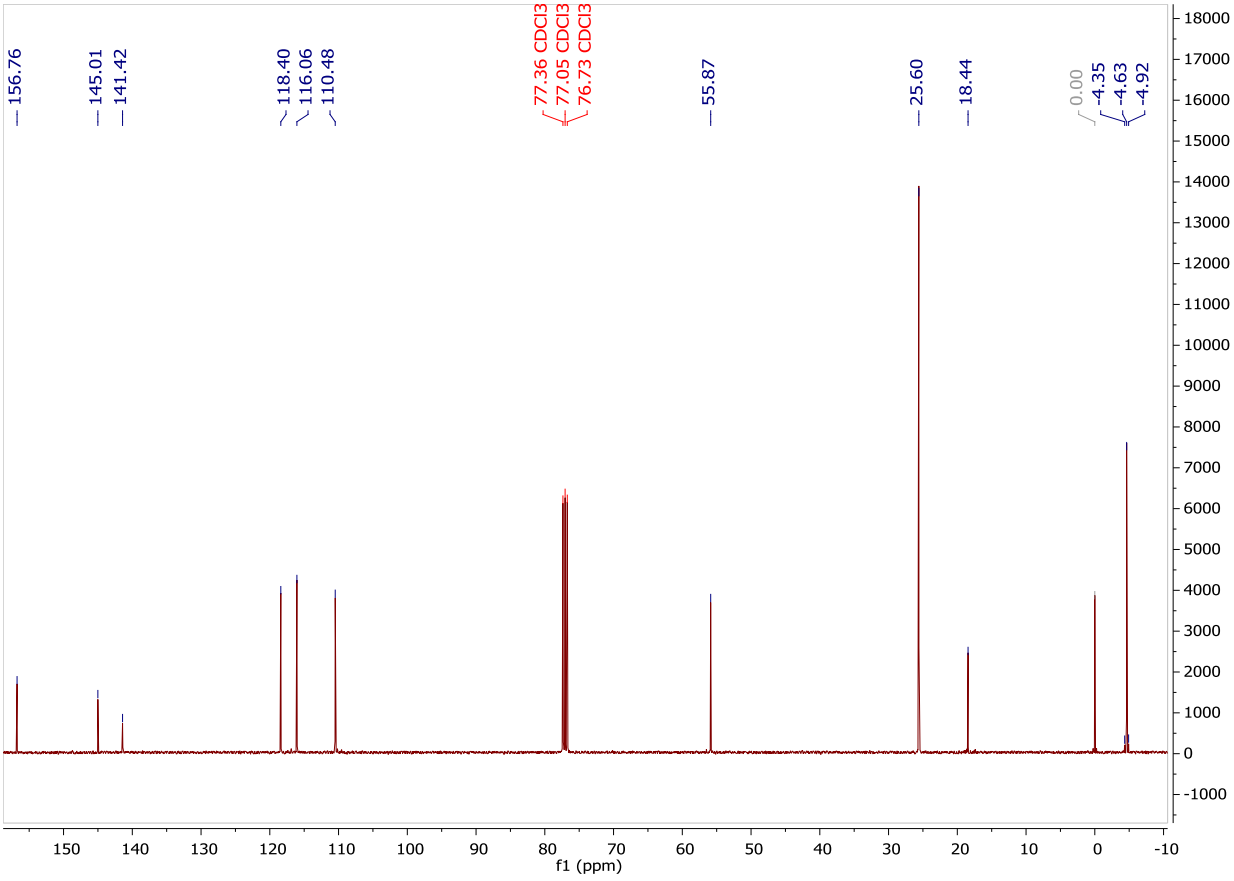

^{1}H NMR of 3-((*tert*-butyldimethylsilyl)oxy)-4-methoxyaniline, 2.2.

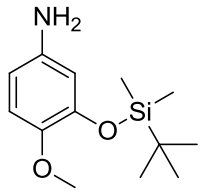

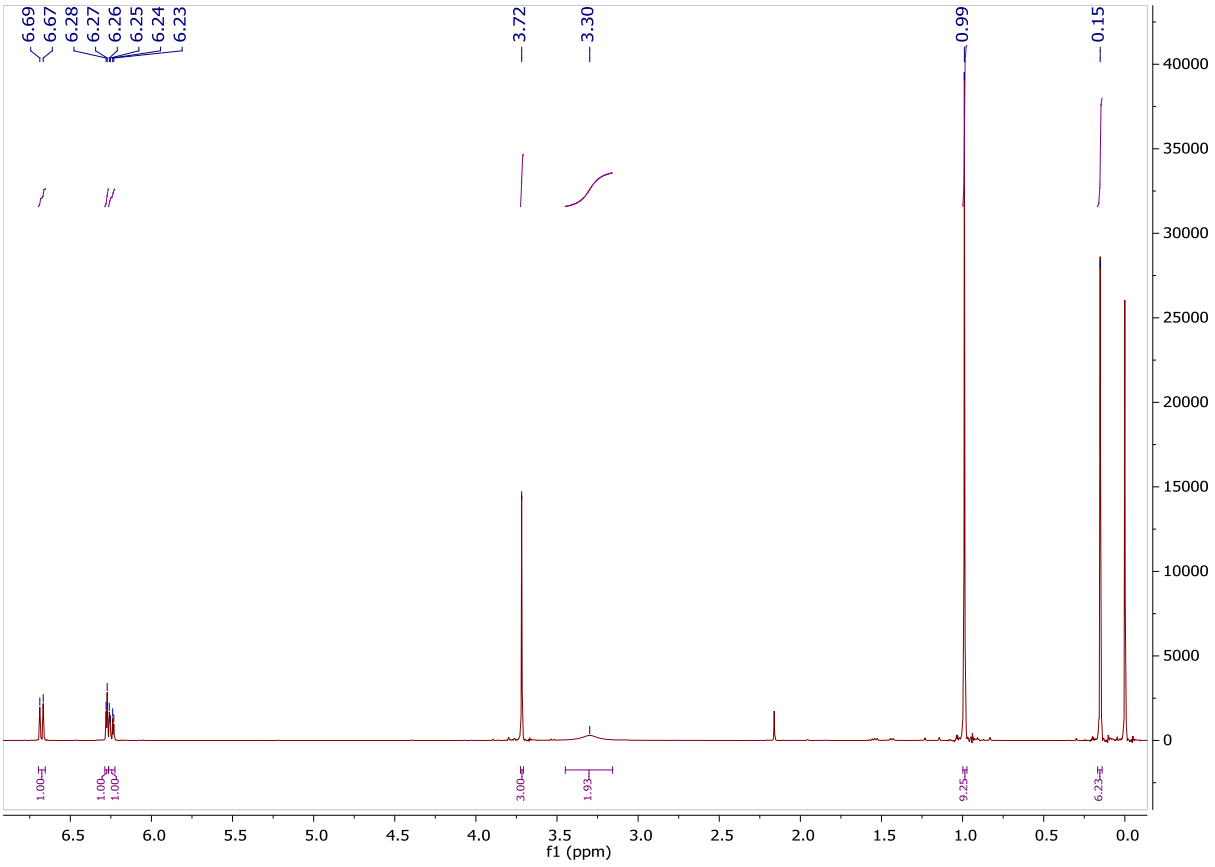

^{13}C NMR of 3-((*tert*-butyldimethylsilyl)oxy)-4-methoxyaniline, 2.2.

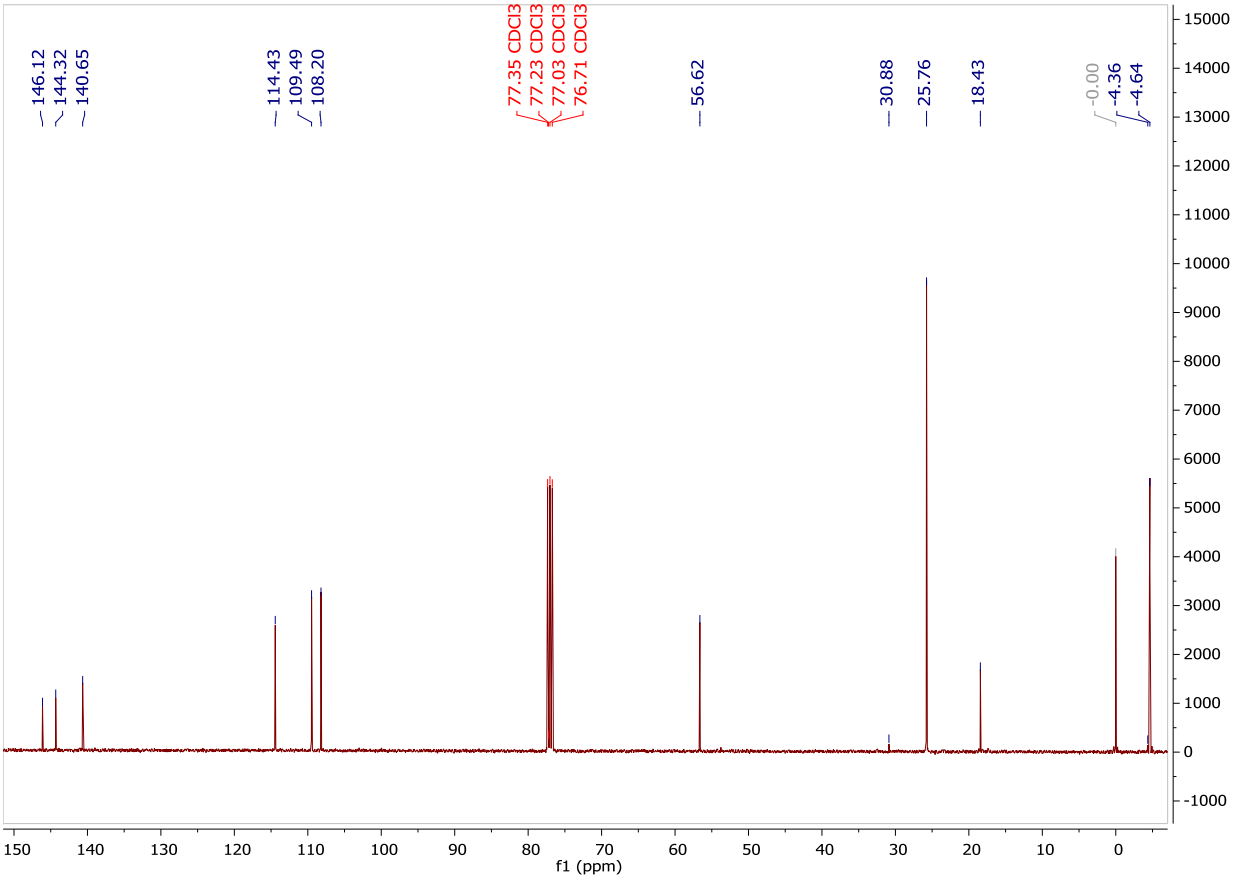

^{1}H NMR of (*E*)-1-(3-((*tert*-butyldimethylsilyl)oxy)-4-methoxyphenol)-2-(3,4,5-trimethoxyphenyl)diazene, 2.3.

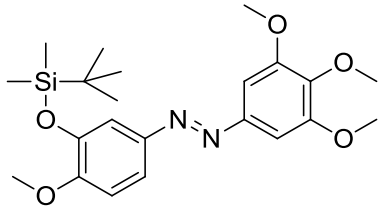

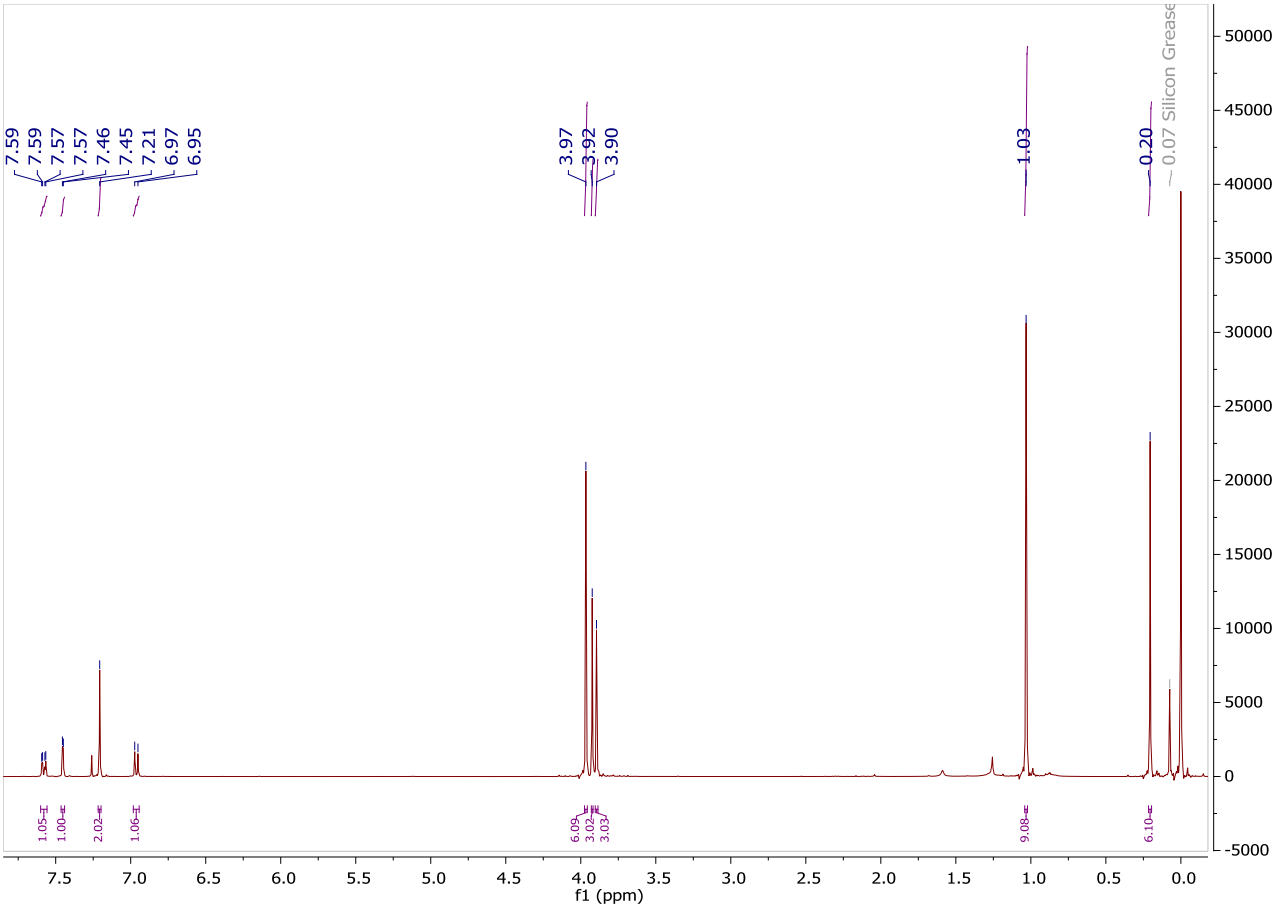

^{13}C NMR of (*E*)-1-(3-((*tert*-butyldimethylsilyl)oxy)-4-methoxyphenol)-2-(3,4,5-trimethoxyphenyl)diazene, 2.3.

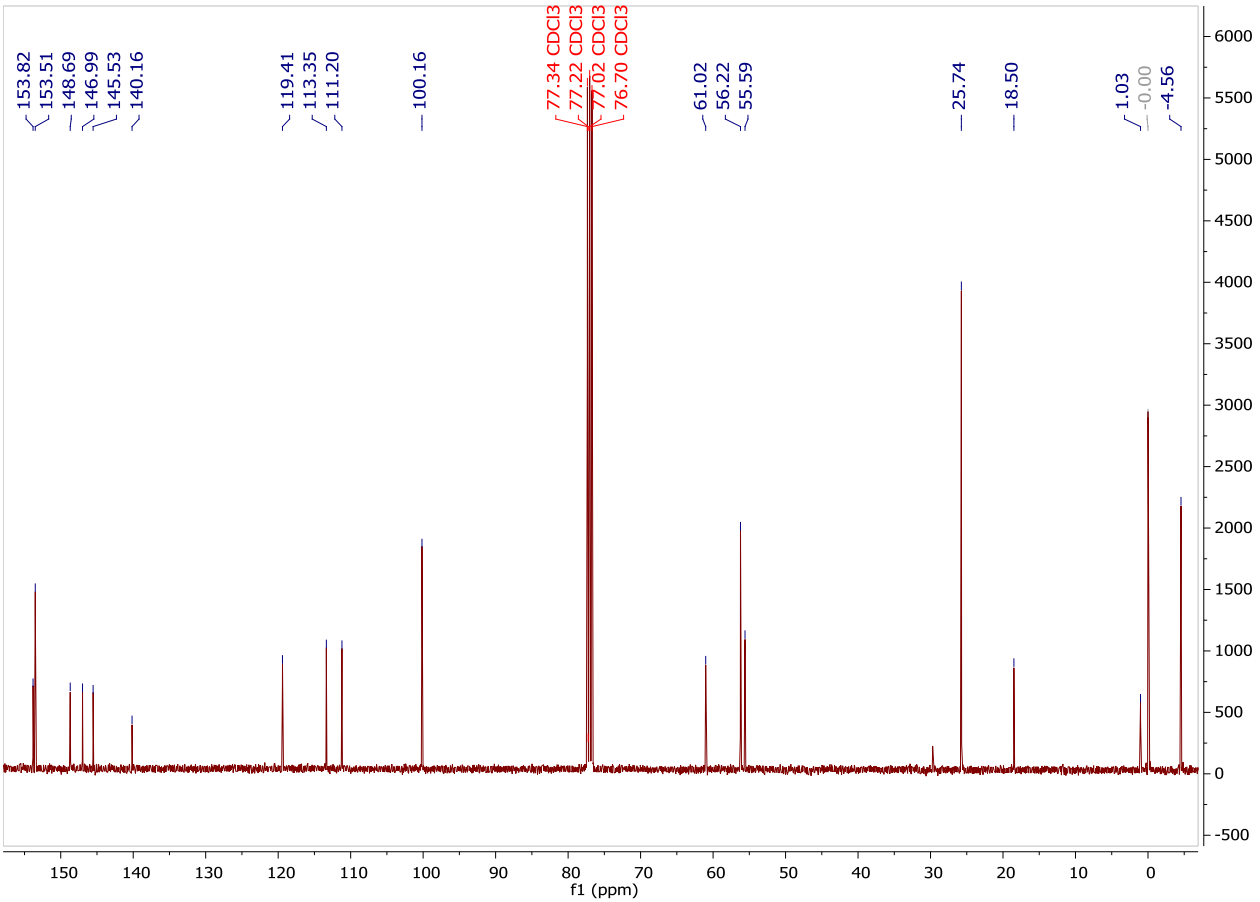

^{1}H NMR of (*E*)-2-methoxy-5-((3,4,5-trimethoxyphenyl)diazenyl)phenol, 2.4.

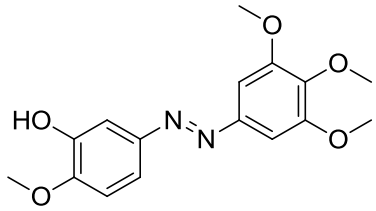

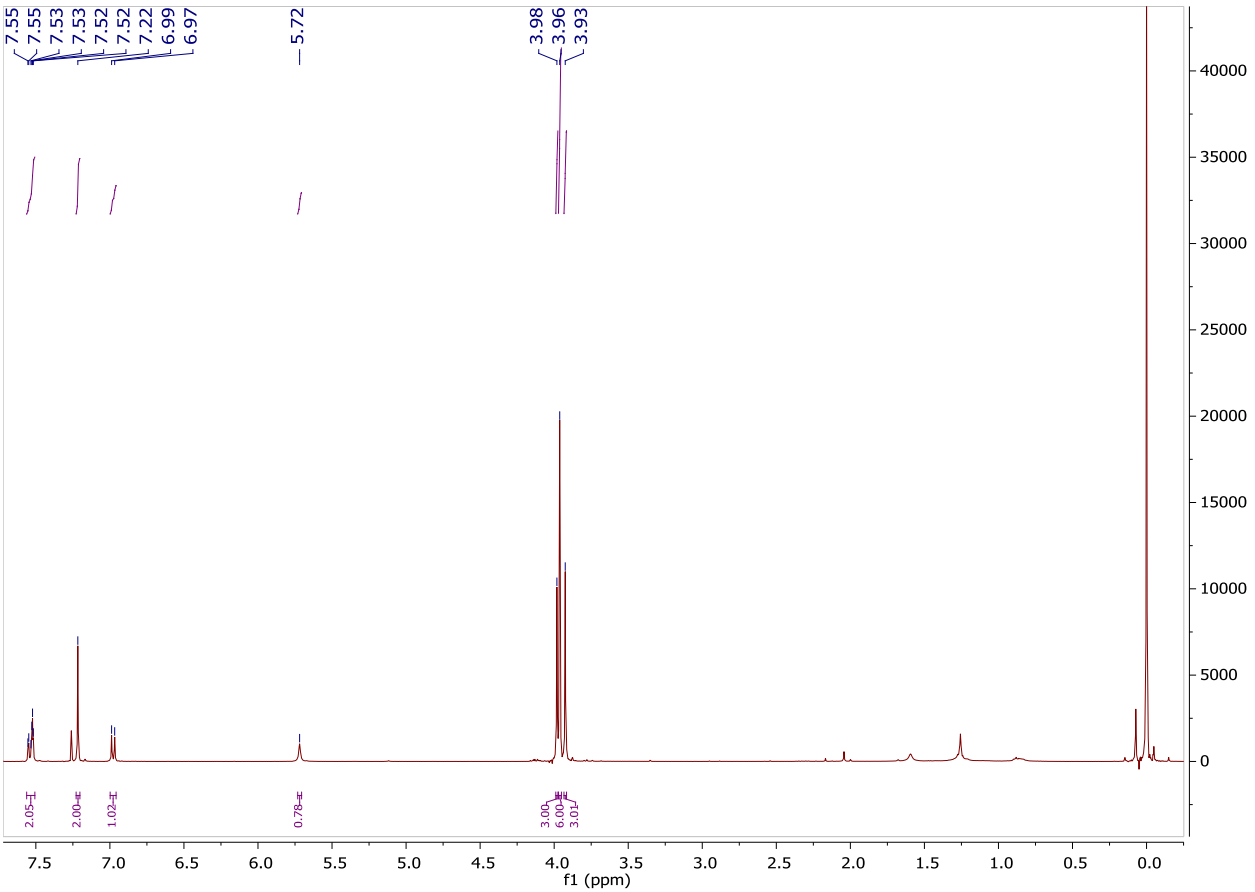

^{13}C NMR of (*E*)-2-methoxy-5-((3,4,5-trimethoxyphenyl)diazenyl)phenol, 2.4.

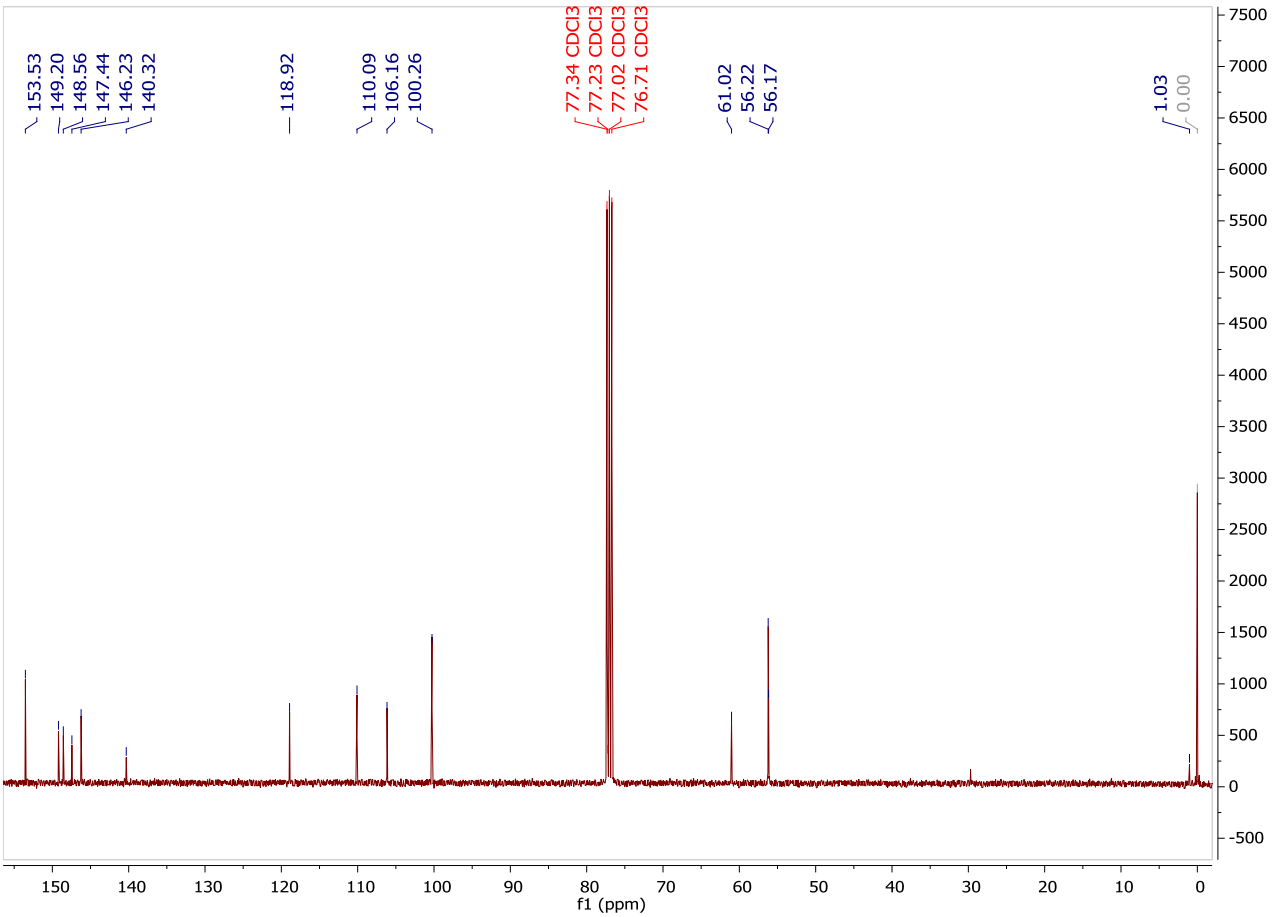

^{1}H NMR of Bis-p-tosyltriethylene glycol, 3.1

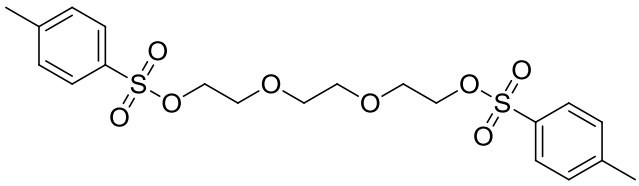

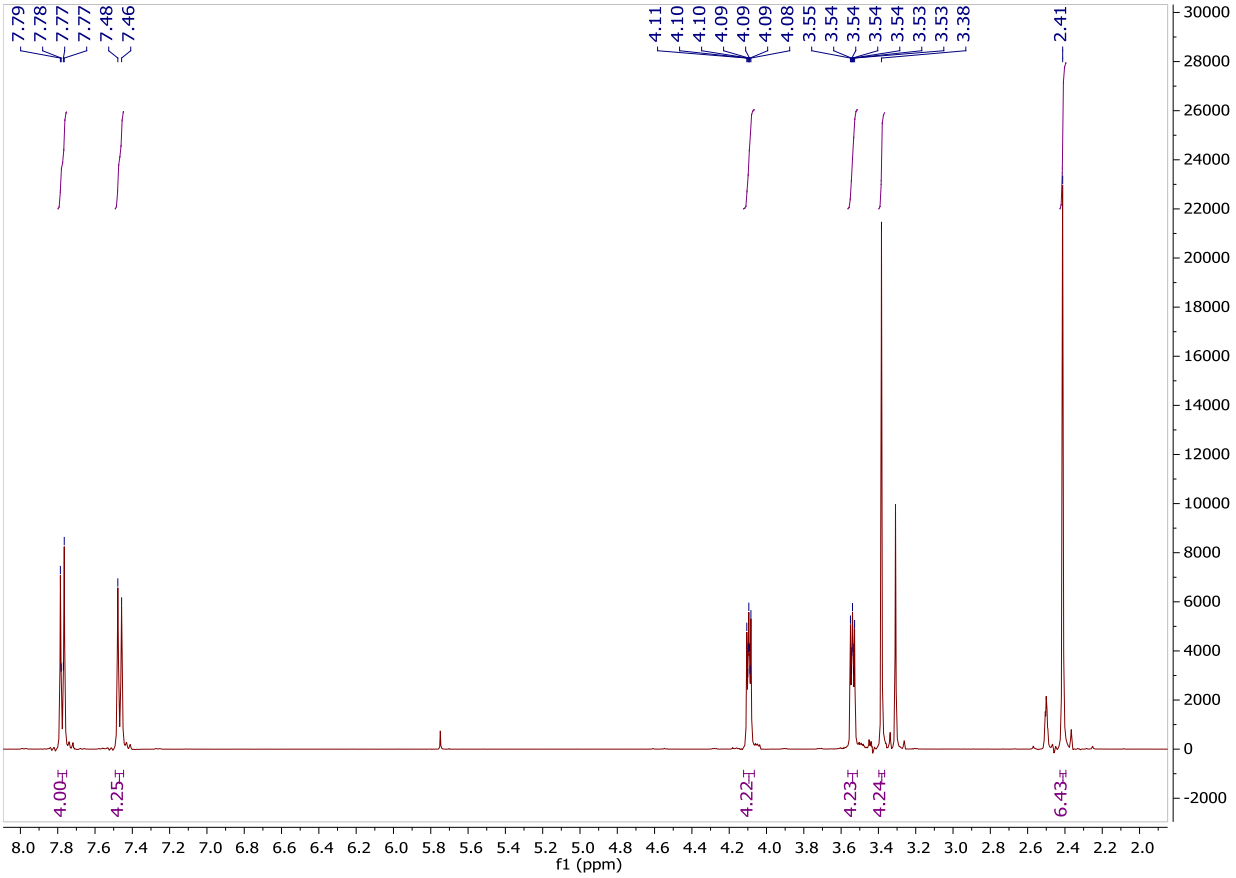

^{1}H NMR of bis-azidetriethylene glycol, 3.2

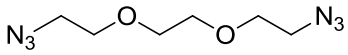

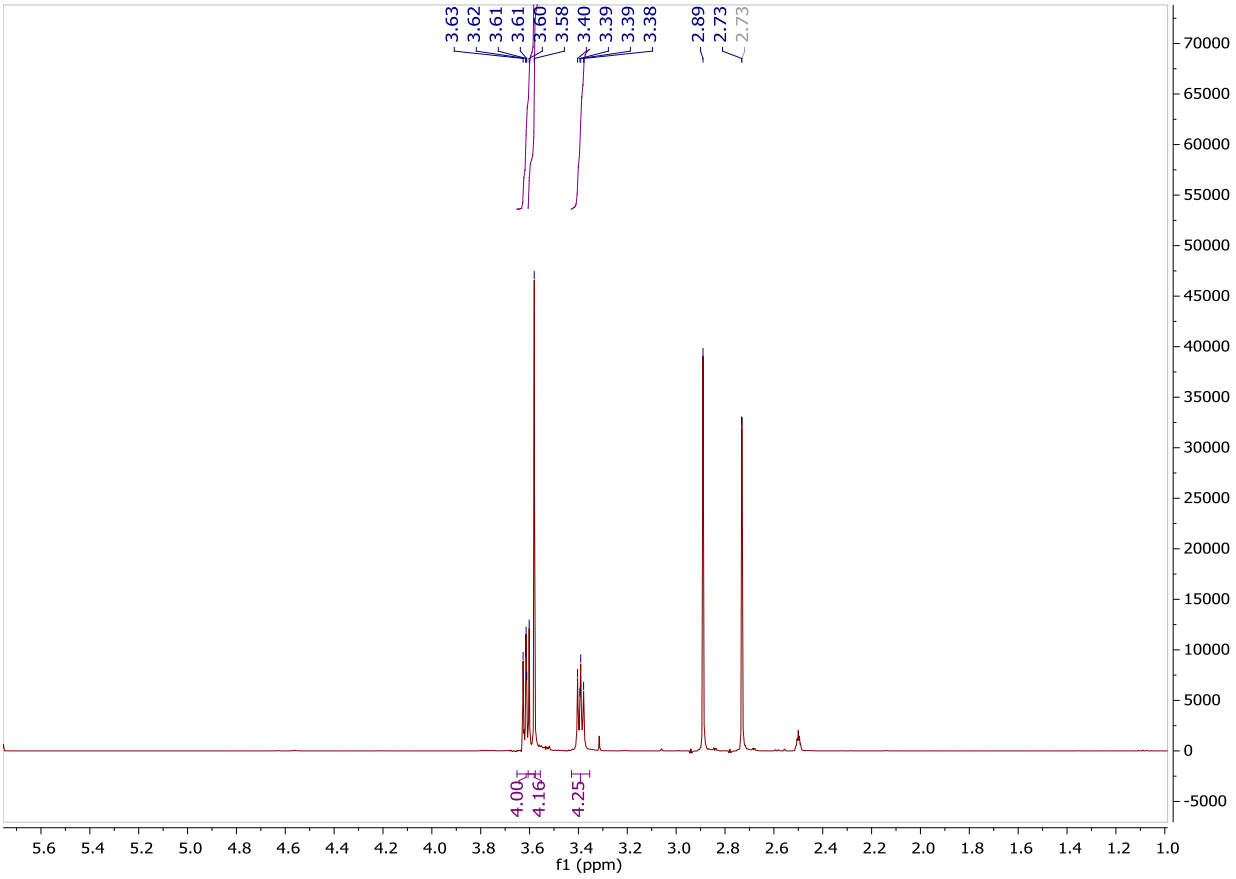

^{1}H NMR of 2-(2-(2-azidoethoxy)ethoxy)ethanamine, 3.3.

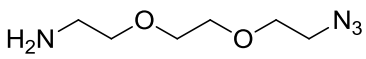

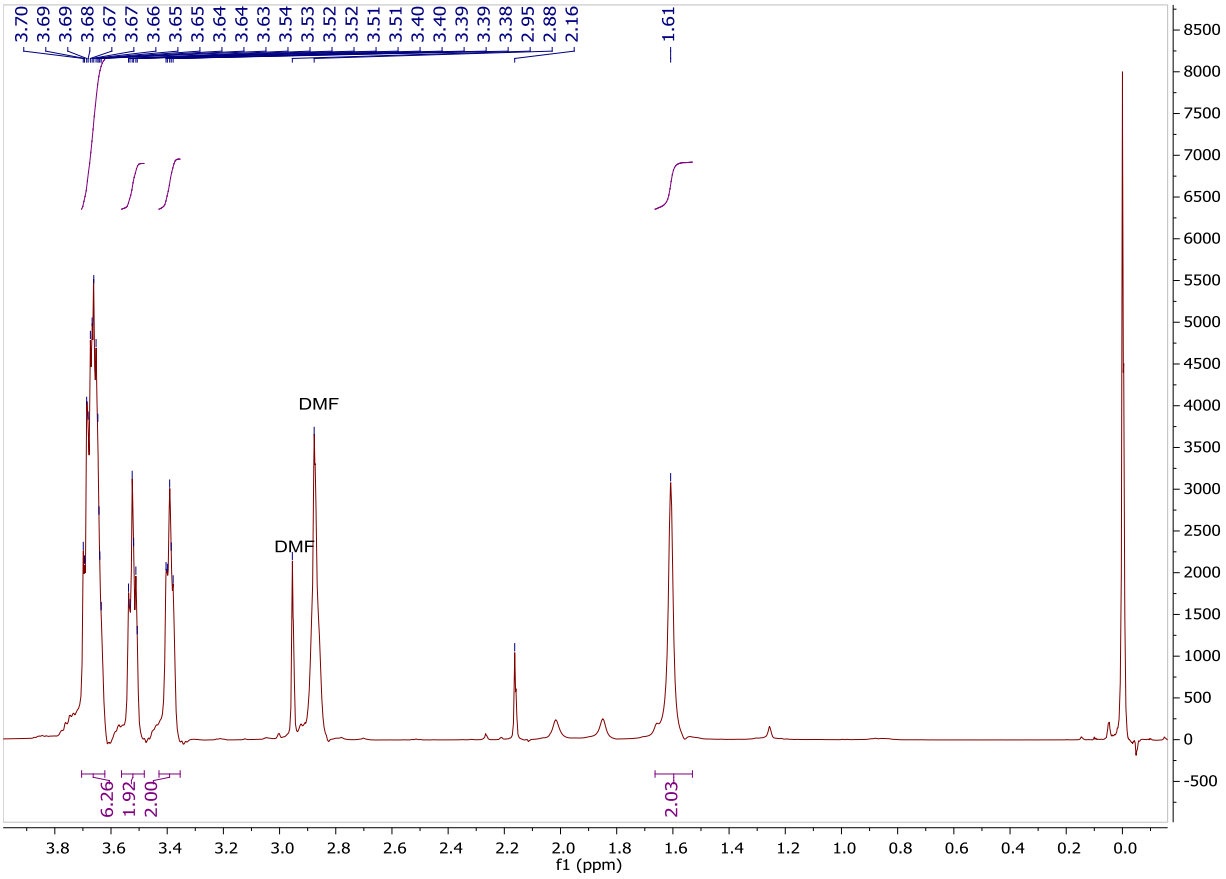

^{19}F NMR of N ^{2,10}-Bis(trifluoroacetyl)pyrofolic acid/anhydride, 3.4.

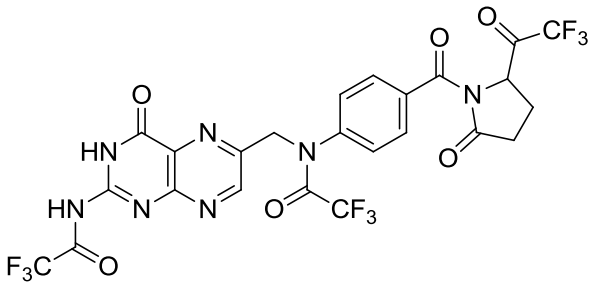

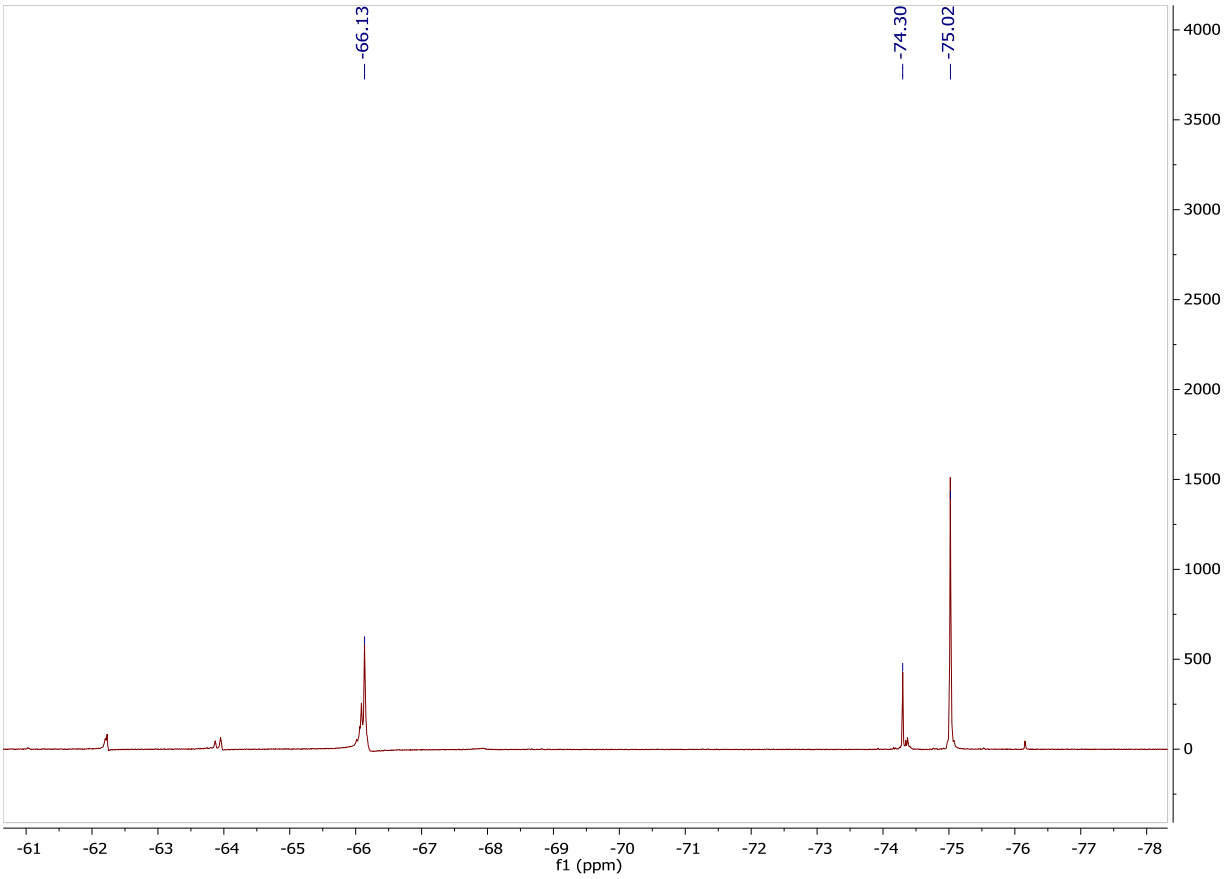

^{1}H NMR of N^{10}-(Trifluoroacetyl)pyrofolic acid, 3.5.

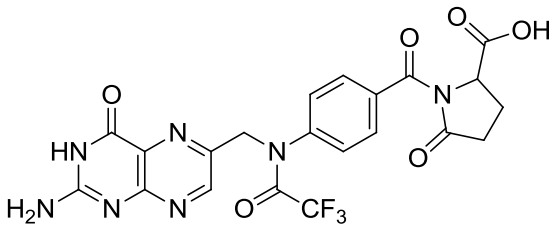

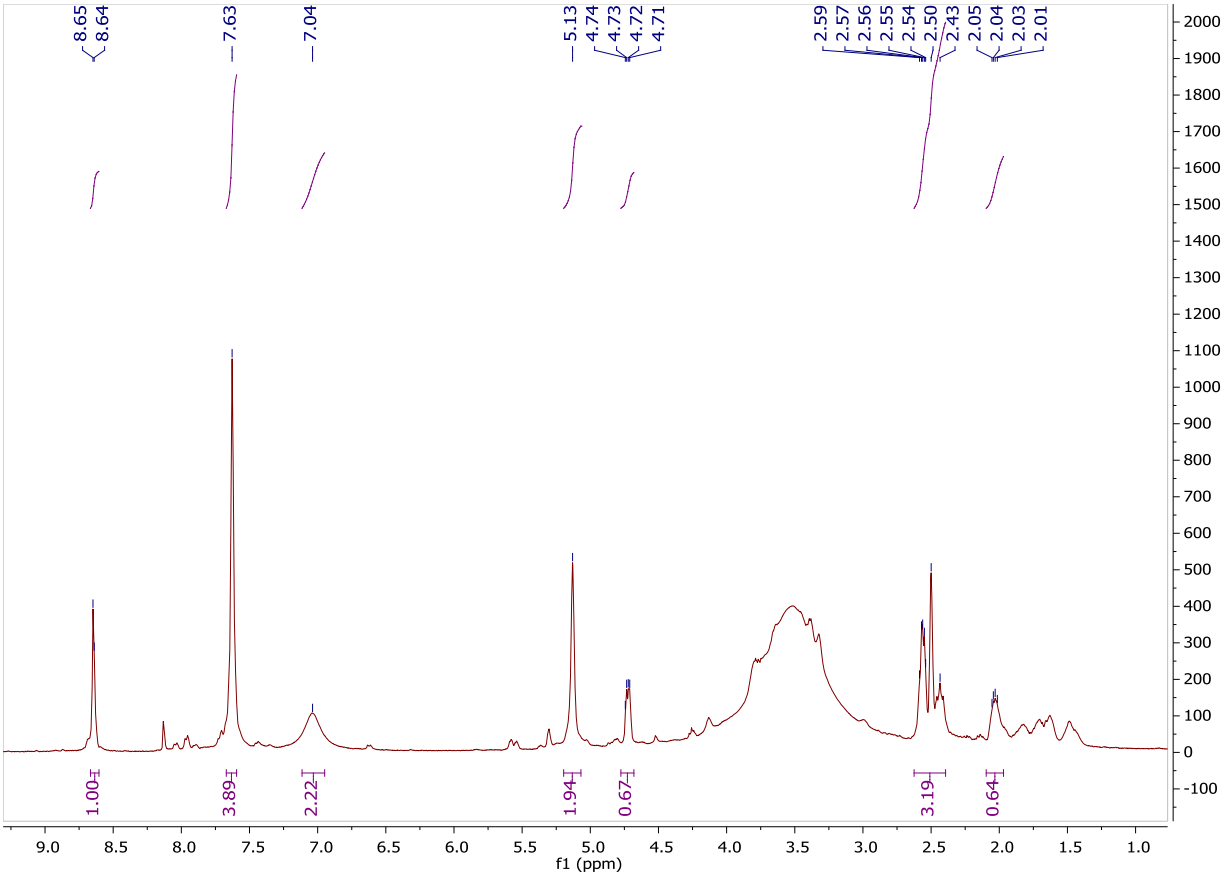

^{1}H NMR of Pteroyl hydrazide, 3.6.

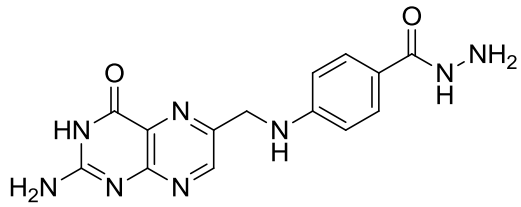

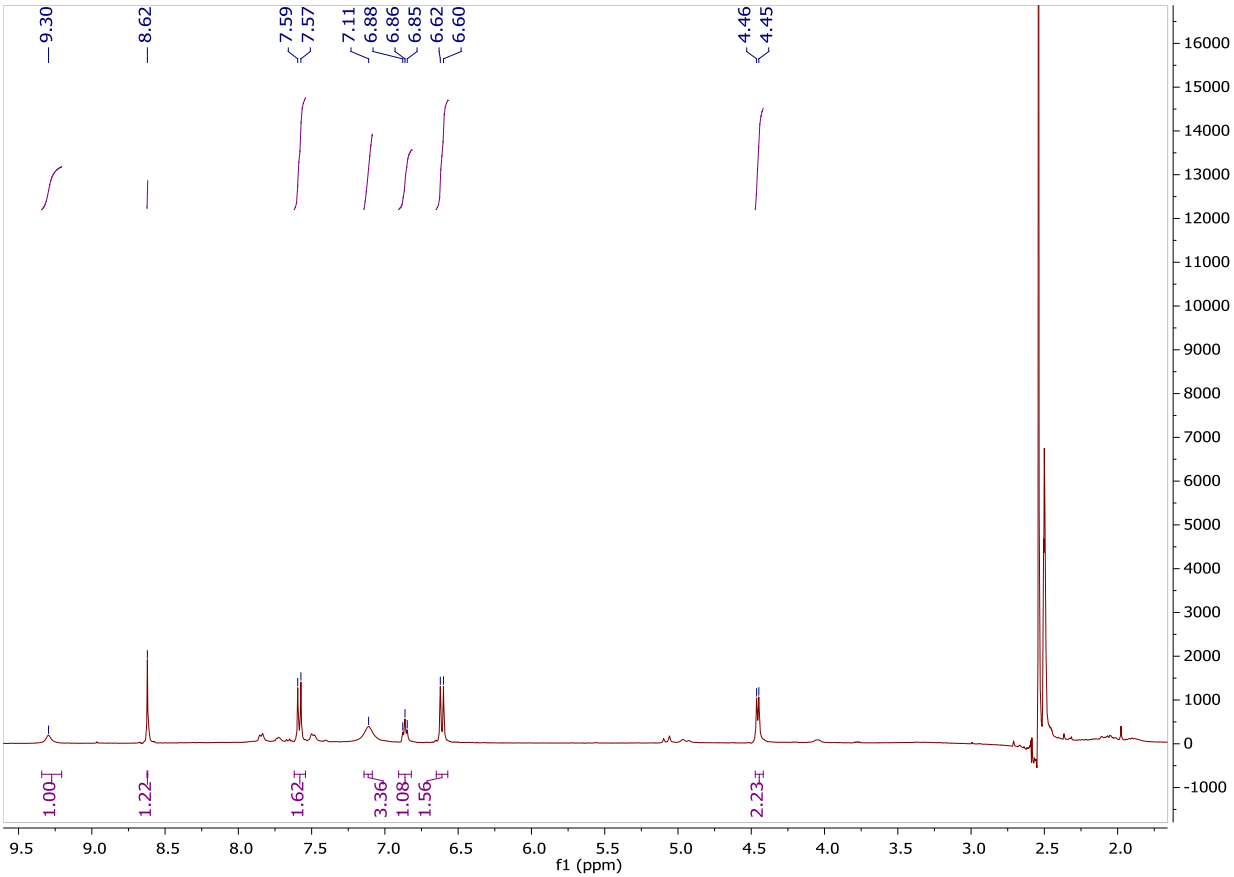

^{1}H NMR of Pteroyl azide, 3.7.

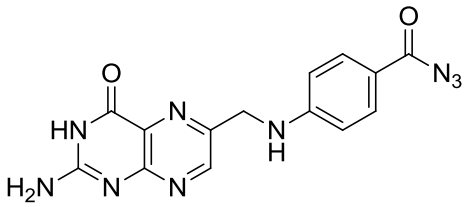

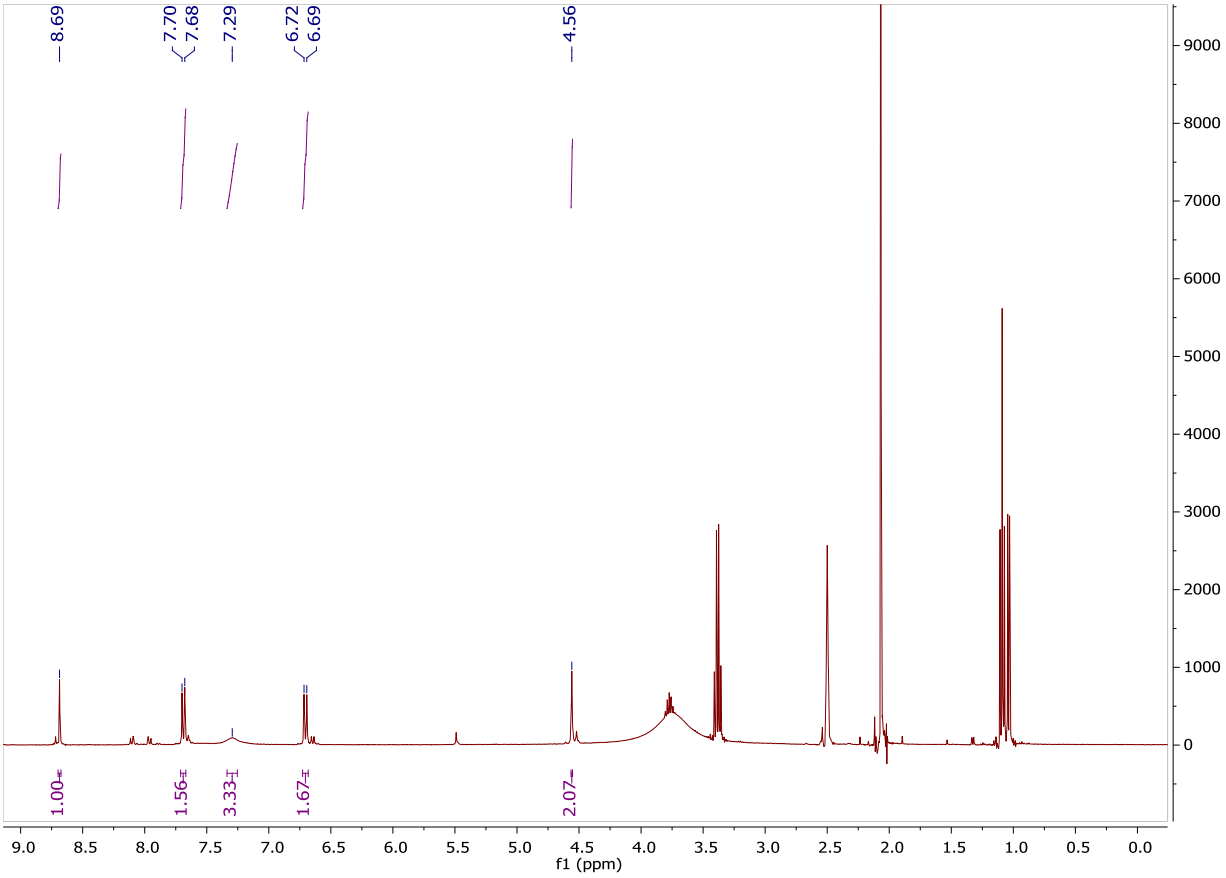

^{1}H NMR of Boc-Glu-OtBu-NHS, 3.8.

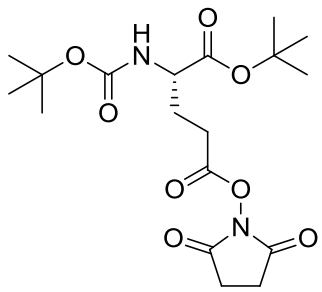

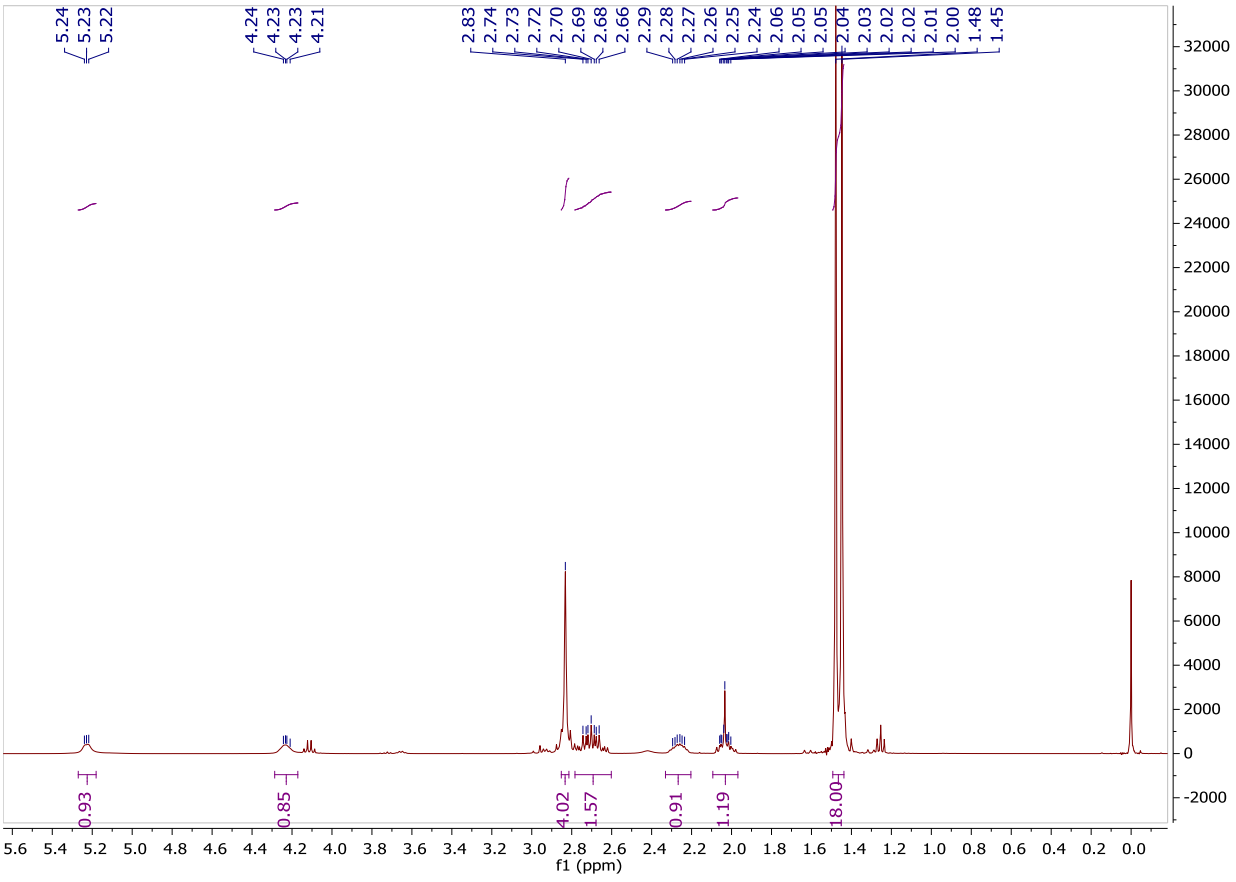

^{1}H NMR of Boc-Glu-OtBu-PEG-Azide, 3.9.

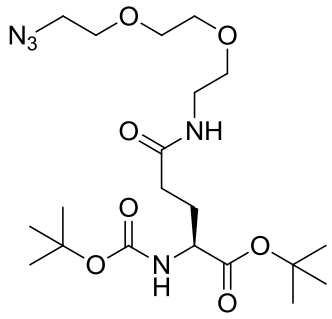

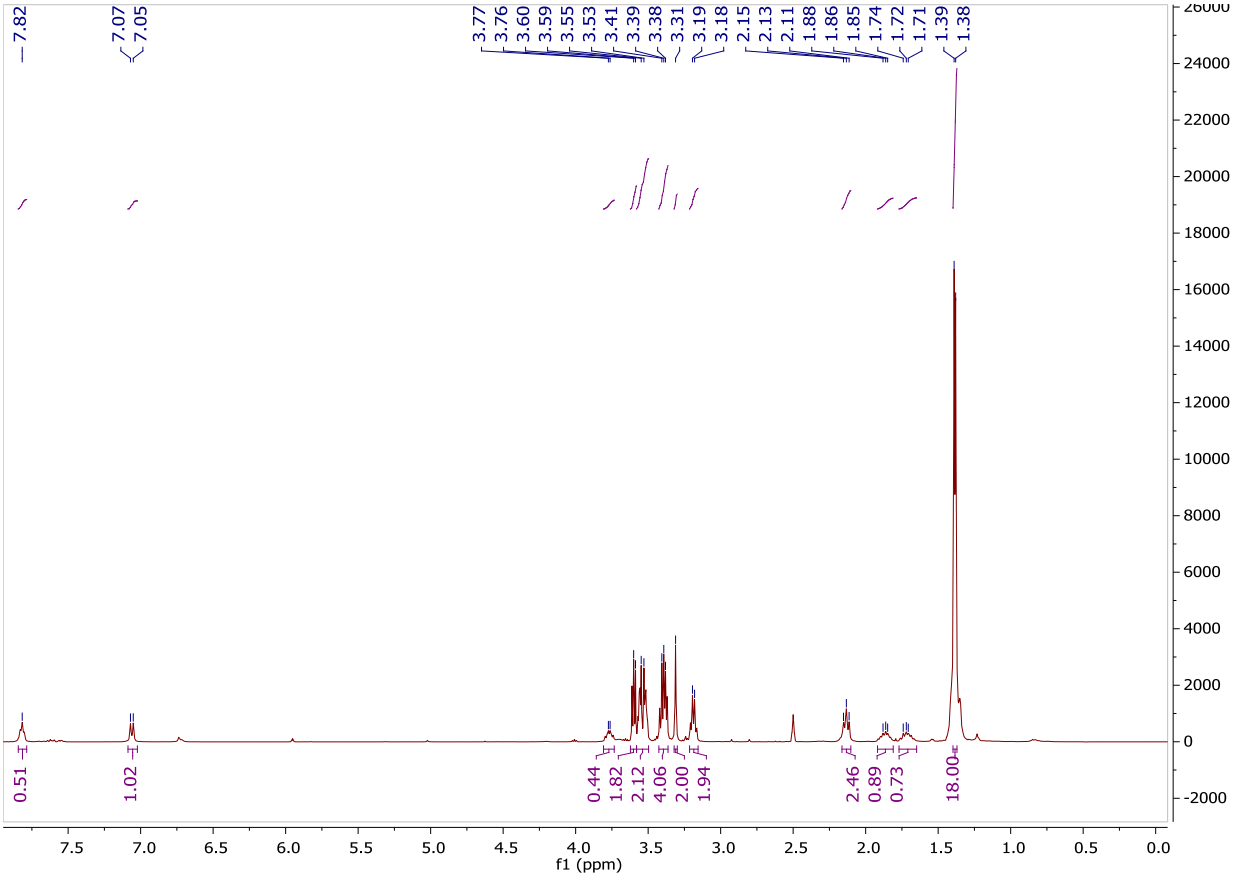

^{13}C NMR of Boc-Glu-OtBu-PEG-Azide, 3.9.

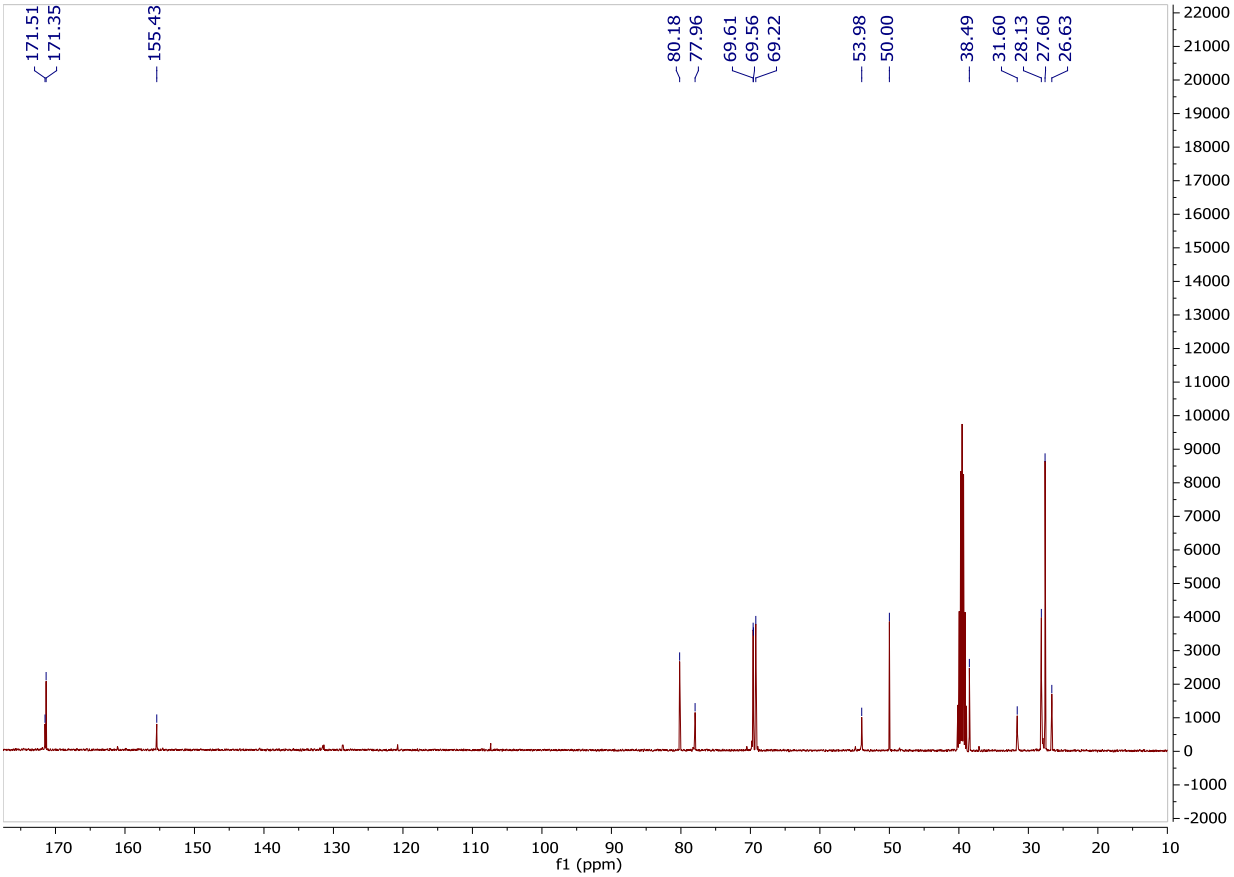

^{1}H NMR of Glu-PEG-Azide, 3.10

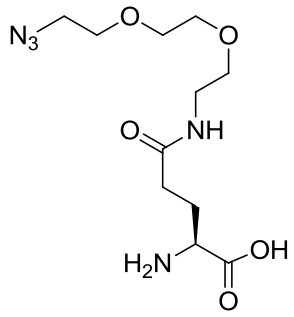

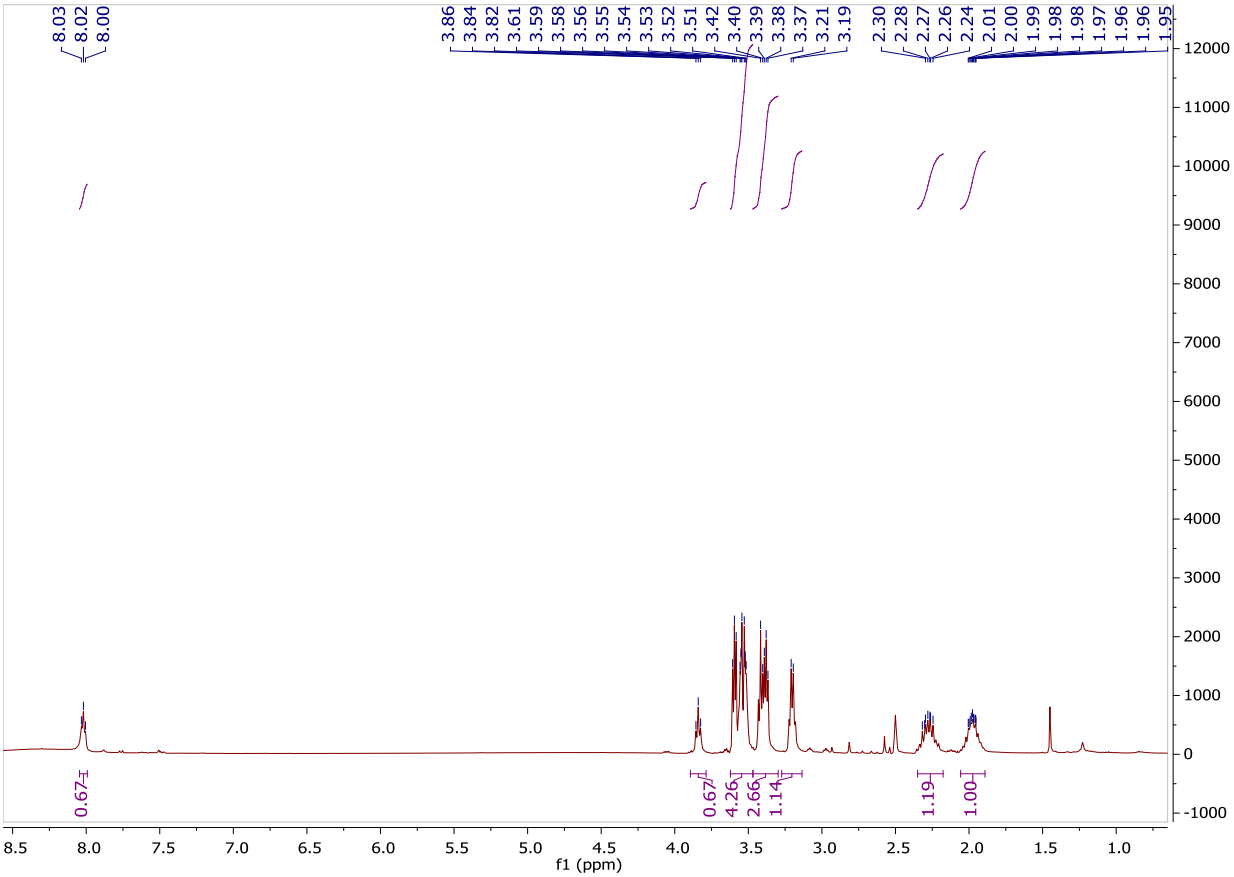

^{1}H NMR of 2,5-dioxopyrrolidin-1-yl 4-(4-(1-hydroxyethyl)-2-methoxy-5-nitrophenoxy)butanoate, 3.12.

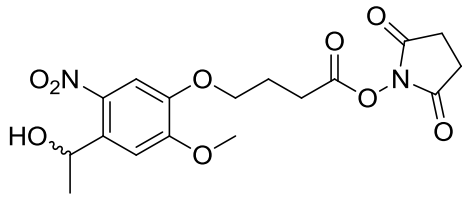

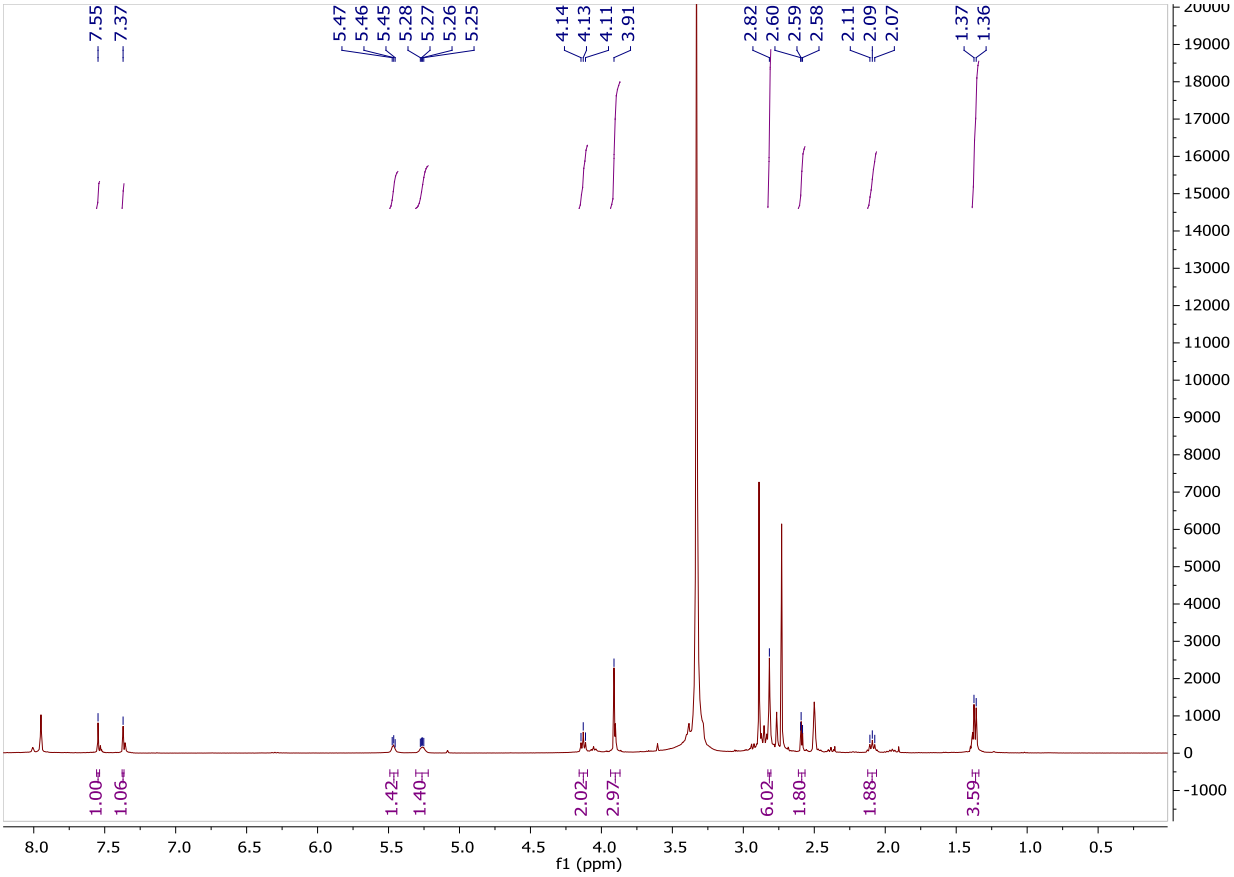

^{1}H NMR of 4-(4-(1-hydroxyethyl)-2-methoxy-5-nitrophenoxy)-N-(prop-2-yn-1-yl)butanamide, 3.13.

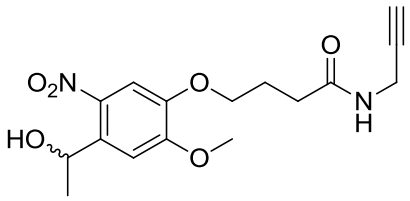

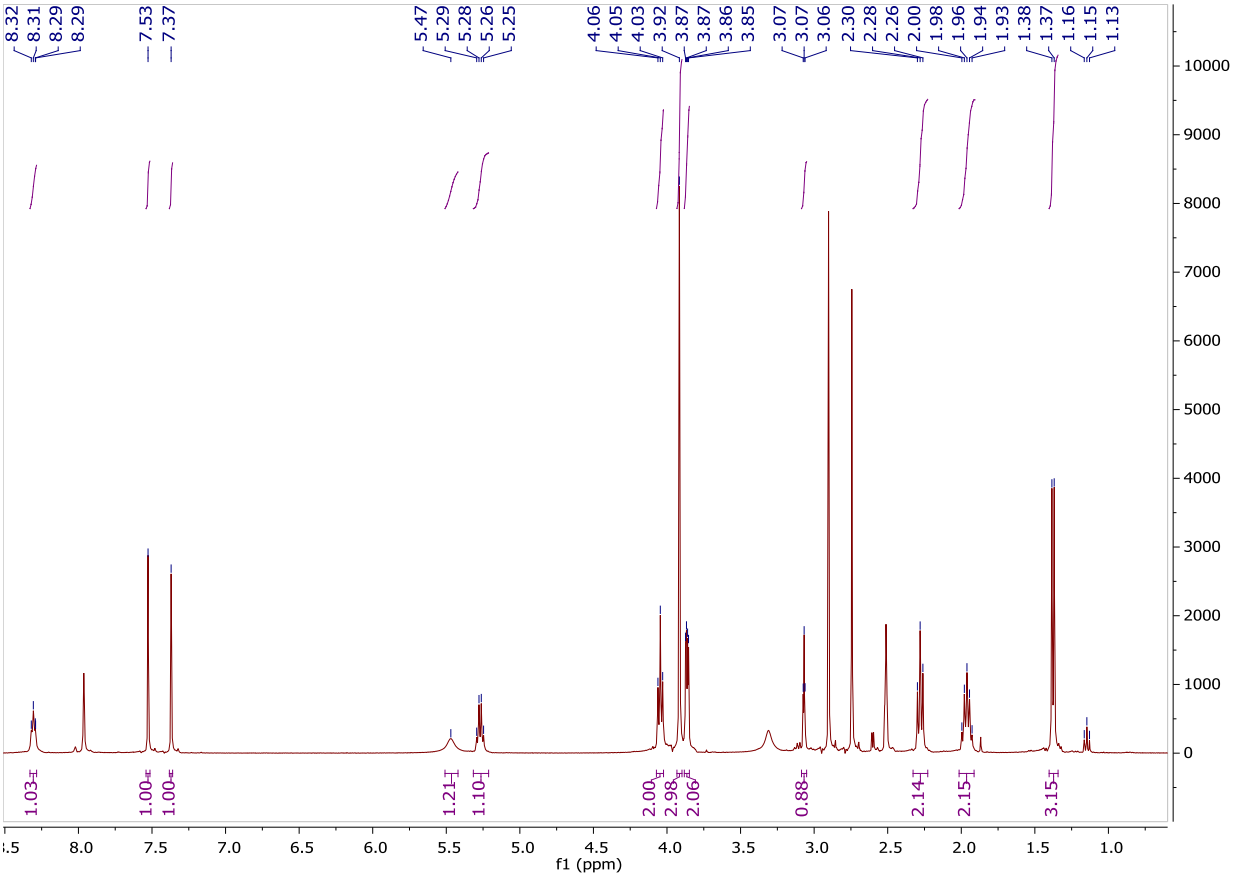

^{1}H NMR of 1-(5-methoxy-2-nitro-4-(4-oxo-4-(prop-2-yn-1-ylamino)butoxy)phenyl)ethyl (4- nitrophenyl) carbonate, 3.14

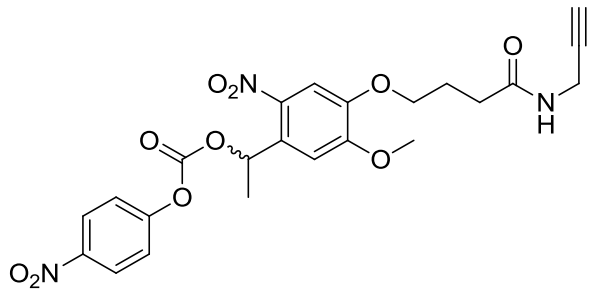

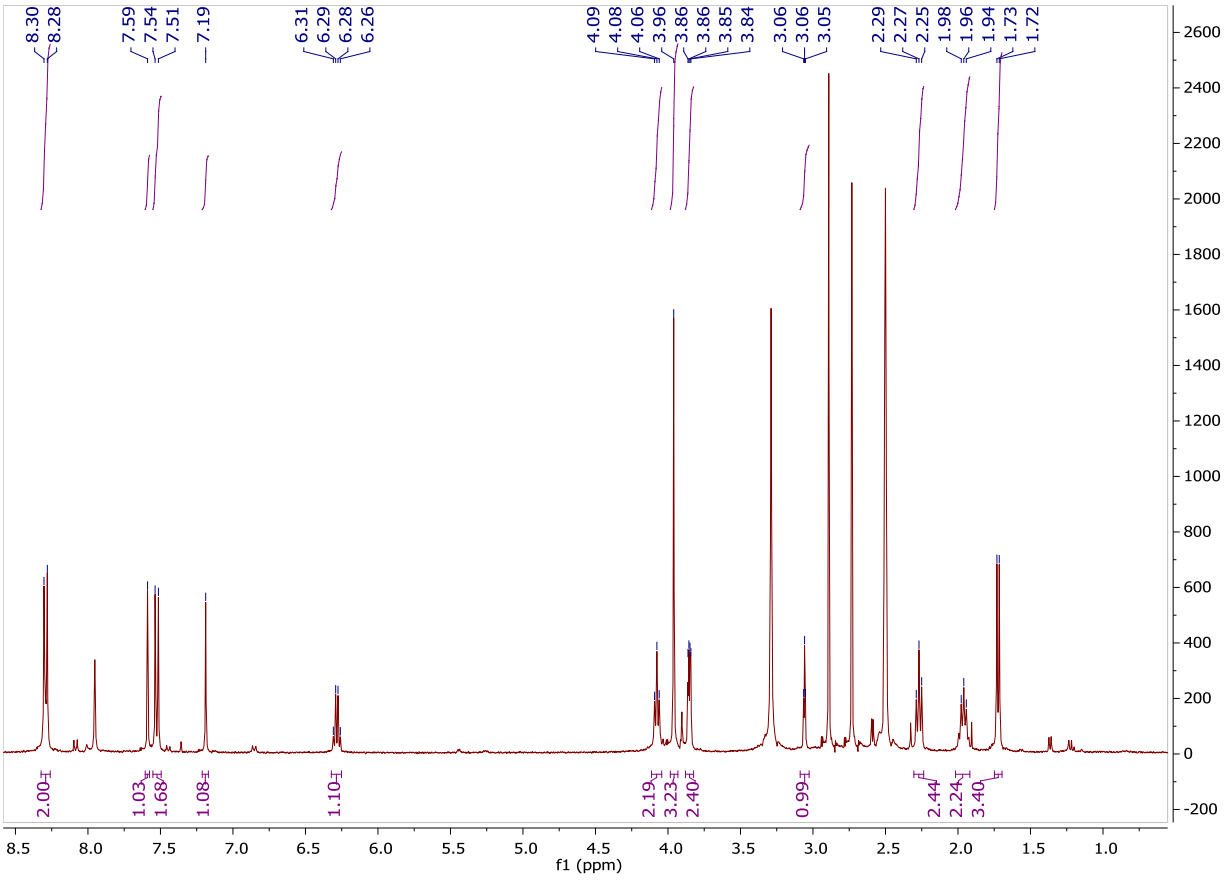

^{1}H NMR of Dox-NV-alkyne, 3.15.

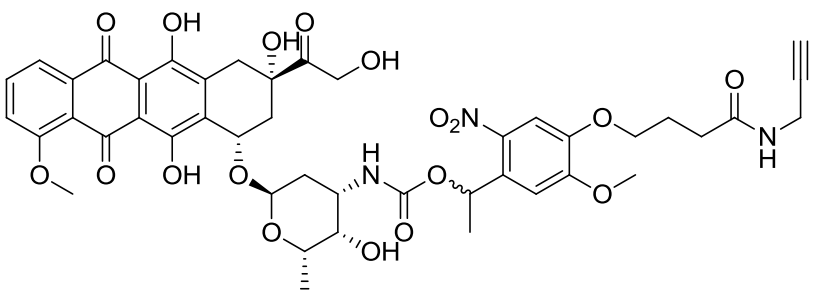

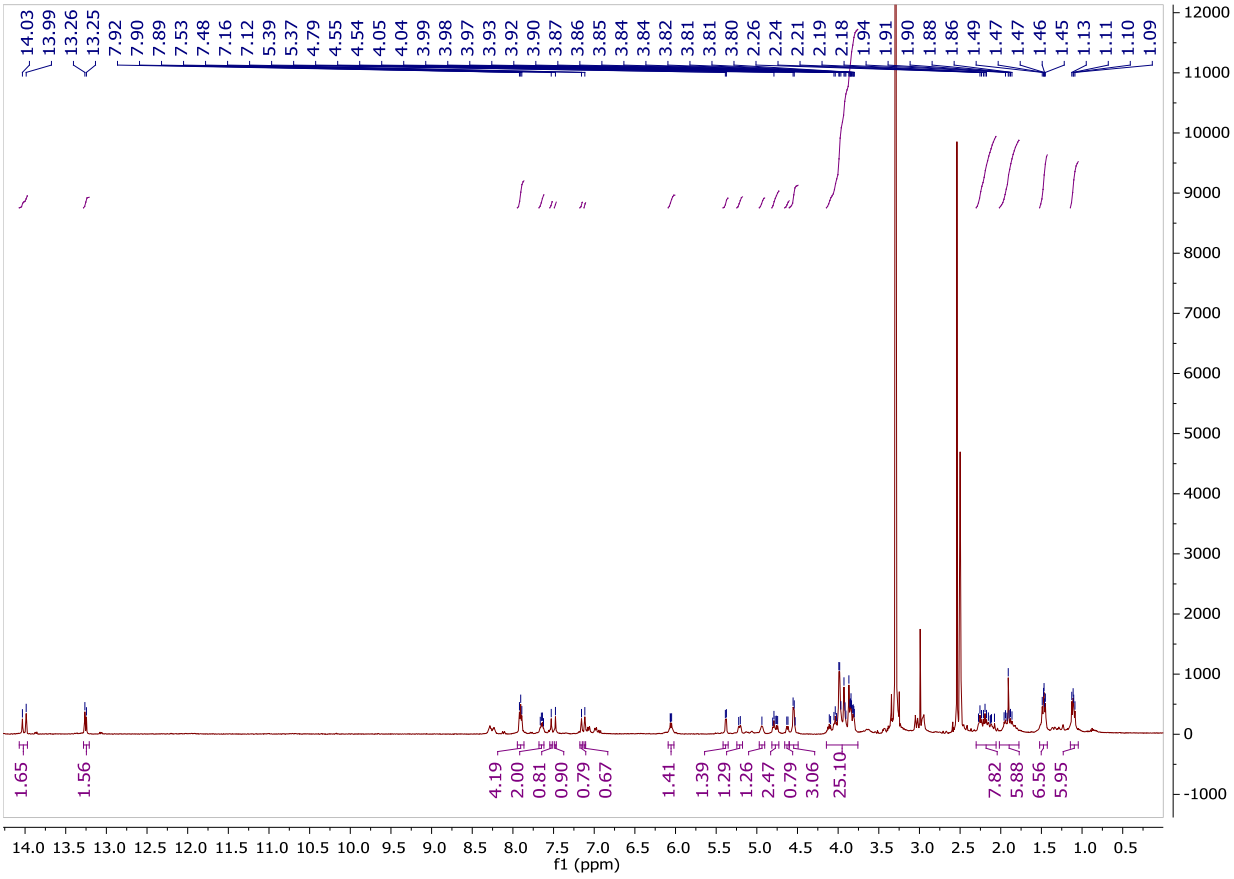

^{1}H NMR of 2,5-dioxopyrrolidin-1-yl 4-azidobenzoate, 3.16.

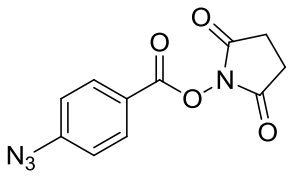

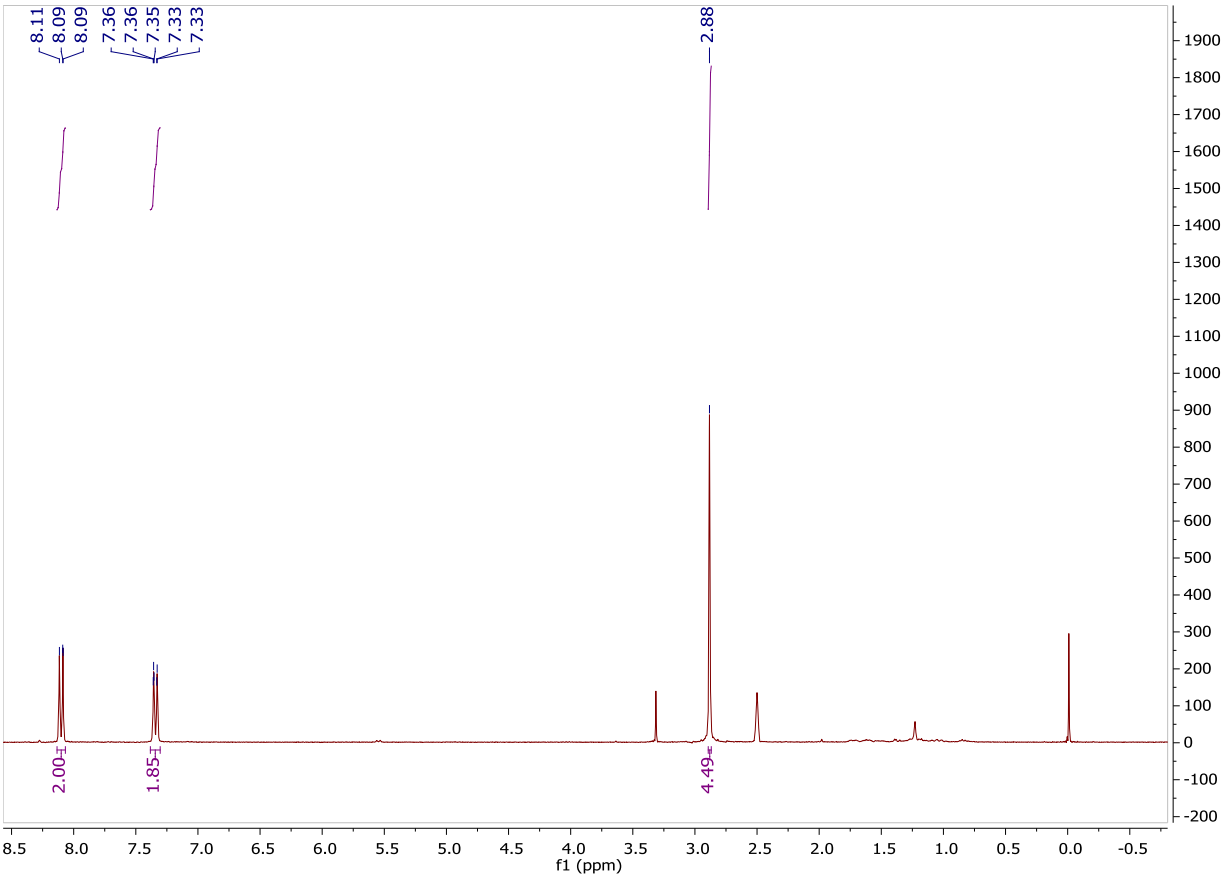

^{1}H NMR of 5-((2-(4-azidobenzamido)ethyl)amino)naphthalene-1-sulfonic acid, 3.17.

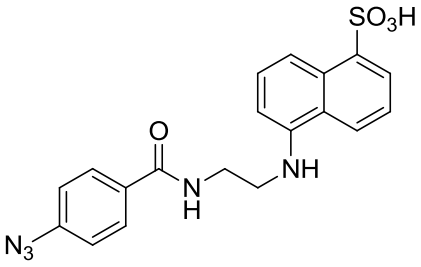

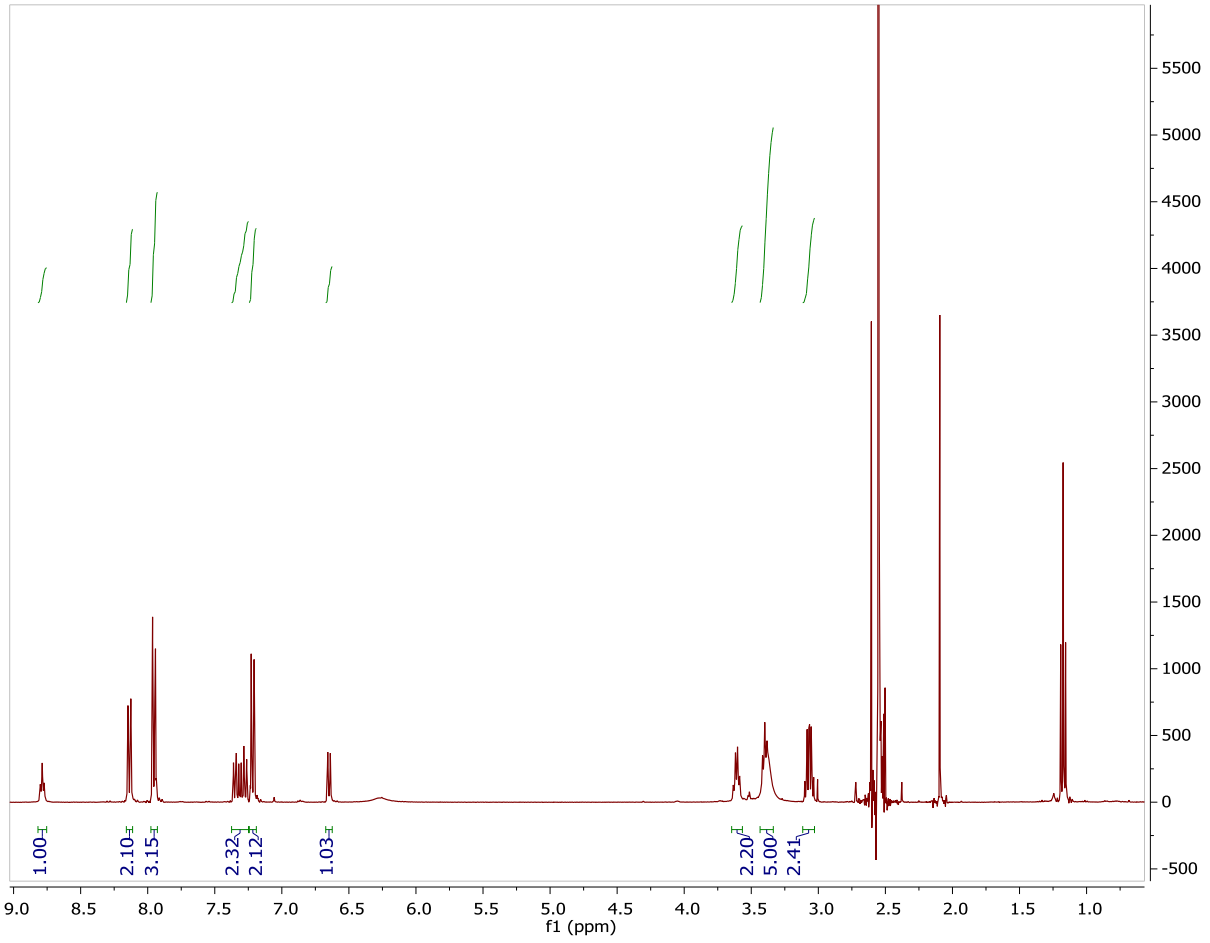

^{1}H NMR of Dox-NV-EDANS, 3.18.

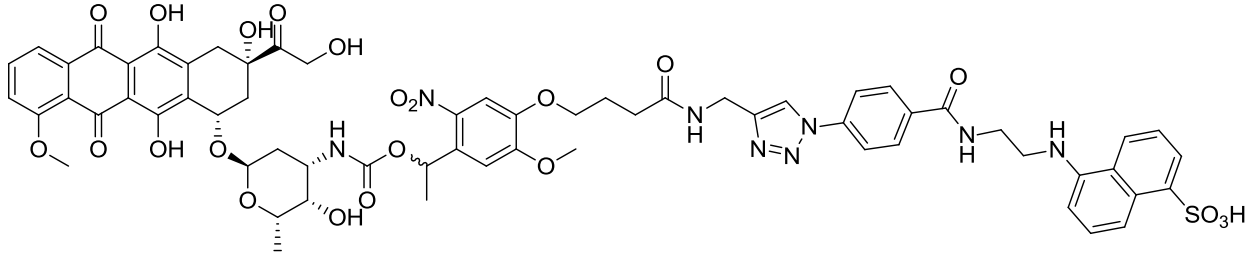

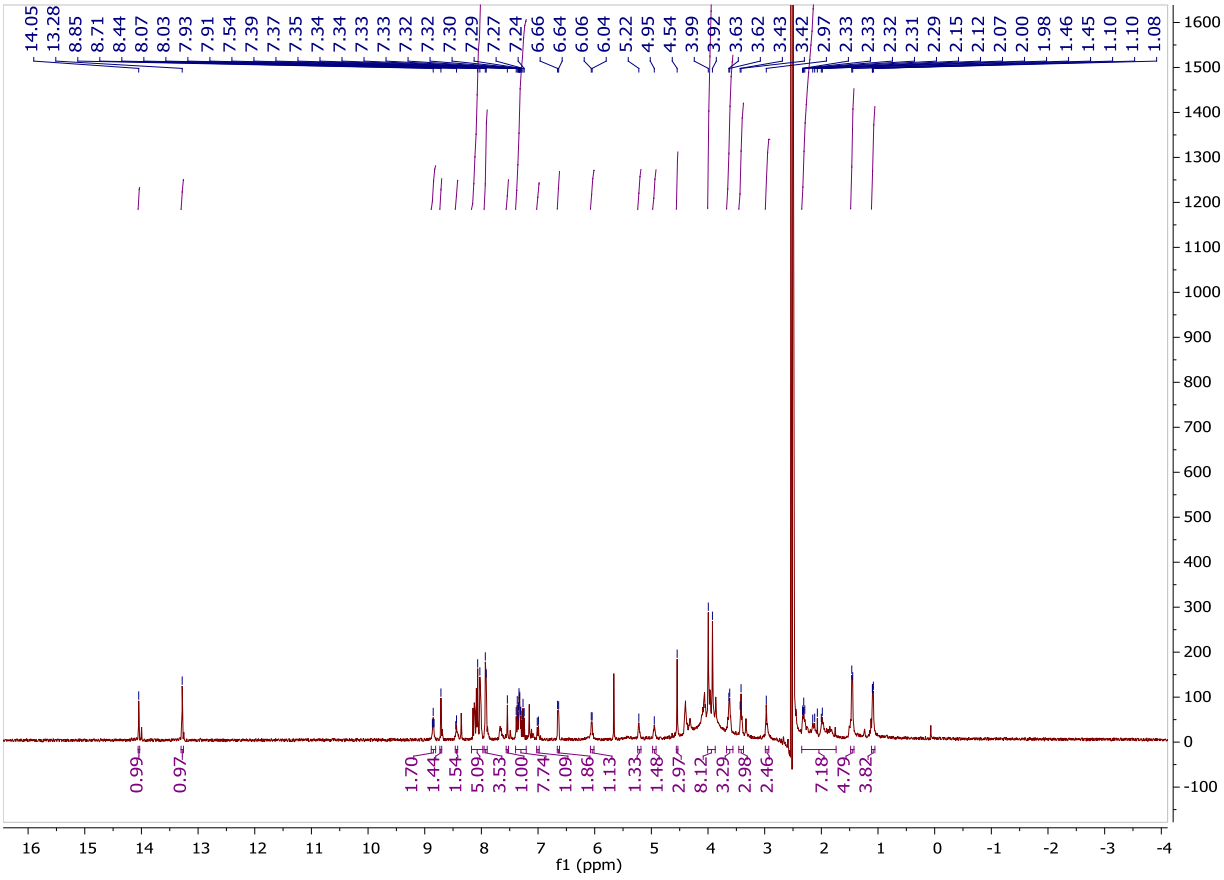

^{1}H NMR of Fmoc-Cav-OH, 4.1.

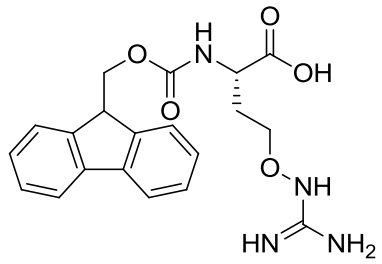

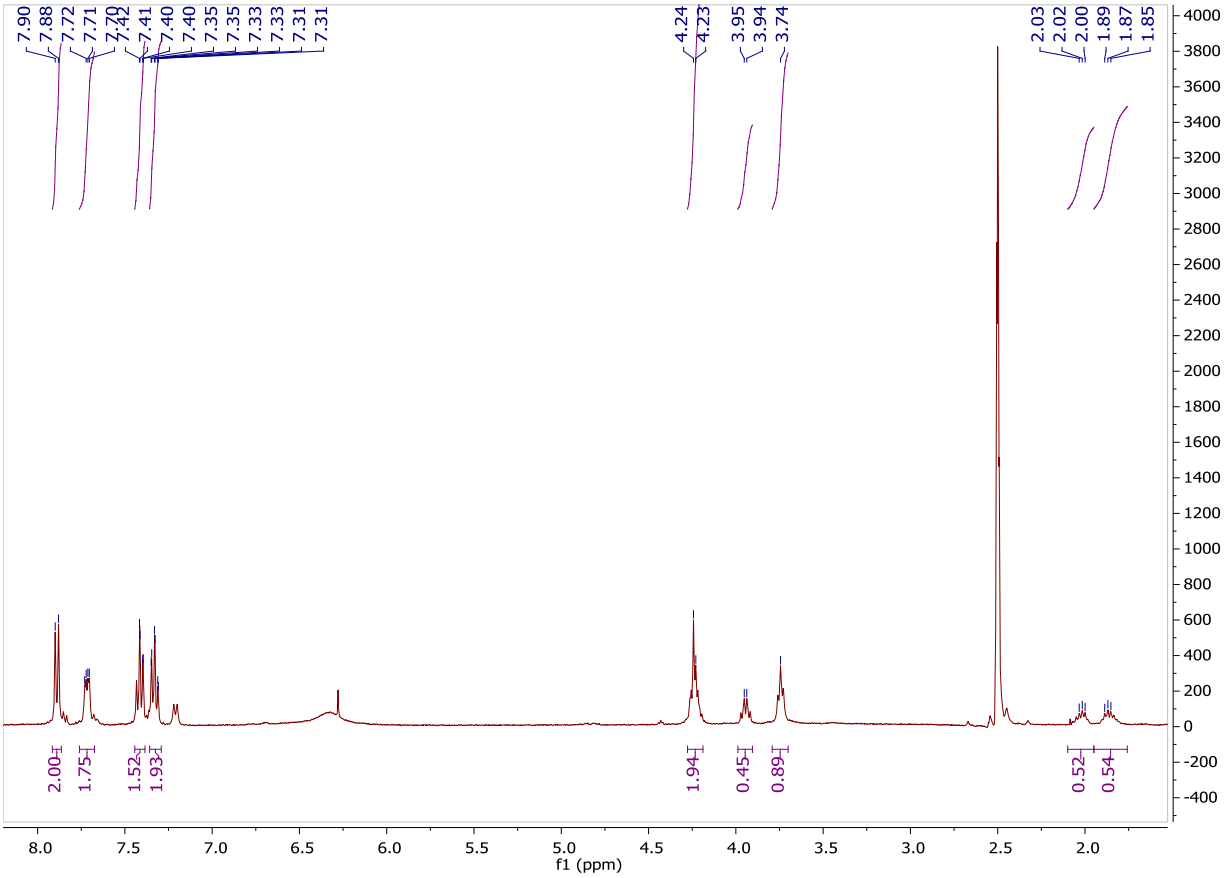

^{1}H NMR of Fmoc-(2-oxotetrahydrofuran-3-yl)carbamate, 4.4.

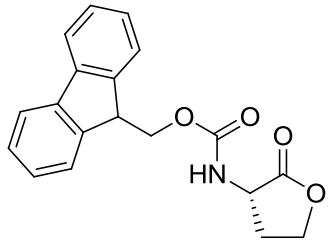

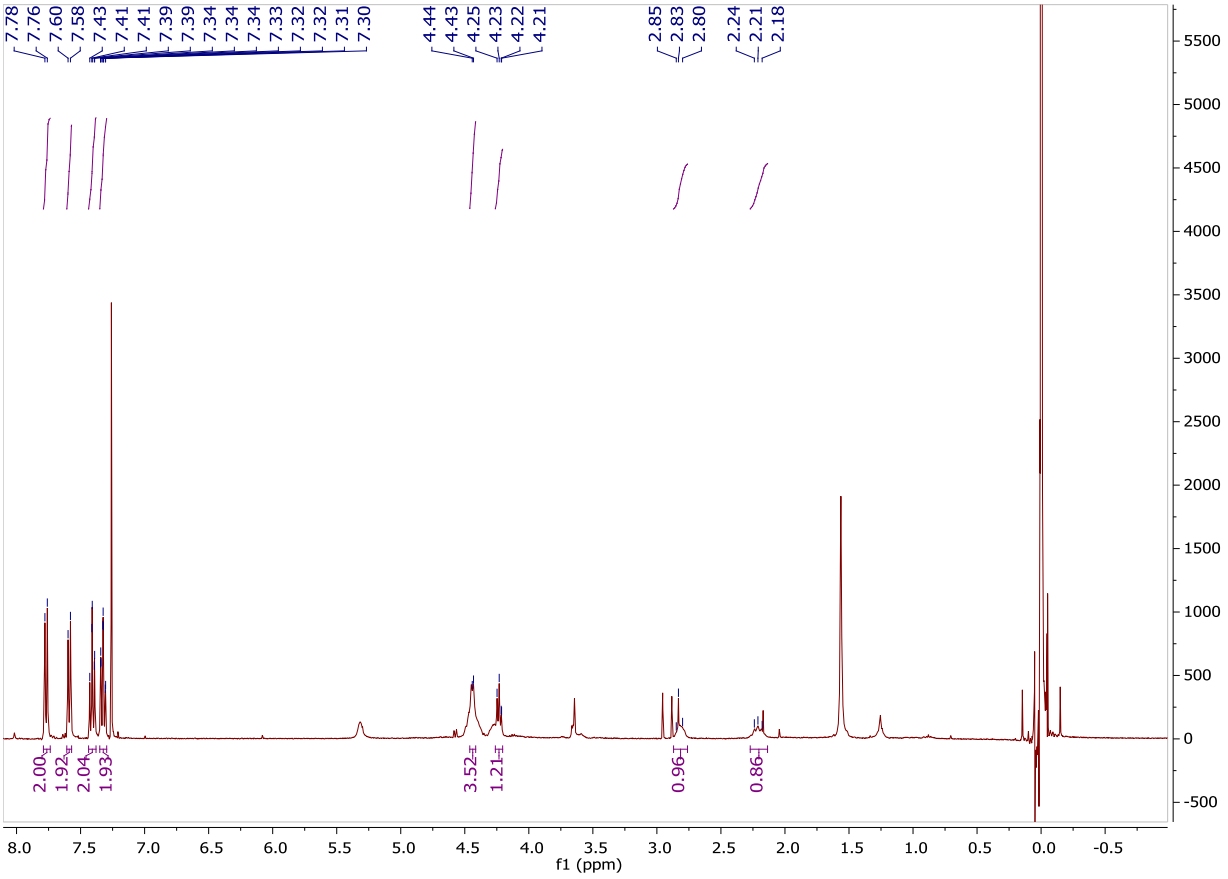

^{1}H NMR of (Z)-tert-butyl(((tert-butoxycarbonyl)imino)(N-hydroxyl)methyl)carbamate, 4.6.

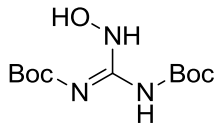

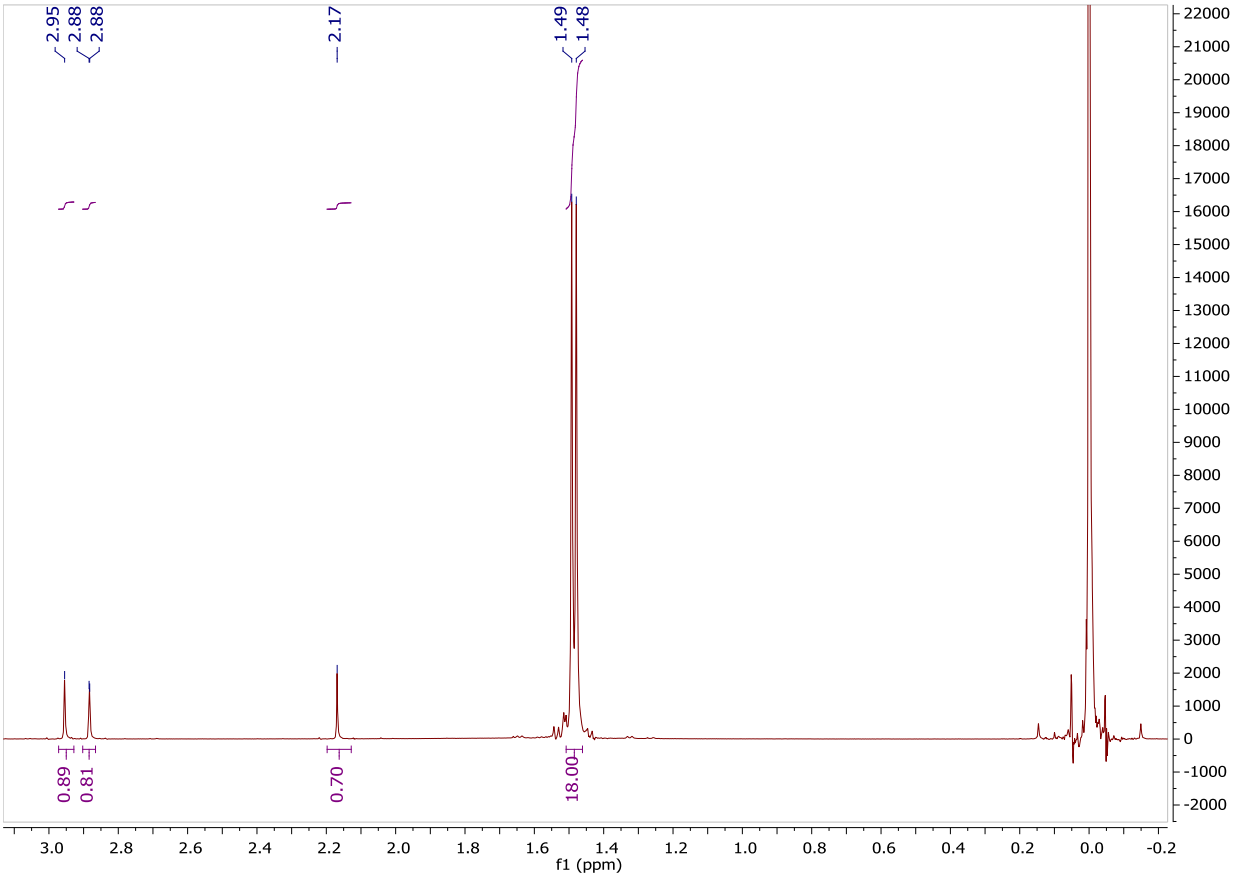

^{1}H NMR of (S)-methyl 2-amino-4-bromobutanoate, 4.7.

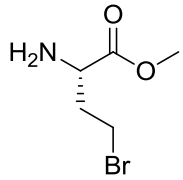

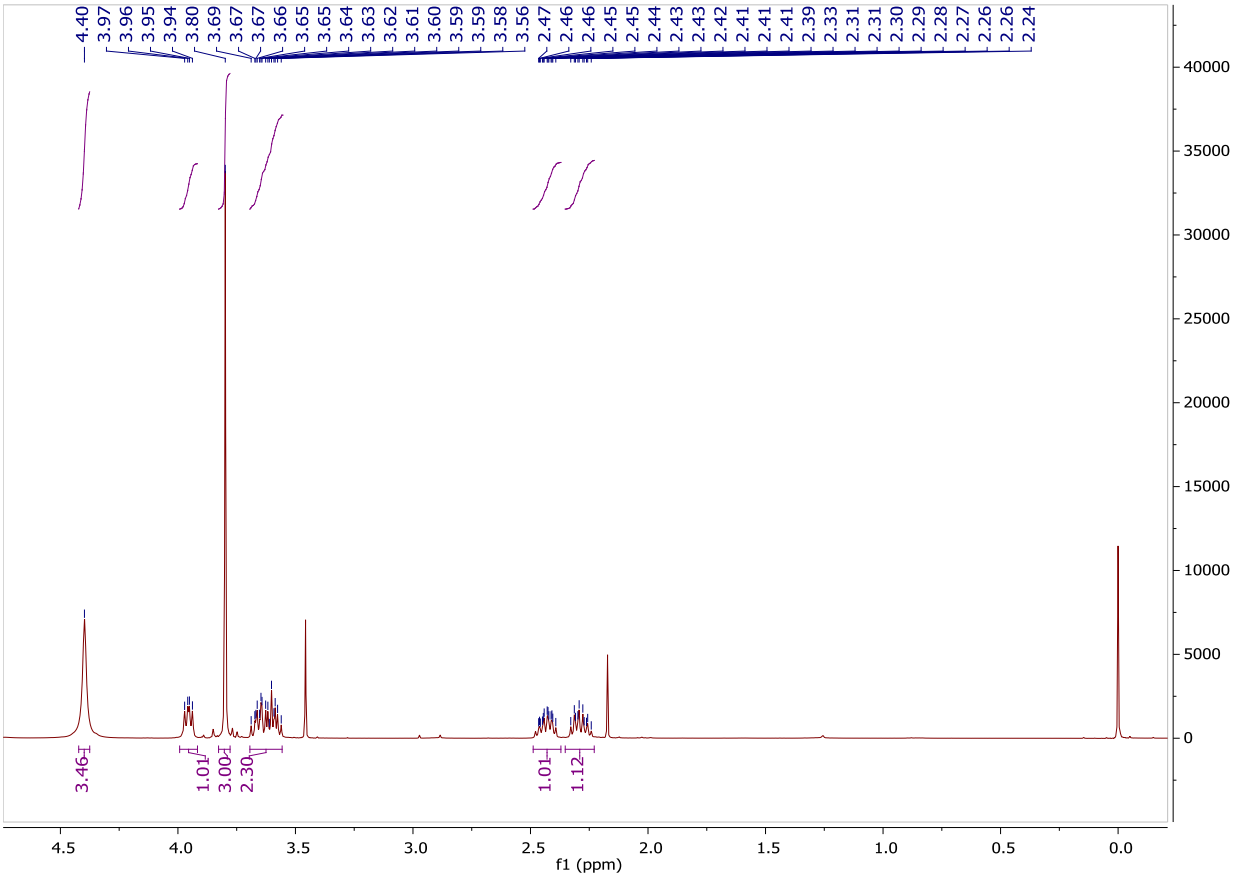

^{1}H NMR of (S)-methyl-2-((((9H-fluoren-9-yl)methoxy)carbonyl)amino)-4-bromobutanoate, 4.8.

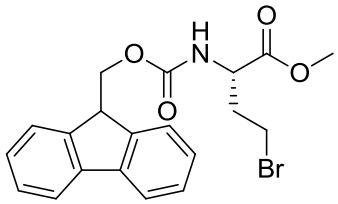

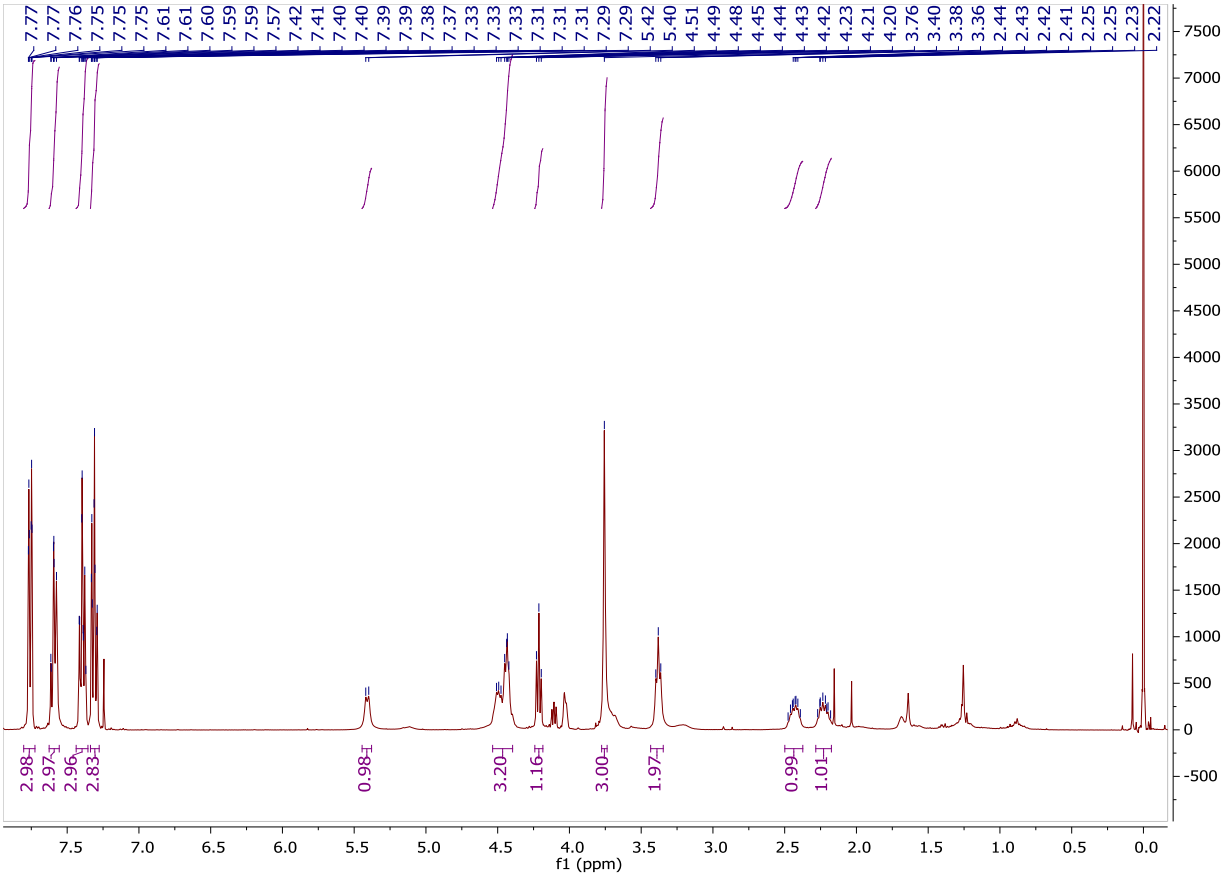

^{1}H NMR Teoc-Cav-OH, 4.10.

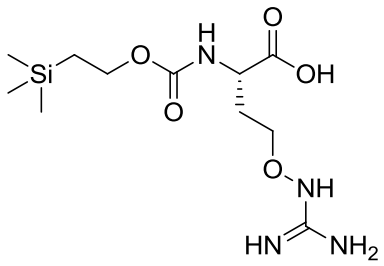

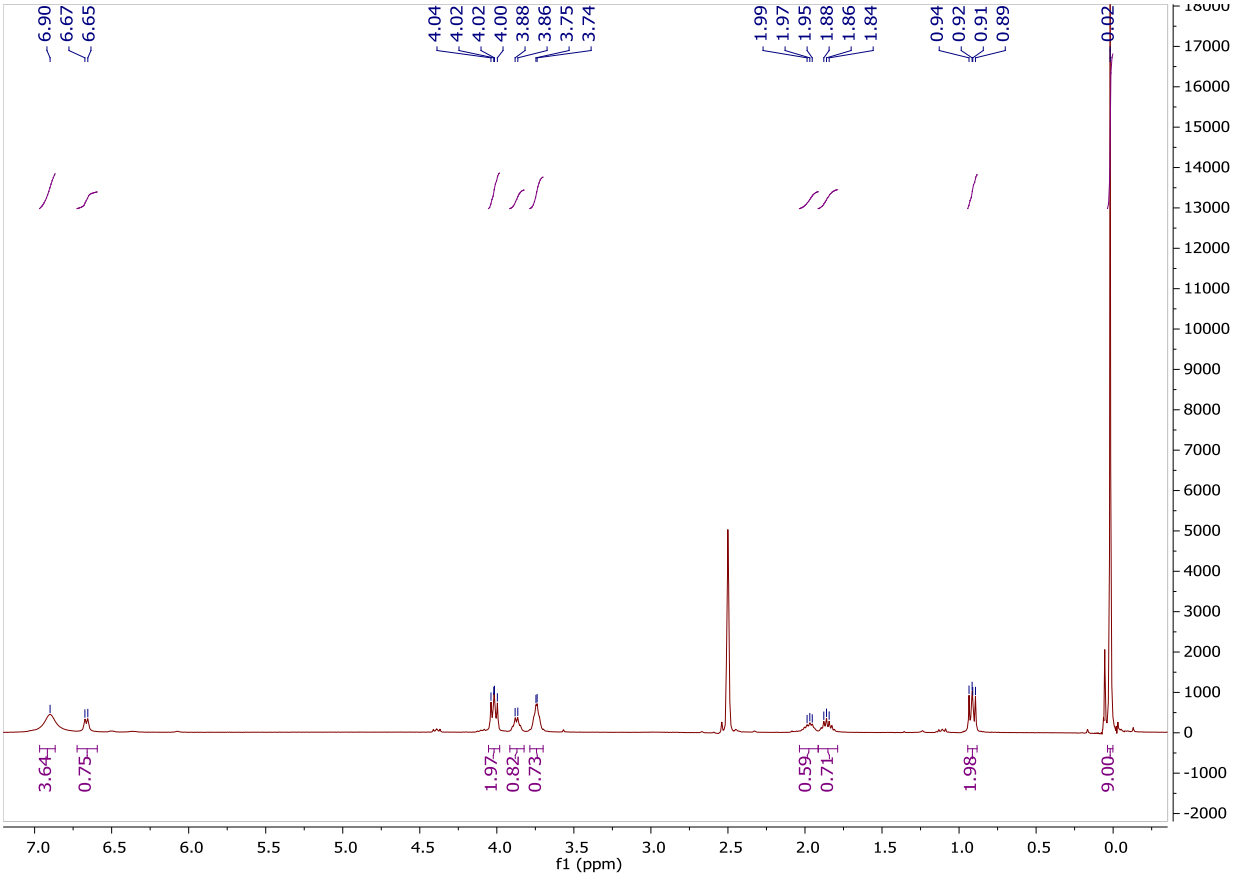

[1] R. L. Siegel, K. D. Miller, A. Jemal, *CA: a cancer journal for clinicians* **2015**, *65*, 5-29.

[2] M. Cushman, D. Nagarathnam, D. Gopal, A. K. Chakraborti, C. M. Lin, E. Hamel, *J. Med. Chem.* **1991**, *34*, 2579-2588.

[3] M. Cushman, D. Nagarathnam, D. Gopal, H. M. He, C. M. Lin, E. Hamel, *J. Med. Chem.* **1992**, *35*, 2293-2306.

[4] C. F. Thorn, C. Oshiro, S. Marsh, T. Hernandez-Boussard, H. McLeod, T. E. Klein, R. B. Altman, *Pharmacogenetics and Genomics* **2011**, *21*, 440-446.

[5] M. M. Dcona, D. Mitra, R. W. Goehe, D. A. Gewirtz, D. A. Lebman, M. C. T. Hartman, *Chem. Commun.* **2012**, *48*, 4755-4757.

[6] N. Parker, M. J. Turk, E. Westrick, J. D. Lewis, P. S. Low, C. P. Leamon, *Anal. Biochem.* **2005**, *338*, 284-293.

[7] M. G. Vander Heiden, L. C. Cantley, C. B. Thompson, *Science* **2009**, *324*, 1029-1033.

[8] S. Farber, L. K. Diamond, R. D. Mercer, R. F. Sylvester, J. A. Wolff, *N. Engl. J. Med.* **1948**, *238*, 787-793.

[9] A. Goldin, J. M. Venditti, S. R. Humphreys, D. Dennis, N. Mantel, S. W. Greenhouse, *Journal of the National Cancer Institute* **1955**, *15*, 1657-1664.

[10] L. P. BIGNOLD, *Anticancer Research* **2006**, *26*, 1327-1336.

[11] Y. Pommier, *Nat Rev Cancer* **2006**, *6*, 789-802.

[12] O. Tacar, P. Sriamornsak, C. R. Dass, *J. Pharm. Pharmacol.* **2013**, *65*, 157-170.

[13] J. R. Jackson, D. R. Patrick, M. M. Dar, P. S. Huang, *Nat Rev Cancer* **2007**, *7*, 107-117.

[14] T. A. Buchholz, D. N. Stivers, J. Stec, M. Ayers, E. Clark, A. Bolt, A. A. Sahin, W. F. Symmans, K. R. Hess, H. M. Kuerer, V. Valero, G. N. Hortobagyi, L. Pusztai, *Cancer J.* **2002**, *8*, 461-461.

[15] G. Minotti, P. Menna, E. Salvatorelli, G. Cairo, L. Gianni, *Pharmacological Reviews* **2004**, *56*, 185-229.

[16] M. Cushman, D. Nagarathnam, D. Gopal, A. K. Chakraborti, C. M. Lin, E. Hamel, *J. Med. Chem.* **1991**, *34*, 2579-2588.

[17] D. W. Siemann, D. J. Chaplin, P. A. Walicke, *Expert Opin. Investig. Drugs* **2009**, *18*, 189-197.

[18] M. Zweifel, G. C. Jayson, N. S. Reed, R. Osborne, B. Hassan, J. Ledermann, G. Shreeves, L. Poupard, S. -. Lu, J. Balkissoon, D. J. Chaplin, G. J. S. Rustin, *Annals of Oncology* **2011**,.

[19] M. M. Cooney, T. Radivoyevitch, A. Dowlati, B. Overmoyer, N. Levitan, K. Robertson, S. L. Levine, K. DeCaro, C. Buchter, A. Taylor, B. S. Stambler, S. C. Remick, *Clinical Cancer Research* **2004**, *10*, 96-100.

[20] C. J. Mooney, G. Nagaiah, P. Fu, J. K. Wasman, M. M. Cooney, P. S. Savvides, J. A. Bokar, A. Dowlati, D. Wang, S. S. Agarwala, S. M. Flick, P. H. Hartman, J. D. Ortiz, P. N. Lavertu, S. C. Remick, *Thyroid* **2009**, *19*, 233-240.

[21] G. Rustin, G. Jayson, N. Reed, **2008**,.

[22] E. Tagliabue, A. Balsari, M. Campiglio, S. M. Pupa, *Expert Opin. Biol. Ther.* **2010**, *10*, 711-724.

[23] K. R. Kalli, A. L. Oberg, G. L. Keeney, T. J. H. Christianson, P. S. Low, K. L. Knutson, L. C. Hartmann, *Gynecol. Oncol.* **2008**, *108*, 619-626.

[24] S. Wang, R. J. Lee, C. J. Mathias, M. A. Green, P. S. Low, *Bioconjugate Chem.* **1996**, *7*, 56-62.

[25] A. R. Hilgenbrink, P. S. Low, *J. Pharm. Sci.* **2005**, *94*, 2135-2146.

[26] C. P. Leamon, P. S. Low, *Journal of Biological Chemistry* **1992**, *267*, 24966-24971.

[27] C. A. Ladino, R. V. J. Chari, L. A. Bourret, N. L. Kedersha, V. S. Goldmacher, *International Journal of Cancer* **1997**, *73*, 859-864.

[28] E. J. Roy, U. Gawlick, B. A. Orr, D. M. Kranz, *Adv. Drug Deliv. Rev.* **2004**, *56*, 1219-1231.

[29] K. Anderson, L. Eliot, B. Stevenson, J. Rogers, *Pharm. Res.* **2001**, *18*, 316-322.

[30] E. K. Park, S. B. Lee, Y. M. Lee, *Biomaterials* **2005**, *26*, 1053-1061.

[31] P. J. Muller, K. Vousden, *Cancer Cell*, *25*, 304-317.

[32] F. M. Boeckler, A. C. Joerger, G. Jaggi, T. J. Rutherford, D. B. Veprintsev, A. R. Fersht, *Proceedings of the National Academy of Sciences* **2008**, *105*, 10360-10365.

[33] K. D. Davies, R. C. Doebele, *Clinical Cancer Research* **2013**, *19*, 4040-4045.

[34] A. S. Advani, A. M. Pendergast, *Leuk. Res.* **2002**, *26*, 713-720.

[35] Z. Huang, *Technology in cancer research & treatment* **2005**, *4*, 283-293.

[36] T. J. Dougherty, G. B. Grindey, R. Fiel, K. R. Weishaupt, D. G. Boyle, *Journal of the National Cancer Institute* **1975**, *55*, 115-121.

[37] R. R. Allison, C. H. Sibata, *Photodiagnosis and Photodynamic Therapy* **2010**, *7*, 61-75.

[38] G. Kostenich, A. Orenstein, L. Roitman, Z. Malik, B. Ehrenberg, *Journal of Photochemistry and Photobiology B: Biology* **1997**, *39*, 36-42.

[39] M. Höckel, P. Vaupel, *Journal of the National Cancer Institute* **2001**, *93*, 266-276.

[40] E. D. STERNBERG, D. DOLPHIN, *J. Clin. Laser Med. Surg.* **1993**, *11*, 233-241.

[41] K. Plaetzer, B. Krammer, J. Berlanda, F. Berr, T. Kiesslich, *Lasers in Medical Science* **2009**, *24*, 259-268.

[42] N. P. Prasad, *Introduction to Biophotonics* **2003**, p. 624.

[43] T. Patrice, D. Olivier, L. Bourre, **2006**, *25*, 467-486.

[44] E. S. Lee, Z. Gao, Y. H. Bae, *J. Controlled Release* **2008**, *132*, 164-170.

[45] J. Ko, K. Park, Y. Kim, M. S. Kim, J. K. Han, K. Kim, R. Park, I. Kim, H. K. Song, D. S. Lee, I. C. Kwon, *J. Controlled Release* **2007**, *123*, 109-115.

[46] Y. K. Reshetnyak, O. A. Andreev, U. Lehnert, D. M. Engelman, *Proceedings of the National Academy of Sciences* **2006**, *103*, 6460-6465.

[47] O. A. Andreev, A. D. Dupuy, M. Segala, S. Sandugu, D. A. Serra, C. O. Chichester, D. M. Engelman, Y. K. Reshetnyak, *Proceedings of the National Academy of Sciences* **2007**, *104*, 7893-7898.

[48] A. D. Frankel, C. O. Pabo, *Cell* **1988**, *55*, 1189-1193.

[49] D. Derossi, A. H. Joliot, G. Chassaing, A. Prochiantz, *Journal of Biological Chemistry* **1994**, *269*, 10444-10450.

[50] X. Yang, Y. Chen, R. Yuan, G. Chen, E. Blanco, J. Gao, X. Shuai, *Polymer* **2008**, *49*, 3477-3485.

[51] X. Yang, Y. Wang, X. Huang, Y. Ma, Y. Huang, R. Yang, H. Duan, Y. Chen, *Journal of materials chemistry* **2011**, *21*, 3448-3454.

[52] C. A. Robertson, D. H. Evans, H. Abrahamse, *Journal of Photochemistry and Photobiology B: Biology* **2009**, *96*, 1-8.

[53] D. E. J. G. J. Dolmans, D. Fukumura, R. K. Jain, *Nat Rev Cancer* **2003**, *3*, 380-387.

[54] B. W. Henderson, T. J. Dougherty, *Photochem. Photobiol.* **1992**, *55*, 145-157.

[55] Brian C Wilson and Michael,S.Patterson, *Phys. Med. Biol.* **2008**, *53*, R61.

[56] M. Michael Dcona, Q. Yu, J. A. Capobianco, M. C. T. Hartman, *Chem. Commun.* **2015**, *51*, 8477-8479.

[57] S. Ki Choi, T. Thomas, M. Li, A. Kotlyar, A. Desai, J. Baker James R., *Chem. Commun.* **2010**, *46*, 2632-2634.

[58] J. You, G. Zhang, C. Li, *ACS Nano* **2010**, *4*, 1033-1041.

[59] J. You, P. Zhang, F. Hu, Y. Du, H. Yuan, J. Zhu, Z. Wang, J. Zhou, C. Li, *Pharm. Res.* **2014**, *31*, 554-565.

[60] S. S. Agasti, A. Chompoosor, C. You, P. Ghosh, C. K. Kim, V. M. Rotello, *J. Am. Chem. Soc.* **2009**, *131*, 5728-5729.

[61] L. L. Fedoryshin, A. J. Tavares, E. Petryayeva, S. Doughan, U. J. Krull, *ACS Appl. Mater. Interfaces* **2014**, *6*, 13600-13606.

[62] Q. Xing, N. Li, Y. Jiao, D. Chen, J. Xu, Q. Xu, J. Lu, *RSC Adv.* **2015**, *5*, 5269-5276.

[63] X. Hu, J. Tian, T. Liu, G. Zhang, S. Liu, *Macromolecules* **2013**, *46*, 6243-6256.

[64] A. Presa, R. F. Brissos, A. B. Caballero, I. Borilovic, L. Korrodi-Gregório, R. Pérez-Tomás, O. Roubeau, P. Gamez, *Angewandte Chemie International Edition* **2015**, *54*, 4561-4565.

[65] G. R. Pettit, S. S. FAU, Hamel E FAU - Lin,,C.M., L. C. FAU, A. D. FAU, D. Garcia-Kendall, *Experientia JID - 0376547* **0410**,.

[66] G. R. Pettit, S. B. Singh, M. R. Boyd, E. Hamel, R. K. Pettit, J. M. Schmidt, F. Hogan, *J. Med. Chem.* **1995**, *10*, 1666-1672.

[67] G. PETTIT, S. SINGH, E. HAMEL, C. LIN, D. ALBERTS, D. GARCIAKENDALL, *Experientia* **1989**, *45*, 209-211.

[68] V. M. Sharma, K. V. Adi Seshu, C. Vamsee Krishna, P. Prasanna, V. Chandra Sekhar, A. Venkateswarlu, S. Rajagopal, R. Ajaykumar, D. S. Deevi, N. V. S. Rao Mamidi, R. Rajagopalan, *Bioorg. Med. Chem. Lett.* **2003**, *13*, 1679-1682.

[69] R. Dorr, K. Dvorakova, K. Snead, D. Alberts, S. Salmon, G. R. Pettit, *Invest. New Drugs* **1996**, *14*, 131-137.

[70] P. Nathan, M. Zweifel, A. R. Padhani, D. Koh, M. Ng, D. J. Collins, A. Harris, C. Carden, J. Smythe, N. Fisher, N. J. Taylor, J. J. Stirling, S. Lu, M. O. Leach, G. J. S. Rustin, I. Judson, *Clinical Cancer Research* **2012**, *18*, 3428-3439.

[71] G. J. S. Rustin, S. M. Galbraith, H. Anderson, M. Stratford, L. K. Folkes, L. Sena, L. Gumbrell, P. M. Price, *Journal of Clinical Oncology* **2003**, *21*, 2815-2822.

[72] N. J. Lawrence, D. Rennison, M. Woo, A. T. McGown, J. A. Hadfield, *Bioorg. Med. Chem. Lett.* **2001**, *11*, 51-54.

[73] T. Figueiras, M. Neves-Petersen, S. Petersen, *J. Fluoresc.* **2011**, *21*, 1897-1906.

[74] L. Rocha, C. Păiuş, A. Luca-Raicu, E. Resmerita, A. Rusu, I. Moleavin, M. Hamel, N. Branza-Nichita, N. Hurduc, *J. Photochem. Photobiol. A.* **2014**, *291*, 16-25.

[75] S. Samanta, C. Qin, A. J. Lough, G. A. Woolley, *Angewandte Chemie International Edition* **2012**, *51*, 6452-6455.

[76] S. Pittolo, X. G ├│mez-Santacana, K. Eckelt, X. Rovira, J. Dalton, C. Goudet, J. Pin, A. Llobet, J. Giraldo, A. Llebaria, P. Gorostiza, *Nat Chem Biol* **2014**, *10*, 813-815.

[77] A. A. Beharry, G. A. Woolley, *Chem. Soc. Rev.* **2011**, *40*, 4422-4437.

[78] J. Broichhagen, M. Sch ├╢nberger, S. C. Cork, J. A. Frank, P. Marchetti, M. Bugliani, A. M. J. Shapiro, S. Trapp, G. A. Rutter, D. J. Hodson, D. Trauner, *Nat Commun* **2014**, *5*.

[79] J. R. Kumita, O. S. Smart, G. A. Woolley, *Proc. Natl. Acad. Sci. U. S. A.* **2000**, *97*, 3803-3808.

[80] A. E. Reed, R. B. Weinstock, F. Weinhold, *J. Chem. Phys.*, http://dx.doi.org/10.1063/1.449486.

[81] R. Zhao, C. Tan, Y. Xie, C. Gao, H. Liu, Y. Jiang, *Tetrahedron Lett.* **2011**, *52*, 3805-3809.

[82] K. Monir, M. Ghosh, S. Mishra, A. Majee, A. Hajra, *European Journal of Organic Chemistry* **2014**, *2014*, 1096-1102.

[83] H. M. D. Bandara, S. C. Burdette, *Chem. Soc. Rev.* **2012**, *41*, 1809-1825.

[84] P. P. Birnbaum, J. H. Linford, D. W. G. Style, *Trans. Faraday Soc.* **1953**, *49*, 735-744.

[85] D. Liu, J. Karanicolas, C. Yu, Z. Zhang, G. A. Woolley, *Bioorg. Med. Chem. Lett.* **1997**, *7*, 2677-2680.

[86] L. Vincent, P. Kermani, L. M. Young, J. Cheng, F. Zhang, K. Shido, G. Lam, H. Bompais-Vincent, Z. Zhu, D. J. Hicklin, P. Bohlen, D. J. Chaplin, C. May, S. Rafii, *J. Clin. Invest.* **2005**, *115*, 2992-3006.

[87] G. G. Dark, S. A. Hill, V. E. Prise, G. M. Tozer, G. R. Pettit, D. J. Chaplin, *Cancer Research* **1997**, *57*, 1829-1834.

[88] S. Parihar, A. Kumar, A. K. Chaturvedi, N. K. Sachan, S. Luqman, B. Changkija, M. Manohar, O. Prakash, D. Chanda, F. Khan, C. S. Chanotiya, K. Shanker, A. Dwivedi, R. Konwar, A. S. Negi, *J. Steroid Biochem. Mol. Biol.* **2013**, *137*, 332-344.

[89] S. Samanta, A. A. Beharry, O. Sadovski, T. M. McCormick, A. Babalhavaeji, V. Tropepe, G. A. Woolley, *J. Am. Chem. Soc.* **2013**, *135*, 9777-9784.

[90] S. Samanta, T. M. McCormick, S. K. Schmidt, D. S. Seferos, G. A. Woolley, *Chem. Commun.* **2013**, *49*, 10314-10316.

[91] C. M. Murphy, C. Fenselau, P. L. Gutierrez, *J. Am. Soc. Mass Spectrom.* **1992**, *3*, 815-822.

[92] M. Borowiak, W. Nahaboo, M. Reynders, K. Nekolla, P. Jalinot, J. Hasserodt, M. Rehberg, M. Delattre, S. Zahler, A. Vollmar, *Cell* **2015**,.

[93] A. J. Engdahl, E. A. Torres, S. E. Lock, T. B. Engdahl, P. S. Mertz, C. N. Streu, *Org. Lett.* **2015**, *17*, 4546-4549.

[94] W. A. Velema, W. Szymanski, B. L. Feringa, *J. Am. Chem. Soc.* **2014**, *136*, 2178-2191.

[95] M. Borowiak, W. Nahaboo, M. Reynders, K. Nekolla, P. Jalinot, J. Hasserodt, M. Rehberg, M. Delattre, S. Zahler, A. Vollmar, D. Trauner, O. Thorn-Seshold, *Cell*, *162*, 403-411.

[96] C. Boulègue, M. Löweneck, C. Renner, L. Moroder, *ChemBioChem* **2007**, *8*, 591-594.

[97] R. F. Standaert, S. B. Park, *J. Org. Chem.* **2006**, *71*, 7952-7966.

[98] A. L. Niles, R. A. Moravec, T. L. Riss, *Current Chemical Genomics* **2009**, *3*, 33-41.

[99] Y. Zhao, *The Chemical Record* **2007**, *7*, 286-294.

[100] O. V. Gerasimov, J. A. Boomer, M. M. Qualls, D. H. Thompson, *Adv. Drug Deliv. Rev.* **1999**, *38*, 317-338.

[101] I. ?. Slowing, B. ?. Trewyn, S. Giri, V. ?. -. Lin, *Advanced Functional Materials* **2007**, *17*, 1225-1236.

[102] C. Dohmen, T. Frohlich, U. Lachelt, I. Rohl, H. Vornlocher, P. Hadwiger, E. Wagner, *Mol Ther Nucleic Acids* **2012**, *1*, e7.

[103] D. M. Kranz, T. A. Patrick, K. E. Brigle, M. J. Spinella, E. J. Roy, *Proc. Natl. Acad. Sci. U. S. A.* **1995**, *92*, 9057-9061.

[104] S. Dong, H. J. Cho, Y. W. Lee, M. Roman, *Biomacromolecules* **2014**, *15*, 1560-1567.

[105] A. Bettio, M. Honer, C. Müller, M. Brühlmeier, U. Müller, R. Schibli, V. Groehn, A. P. Schubiger, S. M. Ametamey, *Journal of Nuclear Medicine* **2006**, *47*, 1153-1160.

[106] N. Valiaeva, D. Bartley, T. Konno, J. K. Coward, *J. Org. Chem.* **2001**, *66*, 5146-5154.

[107] S. Tang, G. A. Baker, S. Ravula, J. E. Jones, H. Zhao, *Green Chem.* **2012**, *14*, 2922-2932.

[108] X. Liu, J. Zhou, T. Yu, C. Chen, Q. Cheng, K. Sengupta, Y. Huang, H. Li, C. Liu, Y. Wang, P. Posocco, M. Wang, Q. Cui, S. Giorgio, M. Fermeglia, F. Qu, S. Pricl, Y. Shi, Z. Liang, P. Rocchi, J. J. Rossi, L. Peng, *Angewandte Chemie International Edition* **2014**, *53*, 11822-11827.

[109] T. Uehara, D. Ishii, T. Uemura, H. Suzuki, T. Kanei, K. Takagi, M. Takama, M. Murakami, H. Akizawa, Y. Arano, *Bioconjugate Chem.* **2010**, *21*, 175-181.

[110] F. Tran, A. Odell, G. Ward, N. Westwood, *Molecules* **2013**, *18*, 11639.

[111] D. J. Mitchell, L. Steinman, D. T. Kim, C. G. Fathman, J. B. Rothbard, *The Journal of Peptide Research* **2000**, *56*, 318-325.

[112] D. M. Copolovici, K. Langel, E. Eriste, Ã Langel, *ACS Nano* **2014**, *8*, 1972-1994.

[113] L. Cascales, S. T. Henriques, M. C. Kerr, Y. Huang, M. J. Sweet, N. L. Daly, D. J. Craik, *Journal of Biological Chemistry* **2011**,.

[114] G. A. Eggimann, E. Blattes, S. Buschor, R. Biswas, S. M. Kammer, T. Darbre, J. Reymond, *Chem. Commun.* **2014**, *50*, 7254-7257.

[115] J. Yang, H. Tsutsumi, T. Furuta, M. Sakurai, H. Mihara, *Org. Biomol. Chem.* **2014**, *12*, 4673-4681.

[116] H. Myrberg, L. Zhang, M. M ├ñe, ├ Langel, *Bioconjugate Chem.* **2008**, *19*, 70-75.

[117] P. Wender, D. Mitchell, K. Pattabiraman, E. Pelkey, L. Steinman, J. Rothbard, *Proc. Natl. Acad. Sci. U. S. A.* **2000**, *97*, 13003-13008.

[118] C. Bechara, S. Sagan, *FEBS Lett.* **2013**, *587*, 1693-1702.

[119] A. BOYAR, R. MARSH, *J. Am. Chem. Soc.* **1982**, *104*, 1995-1998.

[120] T. VOLK, E. JAHDE, H. FORTMEYER, K. GLUSENKAMP, M. RAJEWSKY, *Br. J. Cancer* **1993**, *68*, 492-500.

[121] C. Zscherp, R. Schlesinger, J. Tittor, D. Oesterhelt, J. Heberle, *Proc. Natl. Acad. Sci. U. S. A.* **1999**, *96*, 5498-5503.

[122] M. H. Cezari, L. Juliano, *Pept. Res.* **1996**, *2*, 88-91.

[123] H. Rink, P. Sieber, F. Raschdorf, *Tetrahedron Lett.* **1984**, *25*, 621-624.

[124] Y. Kim, S. Binauld, M. H. Stenzel, *Biomacromolecules* **2012**, *13*, 3418-3426.

[125] T. Pajpanova, S. Stoev, E. Golovinsky, G. -. KrauÃŸ, J. Miersch, *Amino Acids* **1997**, *12*, 191-204.

[126] S. P. Singh, A. Michaelides, A. R. Merrill, A. L. Schwan, *J. Org. Chem.* **2011**, *76*, 6825-6831.

[127] C. A. Miller, R. A. Batey, *Org. Lett.* **2004**, *6*, 699-702.

[128] Y. Xiao, K. Lee, P. Liu, *Org. Lett.* **2008**, *10*, 5521-5524.